UNIVERSITÀ
DEGLI STUDI
DI PADOVA

Sede Amministrativa: Università degli Studi di Padova

Dipartimento di Scienze Chimiche

CORSO DI DOTTORATO DI RICERCA IN: SCIENZE MOLECOLARI
CURRICOLO: SCIENZE CHIMICHE
CICLO XXX

SYNTHESIS AND APPLICATION OF NITROGEN BASED POLYDENTATE LIGAND COMPLEXES

Tesi redatta con il contributo finanziario della Fondazione Cariparo

Coordinatore: Ch.mo Prof. Leonard Jan Prins
Supervisore: Ch.mo Prof. Cristiano Zonta

Dottoranda: Nádia Alessandra Carmo dos Santos

Abstract

This Ph.D. thesis describes the versatility of metal complexes with tris(2-pyridylmethyl)amine (TPMA) based ligands to be used either as self-assembling molecular scaffolds with application on molecular recognition and chiroptical probing, or as active catalysts in atom transfer radical polymerization and hydrogen evolving catalysis reactions. Quantitative chirality determination is fundamental due to the broad effect that stereochemistry has in many different scientific fields. Within this subject, there is a strong urge to develop fast and effective methods to perform stereochemical analysis to couple with high throughput screening methods for production or analysis of biological samples. Chiroptical methods are able to provide the speed and accuracy that enantiomeric excess determination measurement needs. Within that scope, three molecular probes for amino acids have been developed allowing to perform enantiomeric determination and absolute configuration by measuring the induced circular dichroism (CD), vibrational circular dichroism (VDC) or circularly polarized luminescence (CPL). The reported systems were able to provide reliable information about the chirality of the studied analytes.

In this dissertation the mechanistic investigation for the elucidation of the self-assembly process of TPMA with amino acids and metals is described. The complex equilibrium that yields the dimeric supramolecular architectures responsible for the chiroptical signals is exposed. The main factor that affects the final products of the reaction as well. Then the effects on the chiroptical response when changing the metal ions on the main structure are reported, some impressive results were obtained by using Co (II) instead of Zn (II) on the VCD measurements. It was actually possible to enhance the signal intensity by two orders of magnitude. Furthermore, after modifying the initial ligand structure to add a quinolinic moiety in order to give fluorescent properties to the system, it was possible to obtain CPL bands.

Moreover, the versatility of the studied ligands was assessed in other areas like catalysis. Eight novel copper complexes were synthesized and applied as active catalysts in atom transfer radical polymerization (ATRP). Hidroxyquinolinic based cobalt, nickel and iron complexes were evaluated as potential catalysts for hydrogen evolving reactions with positive results.

Acknowledgements

I would like to thank God above all things, for giving me this great opportunity of learning and personal growth, and for being by my side in all times of need.

I would like to express my sincere gratitude to my supervisor Prof. Cristiano Zonta for the continuous support of my Ph.D. study and research, for his patience, motivation, and immense knowledge. His guidance helped me in all the time of research and writing of this thesis. Besides my supervisor, I would like to thank Prof. Giulia Licini for being always present and insightful comments and encouragement.

My sincere thanks also goes to everyone that collaborated with my Ph.D. research, specially Prof. Abdirisak Ahmed Isse, Prof. Sergio Abbate and Prof. Giovanna Longhi who provided me an opportunity to work among with them personally, and who gave me access to their laboratories and research facilities. Also Prof. Klaus Wurst, Prof. Lorenzo Di Bari and Dr. Mirco Natali, without their precious support it would not be possible to conduct this research.

To everyone from lab 108, Emanuele, Rosalia, Paolo, Claudia, William, Giulia S., Davide, Elena, Jack, Carlo, Federico, Giulia M., Cesare, Riccardo, Donato, Francesco, Andrea and Irene, my deep gratitude, it was great sharing the laboratory with all of you during these three years. And I would like to take the opportunity to give my special thanks to Emanuele, Rosalia, Claudia and Paolo who welcomed me in Italy, and took me to their homes and hearts and became part of my Italian family.

A very special gratitude goes out to CARIPARO foundation, for the financial support, but also for the great group of friends that I was able make. Obviously to all CARIPARO Ph.D. students, I wish I could name you all, but we are too many. You are the most amazing international group of friends, my eternal thanks.

My deep love and gratitude go to my family in Brazil, that have always supported my decisions and gave me the strength to keep going, and for my sisters and nice thanks for all moral and emotional support provided in my life, no distance can diminish our love that will last until afterlife.

To everyone that I met during these years and became part of life thanks for all your encouragement!

Declaration

The work in this thesis was carried out at the University of Padova from November 2014 to October 2017. The work was carried out personally except where otherwise stated.

Chapter 2 will be submitted to European Journal of Organic Chemistry as: “Diasteroselective Multi-Component Assemblies from Dynamic Covalent Imine Condensation and Metal-Coordination Chemistry. Mechanism and Narcissistic Stereochemistry Self-Sorting” E. Badetti, N. A. Carmo dos Santos, F. A. Scaramuzzo, K. Wurst, G. Licini, C. Zonta

Chapter 3 has been partially published as part of: “Co(II)-induced giant vibrational CD provides a new design of methods for rapid and sensitive chirality recognition” R. Berardozzi, E. Badetti, N. A. Carmo dos Santos, K. Wurst, G. Licini, G. Pescitelli, C. Zonta, L. Di Bari *Chem. Commun.* **2016**, *52*, 8428-8431.

Chapter 4 has been published as: “A Stereodynamic Fluorescent Probe for Amino-Acids. Circular Dichroism and Circularly Polarised Luminescence Analysis” N. A. Carmo dos Santos, E. Badetti, G. Licini, S. Abbate, G. Longhi, C. Zonta *Chirality*, **2017**, 1-9 https://doi.org/10.1002/chir.22780.

Section 5.1 has been published as part of: “Tuning the reactivity and efficiency of copper catalysts for atom transfer radical polymerization by synthetic modification of tris(2-methylpyridyl)amine” N. A. Carmo dos Santos, F. Lorandi, E. Badetti, K. Wurst, A. A. Isse, A. Gennaro, G. Licini, C. Zonta *Polymer*, **2017**, 128, 169-176.

Section 5.2 has been accepted in Dalton Transaction as part of: “Cobalt, nickel, and iron complexes of 8-hydroxyquinoline-di(2-picolyl)amine for light-driven hydrogen evolution” N. A. Carmo dos Santos, M. Natali, E. Badetti, K. Wurst, G. Licini, C. Zonta.

Nádia Alessandra Carmo dos Santos

Padua, October 2017

Contents

CHAPTER 1

General Introduction

1.1. Introduction

Chirality assessment is fundamental due to the important consequences that the spatial arrangement of molecules has in many fields such as synthesis, medicinal chemistry or materials just to cite a few. The urge in the production of asymmetric compounds have led in the recent years to an increasing attention in fast method for high throughput methods for the determination of the enantiomeric excess (*e.e.*).[1] In this context, strong efforts are directed toward the implementation of HTS methods to several analysis techniques ranging from chromatographic to mass spectroscopy (Table 1.1)

This elaborate deals with the synthesis and study of chemical stereodynamic probes for the enhancement of the applicability of chiroptical spectroscopies as fast and reliable tools to reduce the cost and time of stereochemical analysis. An overview of the three main spectroscopies used in the present thesis, namely electronic Circular Dichroism (CD), vibrational Circular Dichroism (VCD) and Circularly Polarized Luminescence (CPL) will follow.

1.2. Molecular Chirality

Analytical methods for the determination of enantiomeric excess and absolute configuration have received great attention from several fields of chemistry since the discovery of molecular chirality by Louis Pasteur. Chirality assessment has a big importance in several fields including, geology, space exploration, environmental sciences, proteomics, pharmacology and health sciences. When researching for effective drugs and new pharmaceutical agents is necessary to have a reasonable understanding of molecular chirality and how it affects biological organisms and targets..[2] Chirality is an important aspect in many scientific studies, geological layering, fossil dating and time of death of an individual can be calculated by the enantiomeric ratio. In humans, chiral compounds can have delicate effects like giving different aromas in some molecules or more harmful ones, a chiral change in a protein structure can cause serious diseases like cancer, multiple sclerosis, Alzheimer's disease and more.[2a, 3]

It is understandable the importance of chirality in chemistry. Hence, chiral detection and separation methods that are efficient, rapid, and sensitive are highly requested. However, the separation and detection of enantiomers are difficult due their similarities in chemical and physical properties. In the 80's, nuclear magnetic resonance spectroscopy has been used for structure confirmation and chiral separations have been primarily achieved by chromatography and capillary electrophoresis.[2a, 4] The chiral separation by liquid chromatography is usually achieved using a chiral stationary phase, the enantiomers interacts differently and the one that forms a more stable interaction with the chiral selector is retained more strongly. The main

drawback of chromatographic separation techniques is the time consumption and high cost of method development. In several essays to avoid and substitute the slow and tedious process of enantiomeric chromatographic determination, chiroptical methods have been developed for the determination of enantiomeric excess and absolute configuration.[2a, 5]

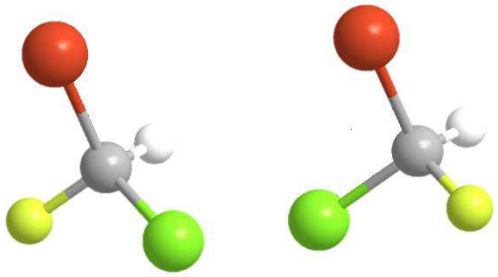

Figure 1.1 CHFClBr enantiomers

1.3. Chiroptical Spectroscopies and Stereodynamic Probes

Optical methods study the interaction between electromagnetic energy and matter. In the case of chiral compounds, while the physical and chemical properties of enantiomeric compounds are identical, the plane of plane-polarized light is rotated in opposite directions when the light passes through a solution of two enantiomers. This optical activity is studied with chiroptical spectroscopy techniques which use polarized electromagnetic radiation. The polarization can be linear, circular or elliptically depending on the direction of the electric (and magnetic) components along the propagation direction.[6] In conventional chiroptical spectroscopies, the sample is irradiated by a light source and the absorbed or emitted light is measured giving information of the sample under characterization. In general, the absorption of the irradiated energy is not carried out by the entire molecule, but by a part of it called chromophore.[7]

Chiroptical methods are commonly used to characterize absolute configuration and to determine the optical purity of chiral compounds. It should be noted, however, that their sensitivity is considered limited in comparison with other analytical techniques. For this reason, chiral spectroscopies are used to do preliminary screening before the employment of other analytical techniques like chiral chromatography.[1a, 8] The low sensitivity is mainly arising from the lack of strong chromophores in most of the analytes. Nevertheless, due the low cost, speed and overall diffusion that optical techniques have, there are strong efforts by the manufacturer to deliver more sensitive instruments. Beside this continuous technological effort, recently, chemical approaches based on a (non)-covalent association between the analyte and a probe containing a chromophore are used to enhance the signal.

Table 1.1. Methods for enantiomeric excess determination and absolute configuration assignment.

Method	Principle	Concept	Requirements
Optical Rotatory Dispersion (ORD)[9]	Variation in the optical rotation with a change in the wavelength of polarized light	Rotating power is measured at different wavelengths of the incident polarized light. It is at the base of the polarimeter.	
Raman Optical Activity (ROA)[10]	Difference between the intensities of the right- and left-handed circularly polarized scattered beams	It uses the difference in intensity of Raman scattered right and left circularly polarized light by reason of molecular chirality	
Chiral Gas Chromatography (Chiral GC)[1h, 11]	Chromatographic separation of enantiomeric compounds	A non-racemic chiral stationary phase (CSP) allow transient diastereomeric interactions with the analyte present in the gas mobile phase. In indirect approaches the chiral compound It is functionalized with a chiral auxiliary. The resulting diastereomers are then separated on an achiral stationary phase.	Derivatization reagents or chiral stationary phase (CPS) and volatile analyte
Chiral High Performance Liquid Chromatography (Chiral HPLC)[1i, 12]	Chromatographic separation of enantiomeric compounds	A non-racemic chiral stationary phase (CSP) allow transient diastereomeric interactions with the analyte present in the liquid mobile phase. Some CSPs are able to separate a wide range of chiral compounds, while others are useful only for specific types of chiral molecules.	Chiral stationary phase (CPS)
Bjovet Pairs[13]	X-ray Crystallography	It is an isomorphous replacement method to reveal a non-centrosymmetric structure on which the abnormal scattering of an atom for a wavelength just beyond its absorption limit is used to identify the correct enantiomorph, of an optically active compound.	Enantiopure crystals
Chiral Ion Mobility Spectroscopy (CIMS)[14]	Chiral discrimination of enantiomeric ions in the gas phase	Gas phase ions, when subjected to a potential gradient are separated at atmospheric pressure due to differences in their shapes and sizes (IMS). In addition to size and shape, CIMS separates ions based on their stereospecific interaction with a chiral gas. Usually the asymmetric environment is provided by doping the drift gas with a volatile chiral reagent.	Necessity to form ions in the gas phase
Coulomb Explosion Imaging (CEI)[15]	Chiral discrimination of enantiomeric ions	Coulomb explosion imaging is a technique which get the structure of small molecules in the gas phase and their ultrafast dynamics by inducing the rapid ionization and dissociation of the molecule into its constituent atomic fragments.	Small cations
Mass Selective – Photo Electron Circular Dichroism (MS-PECD)[16]	Chiral discrimination of enantiomeric ions	It is the detection by imaging techniques of the gaseous chiral molecules and the 3D electron distribution that were previously ionized by circular polarized pulsed laser	Small and simple molecules
Chiral Nuclear Magnetic Resonance (NMR) Spectroscopy[1d, 1j, 17]	NMR chiral discrimination by formation of diasteroisomers	Chiral derivatization agent, chiral lanthanide shift reagents, and chiral solvating agents (CSA) are used to have asynchronous NMR resonances of the chiral molecules	Functionalization of structures

More in detail, a lot of attention has been driven to the use of stereodynamic supramolecular probes. In these cases, the chemosensors own a strong chromophore unit and a labile stereogenic element in a fast racemization equilibrium at room temperature. Through the (non)-covalent interaction with a chiral analyte this equilibrium is shifted to a preferential stereoisomer of the probe that is responsible for the chiroptical readout. A large number of stereodynamic CD probes capable of a rapid and sensitive detection of absolute configuration and *e.e.* of chiral analytes have been reported by exploiting many different systems ranging from small molecular probes to self-assembled structures.[1a, 7b, 9d-f, 18] In the next part, an overview of three main techniques used in this thesis, together with some examples of stereodynamic probes are presented.

1.4. Circular Dichroism (CD)

Circular dichroism (CD) is an important technique used for the interpretation of structural features in chiral systems, it probes electronic transitions in the UV-Vis region of the electromagnetic spectrum. The CD technique measures the difference between the absorption of the right and left circularly polarized light,[19] to provide optical information of chiral samples. Considering circularly polarized light the electric and magnetic vectors rotate around the propagating direction describing a helical path as the wave propagates through the space. The circular polarized light is chiral by itself, therefore interacts differently with the R and S (D or L) enantiomers of a chiral molecule, the left and right circular polarized light are absorbed in different extents.[20] In a typical CD experiment, a sample composed by a chiral molecule in solution is exposed alternatively to L/R-circular polarized light: it is this wavelength-dependent difference between absorption of L/R circularly polarized light that yields the CD spectrum. Thus, a CD signal can be either positive or negative, it depends on whether the left circular polarized light is absorbed more than the right circular polarized light (the CD signal is positive) or less (the CD signal is negative) (Figure 1.2). The CD spectrum is a plot of molar extinction coefficient difference $\Delta\varepsilon$, obtained from the absorbance difference through the Lambert-Beer law, over a range of wavelengths. Enantiomers have mirrored images of the CD spectra, because they have equal, however opposite interaction with the right and left circular polarized light.[7b, 20a, 21] It is also common to find some CD spectra plotted as a correlation between the wavelengths and anisotropy g-factor ($g = \Delta\varepsilon/\varepsilon$). For being a ratio between dichroic signal ($\Delta\varepsilon$) and absorbance (ε), this parameter is proportional to the *e.e*. of the analyte, however has the advantage of being concentration independent.[1l]

Circular dichroism has the advantage of a higher sensibility than other chiroptical methods, therefore the usual host-guest enhancing method is not required in certain cases. Another advantage is the direct correlation between the intensity of the obtained signal and the *e.e*. of the analyte. [1j, 21a, 22]

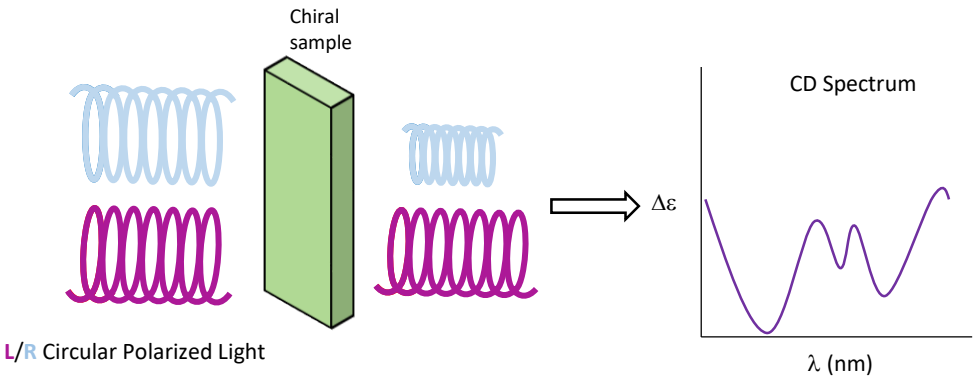

Figure 1.2. Schematic diagram of CD absorption

1.5. Vibrational Circular Dichroism (VCD)

Vibrational circular dichroism (VCD) is similar to the CD differing mainly on the wavelength range used, while CD experiments are performed on the UV-Vis region, the VCD works in the mid-IR region. VCD has been reckoned as one of the best analytical method for determination of *ac* in organic compounds because its spectra might be considered a fingerprint of the molecule configuration.[1j, 21a, 23] Every molecule is capable of absorbing IR radiation, for this reason the VCD technique can be applied in a wider range of compounds than CD. Since the VCD detects the molecular vibrations it is not necessary the derivatization of the analyte with chromophores, however the low signal intensity is an important limitation that induces the samples to be used in high concentrations and with a longer measurement time than others optical methods. The VCD signal is considered weak when compared with the IR absorption, the difference between the VCD signals is about 10^4-10^6 times lower than the intensity of the corresponding vibrational absorption band. To reduce this limitation most measurements are done with concentrated samples, long acquisition time, keen choice of blank, that is normally represented by the racemate and special care to be taken within recording the reference baseline. For this reason, it is more difficult to obtain quality VCD spectra. Although this disadvantage in sensitivity, there are several reasons that have allowed VCD to develop as an essential technique for the identification of absolute configuration of chiral molecules. A common protocol on *ac* determination is the initial collection of baseline and sample spectra in a near series, this way the instrumental drift can be minimized, during this stage a few to several hours can be consumed on the acquisition; followed by the computational studies for geometry optimization and VCD calculation for each enantiomer; the Boltzmann average is calculated using the obtained computed spectra and the calculated energies for a comparison between the experimental and computed spectra.[15] All these passages are crucial on the proper VCD spectrum interpretation, because any small error might cause a wrong *ac* assignment the studied molecule.[1j]

1.6. Circularly Polarized Luminescence (CPL)

Circularly polarized luminescence (CPL) is the differential emission of left and right circularly polarized light in chiral non racemic molecules, frequently it can also be measured by the dissymmetry factor (g_{lum}) that can be described as the ratio between the differential emission of left and right CPL and the average emitted intensity. Only quite special systems (lanthanide complexes or aggregate states with supramolecular chiral order) presents a g_{lum}~ 1: CPL signatures is considered a powerful tool to collect important structural information of chiral compounds in the excited state like the stereochemistry, conformation and spatial configuration. However, the major limitation in this technique is the low dissymmetric factor displayed by most chiral samples, such as biochemical systems, organic molecules and polymers, the g_{lum} value of these systems are on the order of 10^{-2} to 10^{-3}. Literature it has been reported examples where a close examination by CPL of the excited states of chiral molecules has allowed the discovery of interesting features that had not been observed by the related CD technique.[24] Although this technique seems promising in comparison with other chiroptical methods, chiral organic luminophores that exhibit circularly polarized luminescence with high quantum efficiencies are rare what limits the range of compounds that can be analyzed.[24a, 25] The recommended protocol for CPL measurements consists on the initial assay of the adequate analyte concentration by the collection of the CD and absorbance spectra in the same cuvette to be used in the CPL experiment. Then the confirmation of the emission and excitation wavelength by a fast acquisition of the fluorescence spectrum on a fluorimeter, followed by the acquirement of CPL spectra with a single or multiple scans. In the final step redo a CD spectrum to confirm the final state of the sample, more in detail, it is common the degradation of the samples during the CPL measurement.[24d]

1.7. Chiroptical Sensors

The techniques discussed until now have high potential for a rapid *e.e.* determination, however they also have a common limitation. As explained before, some molecules have low absorptions of the irradiated energy, therefore low-intensity of chiroptical signals is obtained. However, strong chromophores can couple with analytes in a (non)-covalent fashion to enhance the signal. In this context, many research groups have been working in the preparation of synthetic receptors as sensors for different kinds of analytes.[18a, 21b, 26] Normally, the enhanced optical signal arises from a host-guest interaction where the overall system electronic structure experience a change after binding, yielding a change in the chiroptical signal that allows the detection and quantification of the analyte.[1a] The use of synthetic sensors to overcome the sensibility limitations have been widely exploited, for this reason frequently a chromogenic or fluorogenic moiety is included into the host scaffold.[27]

Stereodynamic supramolecular probes with strong chromophore units in their backbones that can bind a chiral analyte through (non)-covalent interactions have been receiving great attention in the *e.e*. determination field.[28]

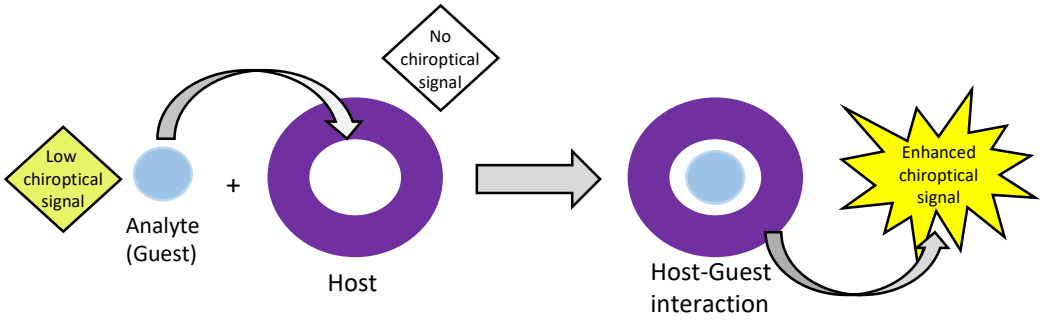

Figure 1.3.Schematic diagram of a generic molecular sensor host-guest interaction

In the past years, in the group were this thesis was carried out, it has been described a series of optical probes that are zinc complexes with a modified version of the widely known tris(2-pyridylmethyl)amine TPMA as ligand. The metallic center with a non-saturated sphere of coordination allows the recognition of carboxylic acids while the aldehyde moiety, from the formyl-phenyl substituent on one of the three arms of the ligand, binds amine groups through imine condensation reaction, thus the system is an adequate amino acid optical probe. Furthermore, the systems were described as quick-formed self-assemblies that yield dimeric supramolecular structures (Figure 1.4). The first probe develop was tested with all natural amino acids, except glycine, and displayed a significant enhancement of the amino acids CD signals, hence the enantiomeric excess was determined with good accuracy. The successive probes included a third metal center in the final architecture. This modification lead to a further improvement on the CD signal.[28b, 28c, 29]

Among the different chemical probes, an intense work has been carried by Berova, Bohan, Wolf, Canary and Anslyn. As example, Wolf reported a method to determine not only the overall concentration but also the *e.e.* and *ac* in cysteine at micromolar concentrations. The sensing investigation described a molecular probe designed to allow a fast detection of this specific amino acid and to generate independent UV and CD data in aqueous media. This optical chemosensing feature was done by covalent substrate modification with the addition of aryl moieties to the thiol and amino groups of cysteine.[30]

Another example has been reported by Li which has combined the zinc porphyrin ability to work as chiroptical sensor of asymmetric compounds and the expected induction of the cooperative effect from dendritic architectures to obtain a significant enhancement of chiroptical CD signals from chiral bidentate guests.[31]

In the study of Agnes *et al.* a metal-linked homochiral macrocycle was designed to work as a chiroptical sensor of electron-rich aromatic molecules, namely ferrocene. The described assembly used a non-covalent interaction

between Pd^{2+} and pyridine moieties from BINOL-based synthon to form the macrocycle probe.[32] R. Peng *et al*. used a racemic N,N'-dioxide-iron(III) complex as an efficient chemosensor, with an accuracy of the *e.e.* measurement of 3% via CD and fluorescence, for simultaneous determination of the absolute configuration, concentration, and enantiomeric excess of hydroxy carboxylic acids in aqueous solution.[33]

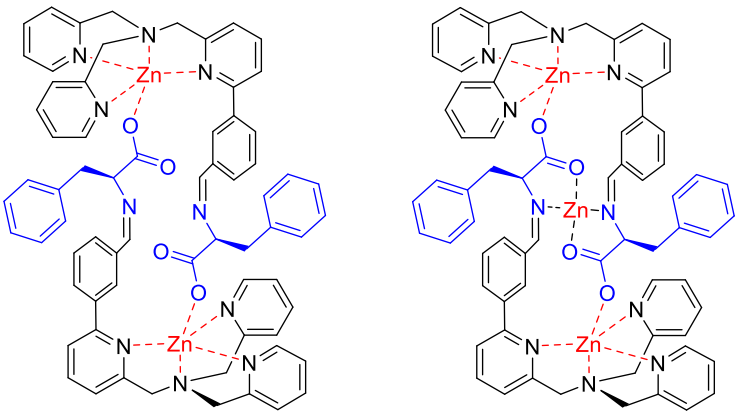

Figure 1.4. *Supramolecular amino acid steriodinamic probes*

An interesting example if offered by Bentley. In this case, stereodynamic metal probes as chiroptical chemosensing to determine the total amount, enantiomeric excess, and absolute configuration of a variety of amines, diamines, amino alcohols, amino acids, carboxylic acids, a-hydroxy acids, and diols.[34] Recently Anslyn and coworkers reported a supramolecular polymeric system built from perylenebisimide (PBI) scaffolds (Figure 1.5) that showed an unusual chiroptical property with an opposite effect to the Yashima's majority-rules effect. This system has been utilized for accurate determination of malic acid enantiopurity at high *e.e*. values via CD.[26] A more recent variation of the CD technique is the photoelectron circular dichroism (PECD), Kastner *et al*.[22b] reports a linear dependence between the quantification of the measurements and the *e.e*. values, however the most promising feature is the described *e.e.* values (denoted as detection limit) of below one percent for almost enantiopure samples, and for nearly racemates. The use of chromophores to overcome the limitations of the weak VCD signals for the determination of absolute configurations is constantly documented in literature. Namely, two complexes from the series of chiral and achiral neutral vanadyl complexes described by Li *et al.* were able to enhance the activity and the red-shifts of the VCD measurements. The complexes structures present the vanadium atom coordinated to lactate, their-alkoxido carboxylate groups, N-heterocycle ligand and terminal oxygen without water molecules. The VCD technique was considered by the authors "an effective tool" on chiral vanadylα-hydroxycarboxylates complexes identification.[35]

Also Burgueño-Tapia and coworkers used an inherently dissymmetric chromophore to assign the absolute configuration of diterpenoids by VCD after density functional theory (DFT) calculations. The analysis protocol

included a molecular model obtained after the contrast between the experimental and calculated VCD curves. In presence of the described chromophores, the differentiation between two epimeric compounds was possible using VCD techinique.[36]

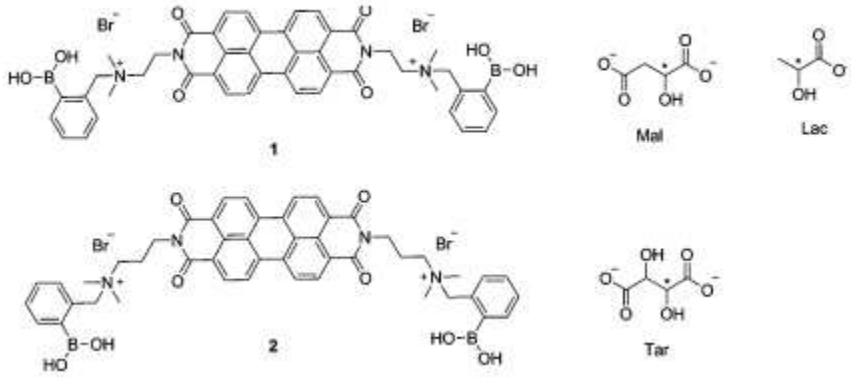

Figure 1.5. *PBI hosts and a-hydroxycarboxylate guests malate. Reproduced from Ref. 26 with permission from The Royal Society of Chemistry*

Lately, the use of organic chromophores able to generate an improvement on the luminescence asymmetry became a widely used strategy, especially with sensors able to self-assemble. Li *et al.* describes the design and synthesis of new chiral tetraphenylethene derivative with two L-leucine-containing attachments (Figure 1.6). This compound emits fairly and gives weak circular dichroism (CD) signals in solutions, however its film displayed circularly polarized luminescence with an emission dissymmetry factor of $+3.2 \times 10^{-3}$.[37]

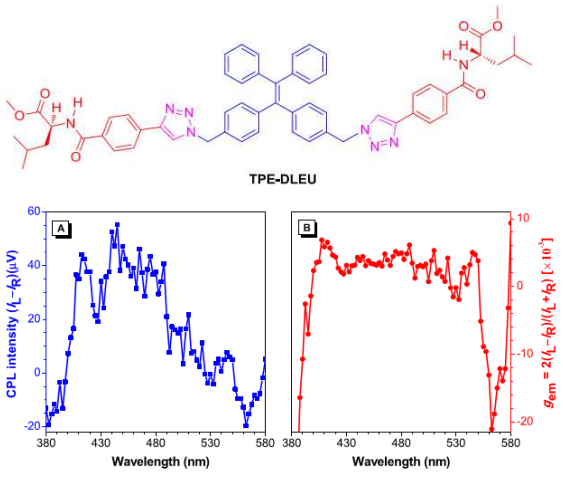

Figure 1.6. TPE-DLEU structure (top) Plots of (A) CPL and (B) luminescence dissymmetry factor (g_{em}) versus wavelength of the cast film of TPE-DLEU prepared by evaporation of its DCE solution (bottom). Adapted from Ref. 37 with permission from Elsevier

Leonzio *et al.* presented a promising CPL probe for biological analytes involving the coordination of *N*,*N*′-bis(2-pyridylmethyl)-*trans*-1,2-diaminocyclohexane-*N*,*N*′-diacetic acid (H_2bpcd), a chiral ligand, and Eu(III) and Tb(III) metal ions in water. The ligand was designed to bind lanthanides ions, however with free coordination sites for further engaging. The metal complexes obtained displayed strong CPL signals. Furthermore, the dissymmetry

factor obtained by the Tb(III) complex was higher than other Tb(III) complexes previously reported in literature.[22d]

Wu, Kessler, Bouř monitored the CPL of a europium complex induced by amino acids by Raman optical activity spectroscopy. The use of a luminophore yielded fluorescent properties to the system and the ROA laser enabled the detection of the weak CPL bands invisible to conventional CPL spectrometers.[38]

1.8. Summary and outlook

The interest in the determination of enantiomeric excess in chiral samples continues to increase, more and more methods are being developed to make the *e.e.* determination cheaper, faster and/or more accurate. And with the ever-growing attention that high-throughput screening methods are getting on the search for new chiral catalysts, the necessity of methods that can solve the analysis bottleneck problem becomes more urgent.

Even if a wide range of techniques available for the *e.e*. determination, not all of them are suitable for HTS analyses. While the chromatographic methods are more traditional and accurate, they are considered high-cost and they lack the necessary speed to handle the amount of samples produced in HTS screening.[1a] Some other techniques could confer rapid analysis, like mass-selective chiral analysis,[39] however the complexity of the necessary equipment and data elaboration are big setbacks. The chiroptical methods, on the other hand, are the ones with the high potential for parallel analysis due the rapid nature of the measurements and simple instrumentation. On the other hand, even if optical signaling methods have disadvantages, for example limited precision and accuracy, many research groups have shown that combined with synthetic sensors important results can be obtained.

Many techniques and methods are being created, new approaches of more traditional methods continue to be developed in attempts to overcome their limitations, there is still much to explore on the determination of *e.e.*

1.9. Aim of the thesis

The overall project deals with the synthesis of new TPMA metal complexes and their application in catalysis and molecular recognition. The research work has been directed to the extension of the chemistry of the dichroic molecular probe towards new metals and the synthesis of new ligands. This is translated in to: *i*) the use of different metals with the same ligand, ii) the synthesis of a new ligand with fluorescence properties, and iii) study of the capability of these metal complexes to perform catalysis. This research has been carried with the aim to increase the sensitivity of the probe and to extend the range of the wavelength to other regions. The possibility to use some of these metal complexes in catalysis has been also evaluated.

1.10. References

[1] (a)D. Leung, S. O. Kang, E. V. Anslyn, *Chem. Soc. Rev.* **2012**, *41*, 448-479; (b)M. Tsukamoto, H. B. Kagan, *Adv. Synth. Catal.* **2002**, *344*, 453-463; (c)M. Mangold, D. Khlopov, E. Temmel, H. Lorenz, A. Seidel-Morgenstern, *Chem. Eng. Sci.* **2017**, *160*, 281-290; (d)G. K. E. Scriba, *J. Chromatogr. A* **2016**, *1467*, 56-78; (e)Y. Hu, Y. Li, J. F. Joung, J. Yin, S. Park, J. Yoon, M. H. Hyun, *Sens Actuators B Chem* **2017**, *241*, 224-229; (f)T. Toyo'oka, *J Biochem Biophys Methods* **2002**, *54*, 25-56; (g)M. E.-A. Said, P. Vanloot, I. Bombarda, J.-V. Naubron, E. M. Dahmane, A. Aamouche, M. Jean, N. Vanthuyne, N. Dupuy, C. Roussel, *Anal. Chim. Acta* **2016**, *903*, 121-130; (h)S.-M. Xie, J.-H. Zhang, N. Fu, B.-J. Wang, L. Chen, L.-M. Yuan, *Anal. Chim. Acta* **2016**, *903*, 156-163; (i)T. Zhang, E. Holder, P. Franco, W. Lindner, *J. Chromatogr. A* **2014**, *1363*, 191-199; (j)P. L. Polavarapu, *Chirality* **2016**, *28*, 445-452; (k)R. Garcia-Rodriguez, S. Hanf, A. D. Bond, D. S. Wright, *Chem. Commun.* **2017**, *53*, 1225-1228. (l) P. Zardi, K. Wurst, G. Licini, C. Zonta, *J. Am. Chem. Soc* **2017**, *139*, 15616-15619.

[2] (a)P. Dwivedi, C. Wu, H. H. Hill, *Anal. Chem.* **2006**, *78*, 8200-8206; (b)O. Buczek, D. Yoshikami, G. Bulaj, E. C. Jimenez, B. M. Olivera, *J. Biol. Chem.* **2005**, *280*, 4247-4253; (c)H.-J. Federsel, *Chirality* **2003**, *15*, S128-S142.

[3] (a)G. Kreil, *Annu. Rev. Biochem.* **1997**, *66*, 337-345; (b)G. F. Russell, J. I. Hills, *Science (New York, N.Y.)* **1971**, *172*, 1043-1044; (c)J. L. Bada, *Science (New York, N.Y.)* **1997**, *275*, 942-943; (d)P. M. Masters, M. R. Zimmerman, *Science (New York, N.Y.)* **1978**, *201*, 811-812; (e)S. A. Fuchs, R. Berger, L. W. J. Klomp, T. J. de Koning, *Mol. Gen. Metab.* **2005**, *85*, 168-180; (f)D. S. Dunlop, A. Neidle, D. McHale, D. M. Dunlop, A. Lajtha, *Biochem. Biophys. Res. Commun.* **1986**, *141*, 27-32; (g)T. Kubo, Y. Kumagae, C. A. Miller, I. Kaneko, *J Neuropathol Exp Neurol* **2003**, *62*, 248-259.

[4] Y. Zhang, D. R. Wu, D. B. Wang-Iverson, A. A. Tymiak, *Drug Discov Today* **2005**, *10*, 571-577.

[5] K. Fulde, A. W. Frahm, *J Chromatogr A* **1999**, *858*, 33-43.

[6] (a)A. J. Adler, N. J. Greenfield, G. D. Fasman, in *Methods in Enzymology, Vol. 27*, Academic Press, **1973**, pp. 675-735; (b)N. J. Greenfield, G. D. Fasman, *Biochem.* **1969**, *8*, 4108-4116; (c)W. C. Johnson, *Proteins: Struct., Funct., Bioinf.* **1990**, *7*, 205-214; (d)F. D. Sonnichsen, J. E. Van Eyk, R. S. Hodges, B. D. Sykes, *Biochem.* **1992**, *31*, 8790-8798.

[7] (a)H. C. Ishikawa-Ankerhold, R. Ankerhold, G. P. C. Drummen, *Molecules* **2012**, *17*, 4047; (b)J. Zhang, H. Gholami, X. Ding, M. Chun, C. Vasileiou, T. Nehira, B. Borhan, *Org. Lett.* **2017**, *19*, 1362-1365.

[8] L. Greene, B. Elzey, M. Franklin, S. O. Fakayode, *Spectrochim. Acta Mol. Biomol. Spectrosc.* **2017**, *174*, 316-325.

[9] (a)J. M. Regenstein, C. E. Regenstein, in *Food Protein Chemistry*, Academic Press, **1984**, pp. 248-254; (b)F. Martínez-Gómez, A. Mansilla, B. Matsuhiro, M. C. Matulewicz, M. A. Troncoso-Valenzuela, *Carbohydr. Polym.* **2016**, *146*, 90-101; (c)H. G. Leemann, *Angew. Chem.* **1962**, *74*, 188-188; (d)M. Evidente, E. Santoro,

A. G. Petrovic, A. Cimmino, J. Koshoubu, A. Evidente, N. Berova, S. Superchi, *Phytochemistry* **2016**, *130*, 328-334; (e)M. Evidente, A. Cimmino, M. C. Zonno, M. Masi, E. Santoro, S. Vergura, A. Berestetskiy, S. Superchi, M. Vurro, A. Evidente, *Tetrahedron* **2016**, *72*, 8502-8507; (f)L. Li, Y.-K. Si, *J. Pharm. Biomed. Anal.* **2011**, *56*, 465-470.

[10] (a)V. Parchansky, J. Kapitan, P. Bour, *RSC Adv.* **2014**, *4*, 57125-57136; (b)M. Magg, Y. Kadria-Vili, P. Oulevey, R. B. Weisman, T. Bürgi, *J. Phys. Chem. Lett.* **2016**, *7*, 221-225; (c)J. Sebestik, F. Teply, I. Cisarova, J. Vavra, D. Koval, P. Bour, *Chem. Commun.* **2016**, *52*, 6257-6260; (d)V. Profant, A. Jegorov, P. Bouř, V. Baumruk, *J. Phys. Chem. B* **2017**, *121*, 1544-1551.

[11] (a)V. Schurig, *Trends Analyt Chem.* **2002**, *21*, 647-661; (b)F. Menestrina, J. Osorio Grisales, C. B. Castells, *Microchem. J.* **2016**, *128*, 267-273; (c)T. Matsukawa, H. Hasegawa, H. Goto, Y. Shinohara, A. Shinohara, Y. Omori, K. Ichida, K. Yokoyama, *J. Pharm. Biomed. Anal.* **2015**, *116*, 59-64; (d)T. Yang, Y. Zhu, C.-Y. Shao, Y. Zhang, J. Shi, H.-P. Lv, Z. Lin, *Ind Crops Prod.* **2016**, *83*, 17-23; (e)J. Yang, S. G. Carmella, S. S. Hecht, *J. Chromatogr. B* **2017**, *1044-1045*, 127-131.

[12] (a)J. Tang, L. Pang, J. Zhou, S. Zhang, W. Tang, *Anal. Chim. Acta* **2016**, *946*, 96-103; (b)J. Qiu, S. Dai, T. Chai, W. Yang, S. Yang, H. Zhao, in *Cellulose - Medical, Pharmaceutical and Electronic Applications* (Eds.: T. v. d. Ven, L. Godbout), InTech, Rijeka, **2013**, p. Ch. 11; (c)M. E. Casas, A. C. Kretschmann, L. Andernach, T. Opatz, K. Bester, *J Chromatogr A* **2016**, *1452*, 116-120; (d)H. Li, X. Jiang, W. Xu, Y. Chen, W. Yu, J. Xu, *J. Chromatogr. A* **2016**, *1435*, 92-99; (e)T. Alizadeh, A. N. Shamkhali, *J Chromatogr B Analyt Technol Biomed Life Sci* **2016**, *1009-1010*, 96-106.

[13] D. M. Blow, in *Methods in Enzymology, Vol. 374*, Academic Press, **2003**, pp. 3-22.

[14] (a)E. Waraksa, U. Perycz, J. Namieśnik, M. Sillanpää, T. Dymerski, M. Wójtowicz, J. Puton, *Trends Analyt Chem.* **2016**, *82*, 237-249; (b)J. Puton, J. Namieśnik, *Trends Analyt Chem.* **2016**, *85*, 10-20; (c)P. Dwivedi, C. Wu, L. M. Matz, B. H. Clowers, W. F. Siems, H. H. Hill, *Anal. Chem.* **2006**, *78*, 8200-8206; (d)M. M. Gaye, G. Nagy, D. E. Clemmer, N. L. B. Pohl, *Anal. Chem.* **2016**, *88*, 2335-2344; (e)J. L. Willems, M. M. Khamis, W. Mohammed Saeid, R. W. Purves, G. Katselis, N. H. Low, A. El-Aneed, *Anal. Chim. Acta* **2016**, *933*, 164-174; (f)J. N. Dodds, J. C. May, J. A. McLean, *Anal. Chem.* **2017**, *89*, 952-959; (g)H. Tian, N. Zheng, S. Li, Y. Zhang, S. Zhao, F. Wen, J. Wang, *Sci. Rep.* **2017**, *7*, 46289; (h)A. Troć, J. Gajewy, W. Danikiewicz, M. Kwit, *Chem. Eur. J.* **2016**, *22*, 13258-13264.

[15] (a)M. Pitzer, M. Kunitski, A. S. Johnson, T. Jahnke, H. Sann, F. Sturm, L. P. Schmidt, H. Schmidt-Bocking, R. Dorner, J. Stohner, J. Kiedrowski, M. Reggelin, S. Marquardt, A. Schiesser, R. Berger, M. S. Schoffler, *Science (New York, N.Y.)* **2013**, *341*, 1096-1100; (b)P. Herwig, K. Zawatzky, M. Grieser, O. Heber, B. Jordon-Thaden, C. Krantz, O. Novotný, R. Repnow, V. Schurig, D. Schwalm, Z. Vager, A. Wolf, O. Trapp, H. Kreckel, *Science (New York, N.Y.)* **2013**, *342*, 1084-1086; (c)P. Martin, *J. Phys. B At. Mol. Opt. Phys.* **2017**, *50*, 153001; (d)L. Christensen, J. H. Nielsen, C. S. Slater, A. Lauer, M. Brouard, H. Stapelfeldt, *Phys. Rev. A.* **2015**, *92*, 033411; (e)H. Tanaka, N. Nakashima, T. Yatsuhashi, *J. Phys. Chem. A* **2016**, *120*, 6917-6928; (f)J.

D. Pickering, K. Amini, M. Brouard, M. Burt, I. J. Bush, L. Christensen, A. Lauer, J. H. Nielsen, C. S. Slater, H. Stapelfeldt, *J. Phys. Chem.* **2016**, *144*, 161105; (g)M. Pitzer, G. Kastirke, M. Kunitski, T. Jahnke, T. Bauer, C. Goihl, F. Trinter, C. Schober, K. Henrichs, J. Becht, S. Zeller, H. Gassert, M. Waitz, A. Kuhlins, H. Sann, F. Sturm, F. Wiegandt, R. Wallauer, L. P. H. Schmidt, A. S. Johnson, M. Mazenauer, B. Spenger, S. Marquardt, S. Marquardt, H. Schmidt-Böcking, J. Stohner, R. Dörner, M. Schöffler, R. Berger, *Chemphyschem* **2016**, *17*, 2465-2472.

[16] (a)D. M. Lubman, *Anal. Chem.* **1987**, *59*, 31A-40A; (b)M. H. M. Janssen, I. Powis, *Phys. Chem. Chem. Phys.* **2014**, *16*, 856-871; (c)C. S. Lehmann, N. B. Ram, I. Powis, M. H. M. Janssen, *J. Phys. Chem.* **2013**, *139*, 234307; (d)M. M. R. Fanood, N. B. Ram, C. S. Lehmann, I. Powis, M. H. M. Janssen, *Nat. Commun.* **2015**, *6*, 7511; (e)X. Yu, Z.-P. Yao, *Anal. Chim. Acta* **2017**, *968*, 1-20.

[17] (a)M. Hernández-Rodríguez, E. Juaristi, *Tetrahedron* **2007**, *63*, 7673-7678; (b)N. Jain, M. B. Mandal, A. V. Bedekar, *Tetrahedron* **2014**, *70*, 4343-4354; (c)C. Peña, J. González-Sabín, I. Alfonso, F. Rebolledo, V. Gotor, *Tetrahedron* **2008**, *64*, 7709-7717; (d)J. Yi, G. Du, Y. Yang, Y. Li, Y. Li, F. Guo, *Tetrahedron: Asymmetry* **2016**, *27*, 1153-1159; (e)G. Bian, S. Yang, H. Huang, H. Zong, L. Song, *Sens Actuators B Chem* **2016**, *231*, 129-134.

[18] (a)S. Matile, N. Berova, K. Nakanishi, S. Novkova, I. Philipova, B. Blagoev, *J. Am. Chem. Soc.* **1995**, *117*, 7021-7022; (b)S. Zahn, J. W. Canary, *Org. Lett.* **1999**, *1*, 861-864; (c)L. A. Joyce, M. S. Maynor, J. M. Dragna, G. M. da Cruz, V. M. Lynch, J. W. Canary, E. V. Anslyn, *J. Am. Chem. Soc.* **2011**, *133*, 13746-13752.

[19] J. W. Steed, J. L. Atwood, in *Supramolecular Chemistry*, John Wiley & Sons, Ltd, **2009**, pp. 49-104.

[20] (a)S. V. Hoffmann, M. Fano, M. van de Weert, in *Analytical Techniques in the Pharmaceutical Sciences* (Eds.: A. Müllertz, Y. Perrie, T. Rades), Springer New York, New York, NY, **2016**, pp. 223-251; (b)T. Levi-Belenkova, A. O. Govorov, G. Markovich, *J. Phys. Chem. C* **2016**, *120*, 12751-12756; (c)J. Lv, K. Hou, D. Ding, D. Wang, B. Han, X. Gao, M. Zhao, L. Shi, J. Guo, Y. Zheng, X. Zhang, C. Lu, L. Huang, W. Huang, Z. Tang, *Angew. Chem.* **2017**, *129*, 5137-5142.

[21] (a)S. S. Wesolowski, D. E. Pivonka, *Bioorganic Med. Chem. Lett.* **2013**, *23*, 4019-4025; (b)M. Tanasova, M. Anyika, B. Borhan, *Angew. Chem. Int. Ed.* **2015**, *54*, 4274-4278.

[22] (a)L. A. Nafie, T. B. Freedman, *ChemInform* **2002**, *33*; (b)A. Kastner, C. Lux, T. Ring, S. Züllighoven, C. Sarpe, A. Senftleben, T. Baumert, *Chemphyschem* **2016**, *17*, 1119-1122; (c)G. Bussi, A. Ruini, E. Molinari, M. J. Caldas, P. Puschnig, C. Ambrosch-Draxl, *Appl. Phys. Lett.* **2002**, *80*, 4118-4120; (d)M. Leonzio, A. Melchior, G. Faura, M. Tolazzi, F. Zinna, L. Di Bari, F. Piccinelli, *Inorg Chem* **2017**, *56*, 4413-4421.

[23] P. Joseph-Nathan, B. Gordillo-Román, in *Progress in the Chemistry of Organic Natural Products 100* (Eds.: A. D. Kinghorn, H. Falk, J. Kobayashi), Springer International Publishing, Cham, **2015**, pp. 311-452.

[24] (a)J. P. Riehl, G. Muller, in *Comprehensive Chiroptical Spectroscopy*, John Wiley & Sons, Inc., **2012**, pp. 65-90; (b)H. Lu, J. Mack, T. Nyokong, N. Kobayashi, Z. Shen, *Coord. Chem. Rev.* **2016**, *318*, 1-15; (c)J. Kumar,

T. Nakashima, T. Kawai, *J. Phys. Chem. Lett.* **2015**, *6*, 3445-3452; (d)G. Longhi, E. Castiglioni, J. Koshoubu, G. Mazzeo, S. Abbate, *Chirality* **2016**, *28*, 696-707.

[25] M. Okazaki, T. Mizusawa, K. Nakabayashi, M. Yamashita, N. Tajima, T. Harada, M. Fujiki, Y. Imai, *J. Photochem. Photobiol., A* **2016**, *331*, 115-119.

[26] X.-X. Chen, Y.-B. Jiang, E. V. Anslyn, *Chem. Commun.* **2016**, *52*, 12669-12671.

[27] (a)T. Ogoshi, A. Harada, *Sensors* **2008**, *8*, 4961; (b)C. Lynam, D. Diamond, *J. Mater. Chem.* **2005**, *15*, 307-314; (c)H. Xia, X. Chen, X. Chen, J. Cheng, Y. Liu, X. Chen, Q. Zhang, G. Zou, *Sens Actuators B Chem* **2018**, *254*, 44-51; (d)M. Tanasova, C. Vasileiou, O. O. Olumolade, B. Borhan, *Chirality* **2009**, *21*, 374-382; (e)L. Zhu, Z. Zhong, E. V. Anslyn, *J. Am. Chem. Soc.* **2005**, *127*, 4260-4269; (f)Y. Zhao, T. M. Swager, *J. Am. Chem. Soc.* **2015**, *137*, 3221-3224; (g)Z. A. De los Santos, C. Wolf, *J. Am. Chem. Soc.* **2016**, *138*, 13517-13520.

[28] (a)M. Anyika, H. Gholami, K. D. Ashtekar, R. Acho, B. Borhan, *J. Am. Chem. Soc.* **2014**, *136*, 550-553; (b)E. Badetti, K. Wurst, G. Licini, C. Zonta, *Chem. Eur. J.* **2016**, *22*, 6515-6518; (c)F. A. Scaramuzzo, G. Licini, C. Zonta, *Chem. Eur. J.* **2013**, *19*, 16809-16813; (d)J. Zhang, M. T. Albelda, Y. Liu, J. W. Canary, *Chirality* **2005**, *17*, 404-420; (e)J. W. Canary, S. Mortezaei, J. Liang, *Coord. Chem. Rev.* **2010**, *254*, 2249-2266.

[29] F. A. Scaramuzzo, E. Badetti, G. Licini, C. Zonta, *Eur. J. Org. Chem.* **2017**, *2017*, 1438-1442.

[30] F. Y. Thanzeel, C. Wolf, *Angew. Chem. Int. Ed.* **2017**, *56*, 7276-7281.

[31] W.-S. Li, D.-L. Jiang, Y. Suna, T. Aida, *J. Am. Chem. Soc.* **2005**, *127*, 7700-7702.

[32] M. Agnes, A. Nitti, D. A. Vander Griend, D. Dondi, D. Merli, D. Pasini, *Chem. Commun.* **2016**, *52*, 11492-11495.

[33] R. Peng, L. Lin, W. Cao, J. Guo, X. Liu, X. Feng, *Tetrahedron Lett.* **2015**, *56*, 3882-3885.

[34] K. W. Bentley, P. Zhang, C. Wolf, *Sci. Adv.* **2016**, *2*.

[35] X. Li, J.-W. Dai, H.-X. Wang, A.-A. Wu, Z.-H. Zhou, *Inorg. Chim. Acta.* **2016**, *453*, 501-506.

[36] E. Burgueño-Tapia, K. Chávez-Castellanos, E. Cedillo-Portugal, P. Joseph-Nathan, *Tetrahedron: Asymmetry* **2017**, *28*, 166-174.

[37] H. Li, W. Yuan, H. He, Z. Cheng, C. Fan, Y. Yang, K. S. Wong, Y. Li, B. Z. Tang, *Dyes Pigm.* **2017**, *138*, 129-134.

[38] T. Wu, J. Kessler, P. Bour, *Phys. Chem. Chem. Phys.* **2016**, *18*, 23803-23811.

[39] (a)U. Boesl, A. Kartouzian, *Annu. Rev. Anal. Chem.* **2016**, *9*, 343-364; (b)O. Plekan, M. Coreno, V. Feyer, A. Moise, R. Richter, M. d. Simone, R. Sankari, K. C. Prince, *Phys. Scripta* **2008**, *78*, 058105.

CHAPTER 2

Diasteroselective Multi-Component Assemblies from Dynamic Covalent Imine Condensation and Metal-Coordination Chemistry. Mechanism and Narcissistic Stereochemistry Self-Sorting

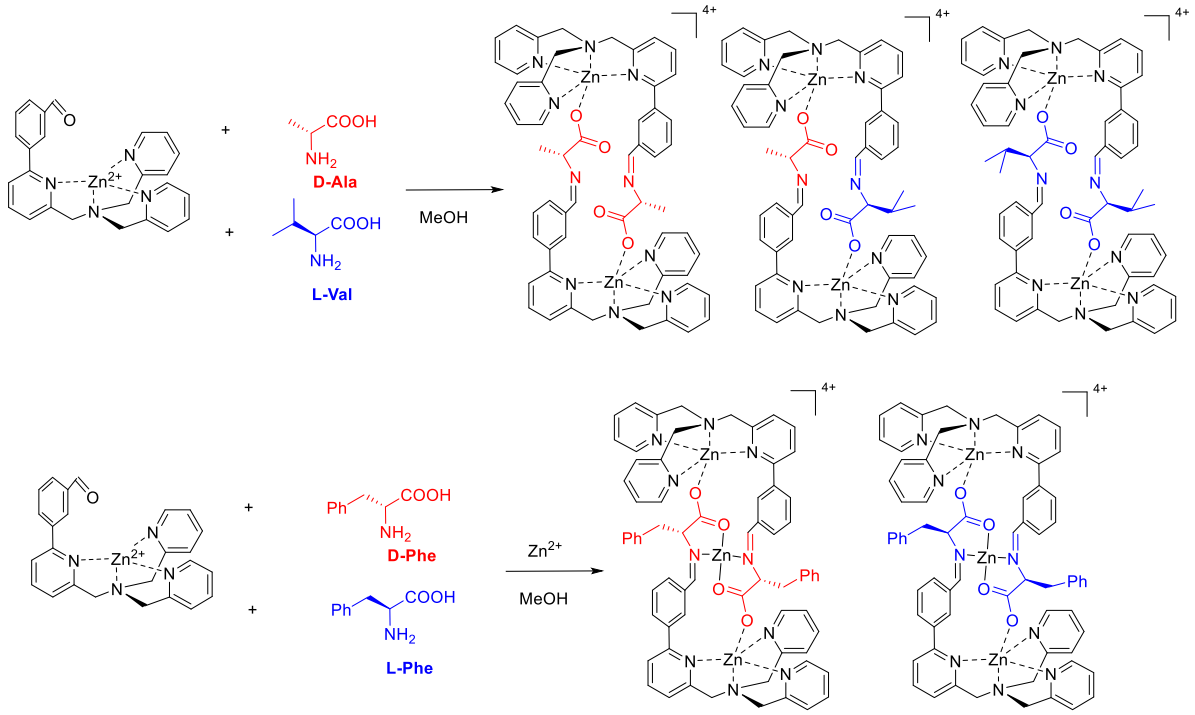

Within this chapter is reported the mechanistic study for the interpretation of the self-assembly process of TPMA with amino acids and metals. The reversibility offered by dynamic covalent and coordination chemistry, gives the possibility to the system composed by a modified tris(2-pyridylmethyl)amine ligand, zinc(II) metal ions and amino acids to exploit different compounds and, within the same compounds, diastereoisomers. This study reveals a complex equilibrium in solution where even small variations in the experimental conditions can profoundly affect the final products of the reaction as well as their stereochemistry. More in detail, tuning the metal concentration is possible to induce a narcissistic self-assembled structure.

2.1. Introduction

One of the leading strategies for the development of complex functional nano-architectures is the use of dynamic covalent chemistry (DCC) in which imine condensation and metal-coordination work simultaneously.[1] These two "orthogonal" thermodynamically driven association processes have successfully and effectively yield a large variety of compounds, ranging from simple complexes to topological structures. This approach has also been effectively used for the development of methods that allow the determination of optical purity.[2] In particular, the focus has been driven towards the development of stereodynamic optical probes[3] for the rapid determination of the enantiomeric excess (*e.e.*) of chiral compounds. In general, these systems are characterized by the presence of at least one labile stereogenic element which, after the addition of a chiral analyte, moves toward the formation of one preferential diasteroisomer. Most of the times, this information is translated into an absorption by the use of optical techniques such as circular dichroism (CD).[4]

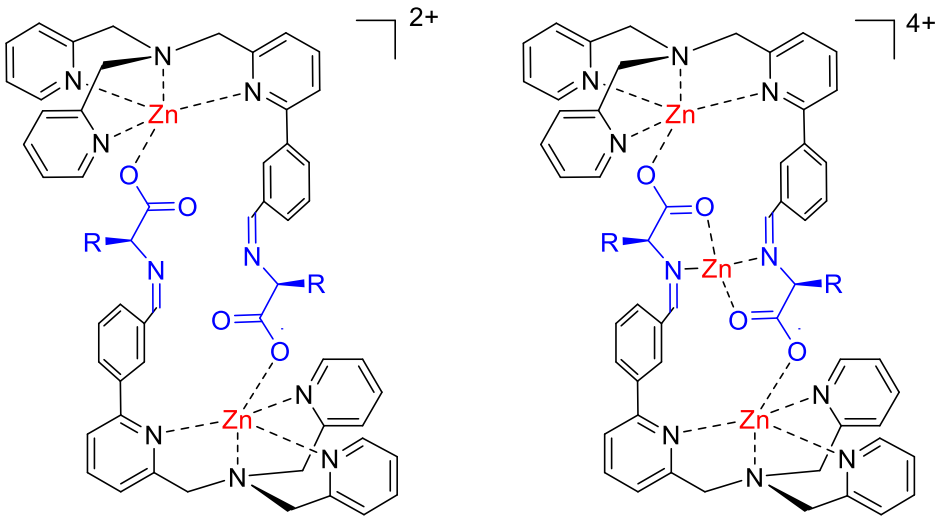

1-Zn-aa **2-Zn-aa**

Scheme 2.1. Dinuclear **1-Zn-aa** and trinuclear **2-Zn-aa** self-assembled structures used as probes for the determination of *e.e.* of amino acids. The counter anions are perchlorates.

Recently, within the research group were this thesis has been carried, tris(2-pyridylmethyl)amine (**TPMA**) metal complexes have been applied both in catalysis and supramolecular chemistry.[6] Within these studies, it has been reported a series of novel molecular architectures that can be used for the determination of the *e.e.* of free amino acids (Scheme 2.1).[7] More in detail, the mix of a modified **TPMA** zinc complex with one equivalent of the desired amino acid resulted in the almost exclusive formation of the dinuclear architecture **1-Zn-aa**. The resulting mixture was used without further purification for CD measurements. The obtained curves directly correlate with the *e.e.* and specular curves were obtained switching the configuration of the amino acids. Beside the capability of the system to be effective with all natural amino acids, it displayed absorptions which were characteristic of the

amino acidic side chain, differentiating clearly the aliphatic or aromatic nature of the backbone. TD-DFT studies have shown that CD signals arise by the helical arrangement of the ligand around the metal, and by the exciton coupling of the atropoisomeric biarylic systems. More recently, from studies on the complex stability, it has been identified the structure **2-Zn-aa**, in which an extra-metal gets coordinated by the cleft formed between the two amino acids. The novel structure, which has also been solved by X-ray diffraction, showed an increase of the CD signal of one order of magnitude. Also in this case, the system was effective in the determination of the optical purity for a series of amino acids.

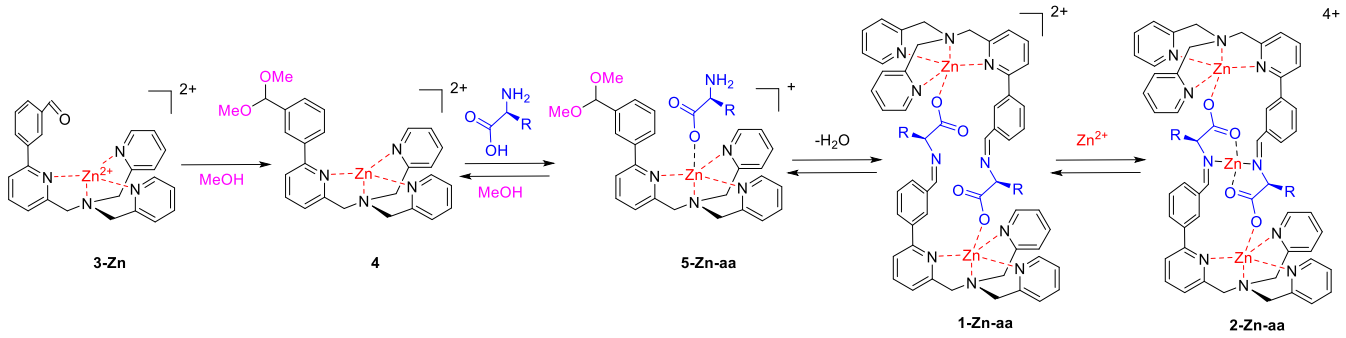

Scheme 2.2. Complex **3** dissolved in methanol give rise to the formation of acetal **4** within hours depending on the initial amount of water. Addition to this mixture of amino acid **L-Phe** leads to adduct **5-Zn-L-Phe** which, in dry conditions, evolves to the dinuclear adduct complex **1-Zn-L-Phe** or to complex **2-Zn-L-Phe** in the presence of an excess of Zn(II) in solution. These initial findings have driven our interest towards the investigation of the whole process taking place in solution, with the two-fold intention of better understanding the self-assembly mechanism and elucidating how the stereochemistry dictates products distribution. The study has revealed how an intricate pattern of variables drive product distribution. The elucidation of the equilibrium present in solution, when imine DCC is used in the presence of metals, highlights that increasing system complexity leads to sharp changes in products distribution and stereochemistry of the processes from small variations in the chemical parameters.

2.2. Results and Discussion

In order to shed light on the mechanism behind the formation of bi- and tri-nuclear dimers, a step-by-step analysis has been performed evaluating how different thermodynamic, kinetic and stereochemical parameters are affecting the assembly formation and, consequently, the dichroic signal. Starting from complex **3-Zn,** the delicate interplay of all the components present in the reaction mixture was revealed.

2.2.1. Intermediates in self-assembly process. Acetal 4 and 5-Zn-L-Phe

The synthesis of the ligand used to obtain the metal complex is done by the aminative reduction reaction between the commercially available 6-Bromo-2-pyridinecarboxaldehyde and dipicolylamine, followed by a Suzuki coupling, and finally a simple complexation reaction using $Zn(ClO_4)_2$ * $6H_2O$. Zinc(II) complex **3**, [7a] bearing a formyl group in meta position to the pyridine ring, is highly soluble in methanol and allows to observe by ^{1}H-NMR, at room temperature, the slow formation of the corresponding acetal **4** (Scheme 2.2 and Figure 2.1).

The complete conversion of **3-Zn** to **4** requires two days at room temperature but only 4 hours at 60 °C. The reaction can be easily monitored by ^{1}H-NMR, following the disappearance of the aldehydic signal of **3-Zn** at 10.02 ppm and the appearance of the signal of acetal **4** at 5.37 ppm. Acetal formation is also confirmed by 2D-NMR HMQC experiment which correlates ^{1}H signal with the characteristic ^{13}C signal at 105 ppm.

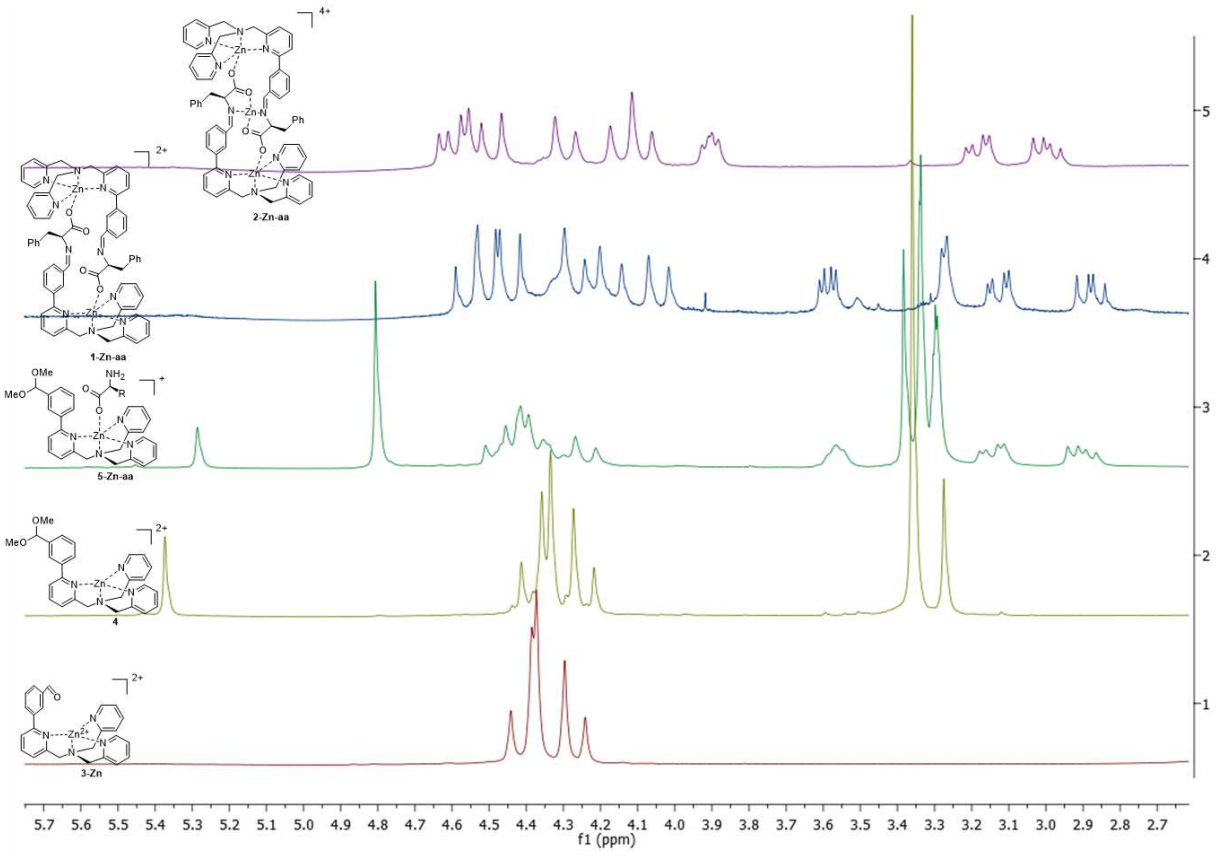

Figure 2.1. Comparison of the signals in the 2.6 to 5.6 ppm region for the compounds **1**, **4**, **5-Zn-L-Phe**, **1-Zn-L-Phe** and **2-Zn-L-Phe**. In this region acetal (5.4 to 5.2 ppm), CH_2 pycolil (4.6 to 3.9 ppm) and amino acid (3.8 to 2.7 ppm) proton signals are present.

Upon adding the amino acid **L-Phe** to acetal **4**, the formation of a new species is instantaneously observed. It is possible to ascribe this structure to the adduct **5-Zn-L-Phe** in which the amino acidic carboxylate binds to the zinc center. This compound is highly stable in solution as variation of ^{1}H NMR signals are not observed: *i*) increasing the temperature, *ii)* leaving the compound in solution for weeks, *iii*) adding extra equivalents of amino acid or iv) extra zinc salt to the sample. In all of these cases, the intensity of the acetal signal remains constant. Moreover, ^{1}H-NMR highlights a broadness of the picolyl CH_2 signals (4.2 – 4.5 ppm) slightly different from the parent compounds **3-Zn** and **4** (Figure 2.1). This observation can indicate the preferential formation of one of the two possible diasteroisomers generated by the helical conformations adopted by the ligand around the metal. However, the absence of any meaningful dichroic signal suggests a poor structural organization of the aromatic chromophores.

2.2.2. Dinuclear complexes 1-Zn-l-Phe

When water is removed from the solution adding activated molecular sieves, the dimeric dinuclear complex **1-Zn-L-Phe** is formed in less than two hours (Scheme 2.1). Compound **1-Zn-L-Phe** has been isolated as a yellow solid simply by evaporation of the solvent and the ^{1}H-NMR indicates predominately the presence of one single species. The disappearance of the signal corresponding to the characteristic acetal proton together with the appearance of the imine signal at 7.7 ppm confirmed the condensation. In this compound, the presence of six doublets (J ~ 16 Hz) between δ = 3.9 and 4.6 ppm, combined with VT-NMR experiments, suggest that the picolyl methylene hydrogens are blocked in a single helical conformation as expressed by the wide separation of the signals. Further confirmation also comes from ESI-MS experiments that show the characteristic isotopic pattern corresponding to the dinuclear zinc complex.

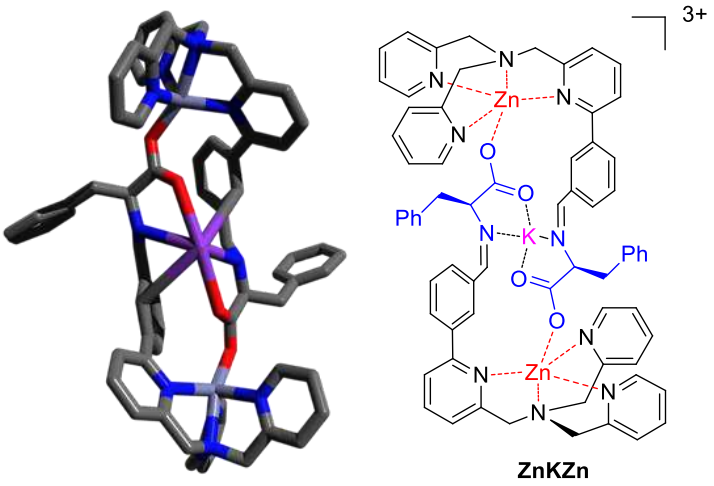

Figure 2.2. X-ray crystal structure of the **ZnKZn** complex arising from the self-assembly of **3-Zn** with **L-Phe** when K is released by molecular sieves.

2.2.3. Trinuclear complexes 2-Zn-L-Phe and ZnKZn

A serendipitous discover has also led to notice, in the dynamic mixture, the formation of a trinuclear complex when an excess of zinc salt is present.[7b] The trinuclear complex **2-L-Phe** can be either obtained starting from the dinuclear complex **1-Zn-L-Phe** by addition of half-equivalent of zinc salt or directly from complex **3-Zn**.

The isolation of the pure compound is possible by crystallization because the tetra positively charged assembly is poorly soluble in methanol. On the other hand, its high solubility in acetonitrile allows registration of ^{1}H-NMR and ESI-MS spectra, the latter showing the characteristic isotopic pattern corresponding to the mono charged species. Surprisingly, in the quest for crystallizing **1-Zn-L-Phe,** small tiny crystals have been obtained leaving the solution of standing, over the molecular sieves, for 24 hours. The crystallographic study was done in collaboration with

Prof. Klaus Wurst (University of Innsbruck). X-ray crystallographic analysis of the crystals reveals that in this case the dimeric system is bound to the potassium released by the molecular sieves to form a new **ZnKZn** trimetallic structure (Figure 2.2). The crystallographic structure obtained, strongly resembles our reported structure of **2-Zn-L-Phe,** indicating a strong tendency of the amino-acidic cleft to incorporate metals.

2.2.4. Stereochemical analysis of 1-Zn-aa and 2-Zn-aa assembly formation

As shown in previous published work of the group, [7a] when **1-Zn-L-Phe** is formed varying amino acid *e.e*., a linear response of the CD signal is observed.

This linearity, besides constituting the bases for a probe, is indicative of a stereochemical recognition process along the formation of a chiral dimeric structure. In principle, two types of structures can be formed starting from a racemic mixture of the amino acid: *i*) homochiral, where both the amino acids incorporated in the structure have the same configuration (narcissistic assembly) or *ii*) heterochiral, where the two amino acids have opposite configuration (meso anti-narcissistic assembly). The linearity in CD response by itself does not give information on which type of structure is more stable in solution. In order to investigate which type of assembly was more stable in solution, we devised an experiment in which the dinuclear **1-Zn-aa** and trinuclear **2-Zn-aa** complexes were prepared from a solution containing a pseudo-racemic solution of **L-Ile** and **D-Ala**.

Starting from the pseudo-racemic mixture the dinuclear **1-Zn-aa** and trinuclear **2-Zn-aa** were obtained following our standard procedure and the resulting mixtures were analysed using ESI-MS experiments in order to understand the stereochemistry of amino acids incorporation in the different compounds (Figure 2.3). In this experiment, assuming a similar response factor for all complexes for the ESI-MS experiment, the dinuclear **1-Zn-aa** and trinuclear **2-Zn-aa** systems behave completely differently. The dinuclear **1-Zn-aa** assembly has a small tendency to prefer, in the presence of a racemic mixture, the hetero-coupled structure (Figure 2.3a). In fact, the mixture obtained is close to the statistical 1:2:1 (measured 1:4:1.2) ratio among the three structures **1-Zn-D-Ala-D-Ala: 1-Zn-L-Val-D-Ala**+**1-Zn-D-Val-L-Ala**: **1-Zn-L-Val-D-Val**, with small preference for the heterochiral structure. On the other hand, it is highly evident that the trinuclear system **2-Zn-aa** shows a complete preference toward the formation of the homochiral assembly.

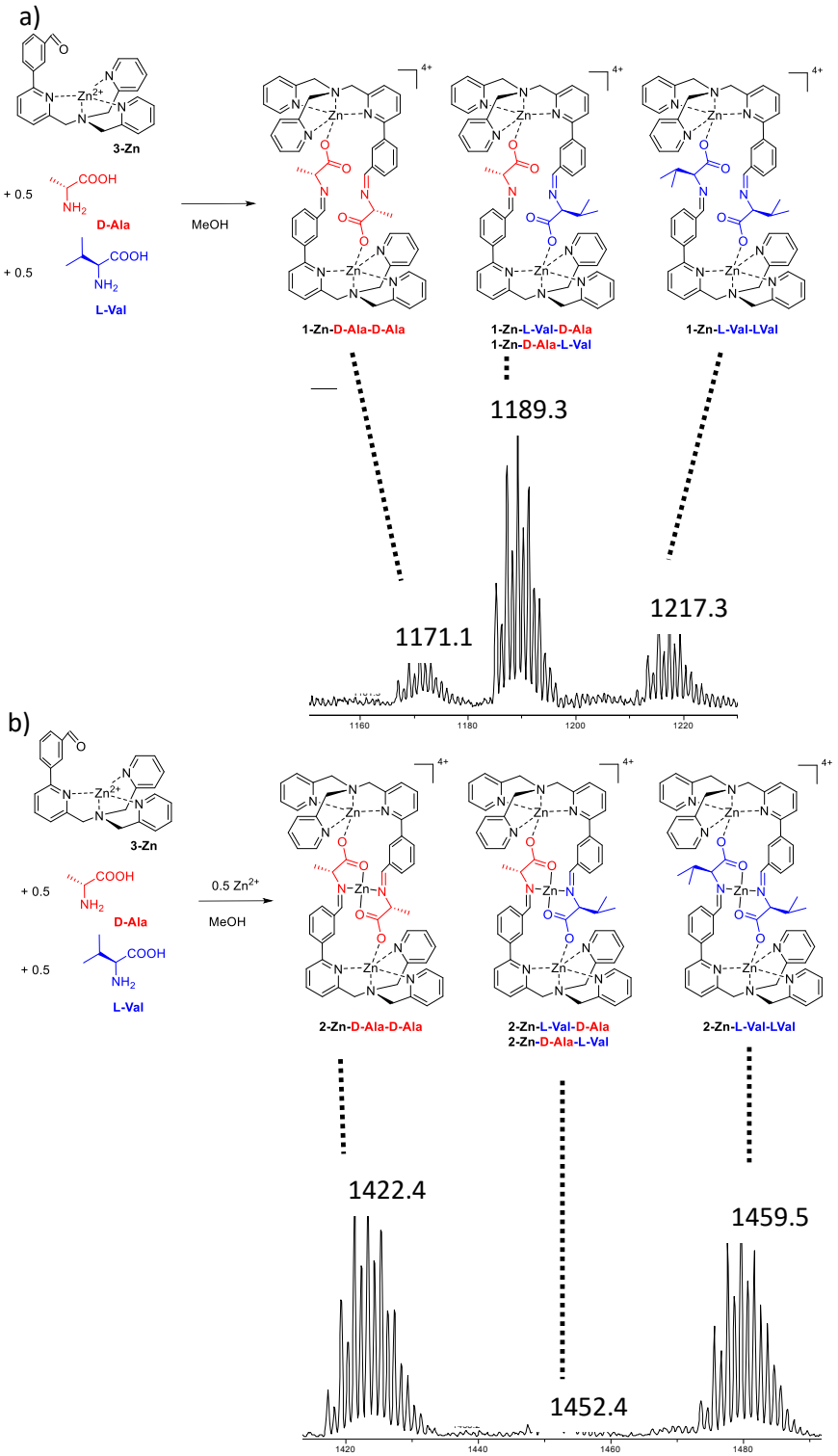

Figure 2.3. a) ESI-MS signals corresponding to a) **1-Zn-D-Ala-D-Ala**, **1-Zn-L-Val-D-Ala** and **1-Zn-D-Ala-L-Val**, **1-Zn-L-Val-L-Val**; b) **2-Zn-D-Ala-D-Ala**, **2-Zn-L-Val-D-Ala** and **2-Zn-D-Ala-L-Val**, **2-Zn-L-Val-L-Val.**

As observed by ESI-MS experiments (Figure 2.3b) the trinuclear species in the presence of a racemic mixture, was formed almost exclusively by the **2-Zn-D-Ala-D-Ala** and the **2-Zn-L-Val-L-Val**. In other words, the presence of the central metal drive toward the formation of the narcissistic structure.

Another proof of the narcissistic behavior of the trinuclear assembly came from the X-ray analysis of crystals grown up when a racemic mixture of **L/D-Phe** was used in the synthesis (Figure 2.4). The diffraction revealed a racemate which had in the same unit cell only the two enantiomeric homochiral narcissistic assemblies.

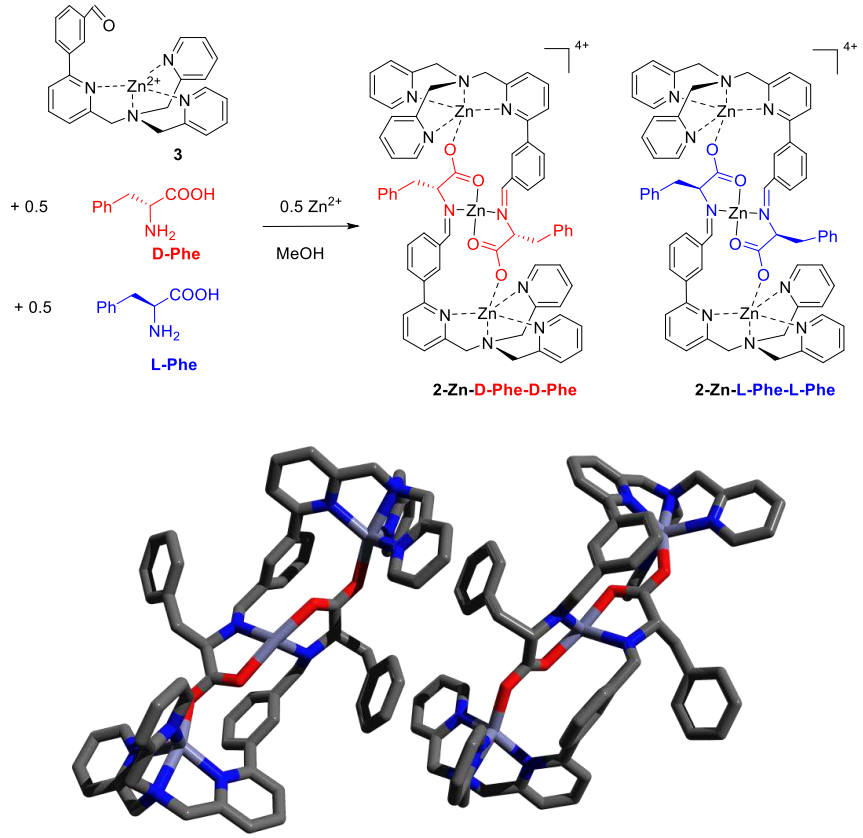

Figure 2.4. X-ray crystal structure of **2-Zn-Phe** starting from the racemic **Phe**. Both **2-Zn-DPhe-DPhe** and the **2-Zn-LPhe-LPhe** are present in the same unit cell.

2.3. Conclusions

In this chapter has been showed that in the novel molecular architectures, the combination of coordination chemistry and DCC results in a delicate and intricate system which can be finely biased by external stimuli of the thermodynamic equilibria. In detail, solvent, molecular sieves (either for removal of water or for the release of potassium), excess of components, temperature, and stereochemistry of the components, can have a profound impact in the outcome of a dynamic library. Even at a first sight this seems a very complicate system, the deep knowledge acquired in each of the process steps allows to drive the synthesis towards the desired products. In other words, it was not only possible to set-up an analytical method for the easy and fast detection of amino acid *e.e.*, but also, through the synthesis and characterization of the pure compounds involved in the dynamic process, to control the self-assembling towards the formation of the homochiral (DL-narcissistic) or heterochiral (meso anti-narcissistic) assembly.

2.4. Experimental Section

2.4.1 General Remarks

Chemicals were purchased from Aldrich, Fluka or Acros and used without further purification. IR spectra were recorded with a Perkin–Elmer FTIR 1650.^{1}H and ^{13}C NMR spectra (referenced to the solvent residual peak) were recorded at 301 K with Bruker AC-300 or 250 MHz instruments. ESI-MS experiments were carried out in positive mode with an Agilent Technologies LC/MSD Trap SL AGILENT instrument (mobile phase methanol). HRMS (ESI-TOF) analyses were performed with an Applied Biosystems ESI-TOF Mariner Biospectrometry Workstation (methanol as mobile phase with internal standards). MALDI-TOF analyses were carried out with an AB-SCIEX TOF-TOF 4800 instrument. Microanalyses were performed with a Flash 2000 Thermo Scientific Analyser. For new compounds, satisfactory determinations were obtained: C±0.3, H±0.27.

2.4.2 Synthesis of Acetal 4

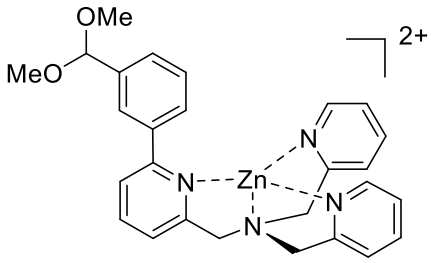

5.2 mg (0.008 mmol) of **complex 3-Zn** [5a] were solubilized in 0.8 mL of deuterated methanol. The solution was let stirring at 60°C for 4 hours to yield a pale yellow solution. ^{1}H NMR (300 MHz, CD_3OD): δ = 8.49 (d, 2H, H_{Ar}), 8.08 (m, 3H, H_{Ar}), 7.60 (m, 10H, H_{Ar}), 5.43 (s, 1H, CH), 4.54 (d, 2H, CH_2), 4.36 (d, 4H, CH_2), the methoxy groups were not detected because of the large excess of MeOD used as reaction solvent.^{13}C NMR (50 MHz, CD_3OD): δ = 155.17, 154.63, 147.65, 141.41, 140.77, 139.72, 138.96, 103.64, 59.13, 58.50, 52.89, 47.83.

2.4.3 Synthesis of Complex 5-Zn-L-Phe

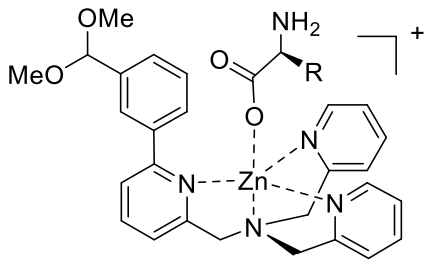

1.3 mg (0.008 mmol) of L-Phe were added to the **Acetal 4** solution in deuterated methanol. The suspension was then sonicated until complete solubilization of the amino acid. ^{1}H NMR (300 MHz, CD_3OD): δ = 8.51 (d, 1H, HAr), 8.31 (d, 1H, HAr), 8.08 (m, 3H, HAr), 7.58 (m, 10H, HAr), 7.30 (m, 7H, HAr) 5.30 (s, 1H, CH), 4.41 (m, 6H, CH_2), 3.46 (t, 1H, $CH_{L\text{-}Phe}$), 3.07 (dd, 1H, $CH_{2L\text{-}Phe}$), 2.90 (dd, 1H, $CH_{2L\text{-}Phe}$), as in the previous case the methoxy groups were not detected because of the deuterated solvent used. ^{13}C NMR (75.4 MHz, CD_3OD): δ =174.05, 157.72, 156.31, 150.41, 150.18, 142.70, 140.79, 140.47, 137.21, 130.59, 129.57, 128.65, 128.10, 127.09, 126.67, 126.18, 124.60, 105.32, 58.35, 57.98, 55.86, 37.68.

2.5. References

[1] (a) J. Bunzen, J. Iwasa, P. Bonakdarzadeh, E. Numata, K. Rissanen, S. Sato, M. Fujita *Angew Chem. Int. Ed.* **2012**, *51*, 3161–3163; (b) Y. Inokuma, S. Yoshioka, J. Ariyoshi, T. Arai, Y. Hitora, K. Takada, S. Matsunaga, K. Rissanen, M. Fujita *Nature* **2013**, *495*, 461-466; (c) D. A. Leigh, R. G. Pritchard, A. J. Stephens *Nature Chem.* **2014**, *6*, 978-982; (d) V. Marcos, A. J. Stephens, J. Jaramillo-Garcia, A. L. Nussbaumer, S. L. Woltering, A. Valero, J.-F. Lemonnier, I. J. Vitorica-Yrezabal, D. A. Leigh *Science* **2016**, *352*, 1555–1559; (e) K. S. Chichak, S. J. Cantrill, A. R. Pease, S.-H. Chiu, G. W. V. Cave, J. L. Atwood, J. F. Stoddart *Science* **2004**, *304*, 1308–1312; (f) J.-N. Rebilly, B. Colasson, O. Bistri, D. Over, O. Reinaud *Chem. Soc. Rev.* 2015, 44, 467-489. (g) Leenders, S. H. A. M.; Doria, R. G.; de Bruin, B.; Reek, J. N. H. Chem. Soc. Rev. 2015, 44, 433-448. (h) Durot, S.; Taesch, J.; Heitz, V. Chem. Rev. 2014, 114, 8542-8578. (i) Xie, T.-Z.; Endres, K. J.; Guo, Z.; Ludlow, J. M.; Moorefield, C. N.; Saunders, M. J.; Wesdemiotis, C.; Newkome, G. R. J. Am. Chem. Soc., 2016, 138, 12344-12347.

[2] (a) D. Leung, S. O. Kang, E. V. Anslyn, *Chem. Soc. Rev.* **2012**, *41*, 448-479. (b) G. Pescitelli, L. Di Bari, N. Berova, *Chem. Soc. Rev.* **2014**, *43*, 5211-5233. (c) N. Berova, L. Di Bari, G. Pescitelli, *Chem. Soc. Rev.* **2007**, *36*, 914–931. (d) C. Wolf, K. W. Bentley, *Chem. Soc. Rev.* **2013**, *42*, 5408-5424.

[3] (a) S. Hayashi, M. Yotsukura, M. Noji, T. Takanami, *Chem. Commun.* **2015**, *51*, 11068-11071. (b) P. Metola, E. V. Anslyn, T. D. James, S. D. Bull, *Chem. Sci.* **2012**, *3*, 156-161. (c) Z. A. De los Santos, C. Wolf, *J. Am. Chem. Soc.* **2016**, *138*, 13517-13520. (d) G. Bian, S. Yang, H. Huang, H. Zong, L. Song, H. Fan, X. Sun, *Chem. Sci.* **2016**, *7*, 932-938. (e) A. Akdeniz, T. Minami, S. Watanabe, M. Yokoyama, T. Ema, P. Anzenbacher Jr, *Chem. Sci.* **2016**, *7*, 2016-2022. (f) Z. A. De los Santos, R. Ding, C. Wolf, *Org. Biomol. Chem.* **2016**, *14*, 1934-1939.

[4] (a) N. Berova, G. Pescitelli, A. G. Petrovic, G. Proni, *Chem. Commun.* **2009**, 5958-5980. (b) M. Tanasova, M. Anyika, B. Borhan, *Angew. Chem. Int. Ed.* **2015**, 54, 4274-4278. (c) S. L. Pilicer, P. R. Bakhshi, K. W. Bentley, C. Wolf, *J. Am. Chem. Soc* **2017**, 139, 1758-1761. (d) Y. Zhou, Y. Ren, L. Zhang, L. You, Y. Yuan, E. V. Anslyn, *Tetrahedron* **2015**, 71, 3515-3527.

[5] N. A. Carmo dos Santos, F. Lorandi, E. Badetti, K. Wurst, A. A. Isse, A. Gennaro, G. Licini, C. Zonta, *Polymer* **2017**, *128*, 169-176.

[6] C. Bravin, E. Badetti, F. A. Scaramuzzo, G. Licini, C. Zonta *J. Am. Chem. Soc.* **2017**, *139*, 6456–6460.

[7] (a) F. A. Scaramuzzo, G. Licini, C. Zonta, *Chem. Eur. J.* **2013**, *19*, 16809–16813. (b) E. Badetti, K. Wurst, G. Licini, C. Zonta, *Chem. Eur. J.* **2016**, *22*, 6515–6518. (c) F. A. Scaramuzzo, E. Badetti, G. Licini, C. Zonta, *Eur. J. Org. Chem*. **2017**, *11*, 1438-1442.

[8] R. Berardozzi, E. Badetti, N. A. Carmo dos Santos, K. Wurst, G. Licini, G. Pescitelli, C. Zonta, L. Di Bari, *Chem. Commun.* **2016**, *52*, 8428-8431

[9] *A Stereodynamic Fluorescent Probe for Amino-Acids. Circular Dichroism and Circularly Polarised Luminescence Analysis.* N. A. Carmo dos Santos, E. Badetti, G. Licini, S. Abbate, G. Longhi, C. Zonta, *Chirality* **2017**, *In press*

[10] For other systems for *e.e*. detection of amino-acids see: (a) F. Biedermann, W. M. Nau, *Angew. Chem. Int. Ed.* **2014**, *53,* 5694–5699; *Angew. Chem.* **2014**, *126,* 5802–5807. (b) E. G. Shcherbakova, V. Brega, T. Minami, S. Sheykhi, T. D. James, P. Anzenbacher Jr, *Chem. Eur. J.* **2016**, *22*,10074–10080. (c) S. Shinoda, K. Terada, H. Tsukube, *Chem. Asian J.* **2012**, *7*, 400–405. (d) E. Faggi, C. Vicent, S. V. Luis, I. Alfonso, *Org. Biomol. Chem.* **2015**, *13*, 11721-11731. (d) K. W. Bentley, Y. G. Nam, J. M. Murphy, C. Wolf, *J. Am. Chem. Soc.* **2013**, *135*, 18052–18055. (e) N. Kameta, M. Masuda, T. Shimizu, *Chem. Commun.* **2015**, *51*, 11104-11107. (f) K. W. Bentley, P. Zhang, C. Wolf, *Sci. Adv.* **2016**, *2*, e1501162. (g) K. W. Bentley, C. Wolf, *J. Org. Chem.* **2014**, *79*, 6517–6531.

CHAPTER 3

Multimetallic Sensors

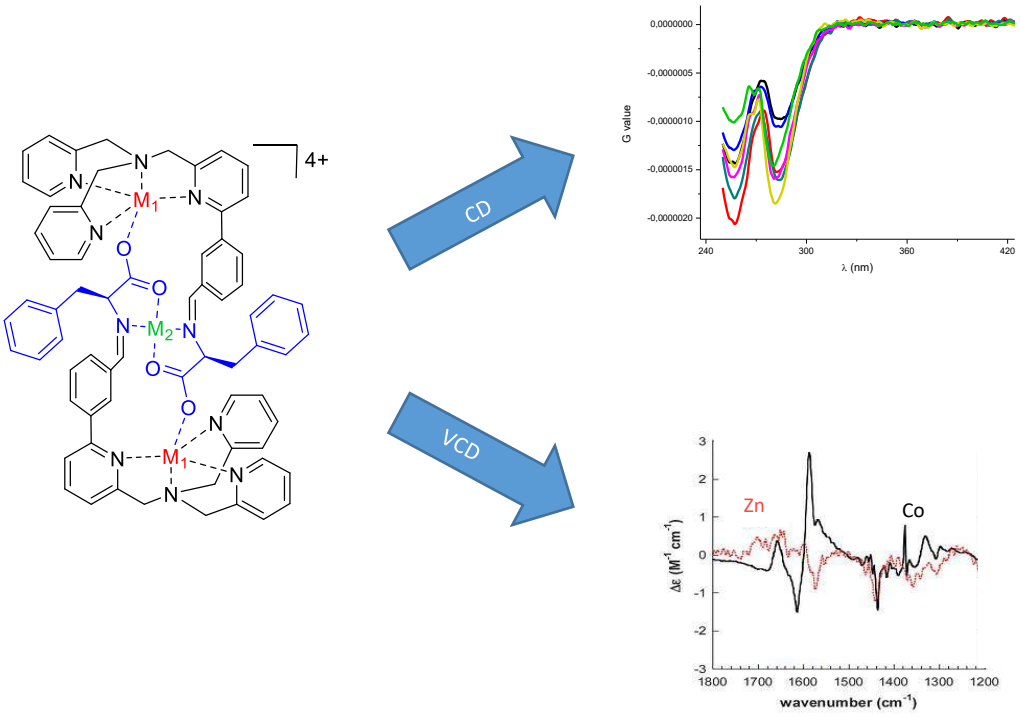

Novel molecular architectures were developed from the self-assembly of a modified tris(2-pyridylmethyl)amine ligand, metal ions, zinc(II), cobalt(II), nickel (II) or manganese (II) and amino acids. In total, seven different combination of metals were obtained and their chiroptical properties were studied. These systems have shown the capability to act effectively as stereo dynamic optical probes for the determination of the enantiomeric excess of free amino acids either using Electronic or Vibrational Circular Dichroism (CD and VCD). In particular, one compound presented giant VCD bands induced by Co(II). This peculiariaty gives the possibility to acquire VCD spectrum in a very short time, therefore overcoming the weak VCD signals limitations.

3.1. Introduction

Amino acids have an important role in organic reaction, pharmaceutical chemistry and biotechnological industry. They can be used as chiral building blocks in peptides and proteins on the development of new drugs.[1] With the development of high-throughput screening methods, that became an important allied to asymmetric synthesis, it is possible to study and evaluate different reaction conditions at the same time. However, the bottleneck in the analysis step continues to be a big drawback in the entire research process. Therefore, the interest on methods that can determine the enantiomeric excess (*e.e.*) in chiral compounds that are fast, robust, accurate, low-cost, and user-friendly continues to increase. [2]

Nowadays the determination of *e.e.* can be done by several different analytical techniques such as HPLC, GC, NMR spectroscopy, UV−vis, circular dichroism (CD), circularly polarized luminescence (CPL), and many others.[3] Unfortunately, not all techniques available are suitable for HTS, mainly because they are time consuming or not accurate enough. Nevertheless, the optical methods have a higher potential to satisfy the HTS needs for parallel analysis, but is limited by accuracy and sensibility.[2a]

The use of synthetic sensors to overcome these limitations and promote enantiodiscrimination have become common in this field, for example, the use of lanthanoid complexes in CPL probes or as NMR shift reagents is well known.[4] Berova[5] and Borhan[6] studied several metallo porphyrins systems in their host-guest interactions with chiral amines and/or chiral carboxylic acids to give high CD signals for absolute configurational assignments analysis. Canary published derivatization methods that use quinolinic tripodal ligand-based Cu(II) complexes in order to assign the absolute configuration of α-amino acids, β-amino alcohols and chiral amines.[7] Wolf's research involves the investigation of the stereodynamics of chiral compounds by the formation of adducts between the analyte and the designed probes either by covalent bond formation or non-covalent interactions.[8] Anslyn and coworkers have developed some methods for *e.e.* determination involving supramolecular interactions such as multicomponent assemblies and molecular recognition,[9] and most recently revealed a supramolecular polymeric system able to determine the enantiopurity of malic acid at high *e.e.* values with an accuracy similar to chromatographic methods.[10]

In the last decades, tris(2-pyridylmethyl)amines (TPMA) based metal complexes have been used as stereodynamic probes on the determination of *e.e.* in chiral chemical systems. TPMA based complexes show M and P helical chirality as a consequence of the wrapping of the ligand around the metal. While in solution an equilibrium between the two isoenergetic forms is present, in presence of a chiral guest, one preferential diasteroisomer is formed and when chromophores are presents chiroptical information can be acquired.[9b,11] Recently, in our research group, TPMA derivatives have been used as building blocks for the formation of supramolecular structures to determine *e.e.* in amino acids.[12] These optical sensors were based on the

dynamic covalent chemistry (DCC) of reversible covalent reaction to form imine bonds. DCC is a powerful tool in the supramolecular field, especially on the design of new molecular sensors. It allows the combination of the building blocks, through the reversible formation of covalent and non-covalent bonds, to yield the most thermodynamic stable products.[13]

Herein, a systematic study on the influence of different metal atoms in the trinuclear molecular structures reported in Chapter 2 is reported. More in detail, after the positive results obtained with the Zn (II) probes within the research group, [12] other metals that could produce a different effect in chiroptical techniques other than CD were considered. In particular, Vibrational Circular Dichroism (VCD), that can be used for the determination of absolute configuration (as explained in Chapter 1), was of high interest because certain transition metals such as Co (II) and Ni (II) enhance the VCD signal due to their specific orbital distribution. This property is believed to be strong enough to alleviate the major drawback of VCD, the weak response it usually gives, when compared with vibrational absorption.

3.2. Results and Discussion

3.2.1. Synthesis and Characterization

While as reported in the previous chapter we were able to form the trinuclear structure just adding an excess of the central metal, in order to understand how molecular properties of the systems were varying changing the metal, a new synthetic procedure was developed to insert a metal on the cleft formed by the amino acids. In order to form a multi-metallic structure a three steps synthesis was planned. Initially, the metallic complex **3-M_1**, that will be the extremity of the final architecture, is formed. This is a normal complexation reaction between the modified TPMA ligand and the desired metal (**M_1**) salt. The following step is the formation of the amino acid core by mixing 0.5 equivalent of a second metal (**M_2**) salt with 1 equivalent of the desired amino acid in methanol. The coordination between the metal and the amino acids is instantaneous to give the intermediate **6**. On the final step, 1 equivalent of complex **3-M_1** is added to the solution of **6** and the mixture is heated to 65 °C for 1h, it was observed that when using cobalt ion either as $Co(ClO_4)_2$ or complex 3-Co the solutions immediately changes colour to a characteristic green indicating the formation of the dimeric structure (Scheme 3.1), similar colour changes were not observed with the other metal ions. The mixture is left at room temperature furnishing the final product as a precipitate. This is recovered by the centrifugation of the reaction mixture and the residual solvent is removed under low pressure.

Since all metals used on this study have paramagnetic properties, except zinc, NMR analyses would be difficult to interpret for the determination of the structure. For this reason, in order to confirm the identity

and purity of the compounds ESI-MS, with the comparison of the isotopic patterns (Figure 3.2), and elemental analysis have been carried out.

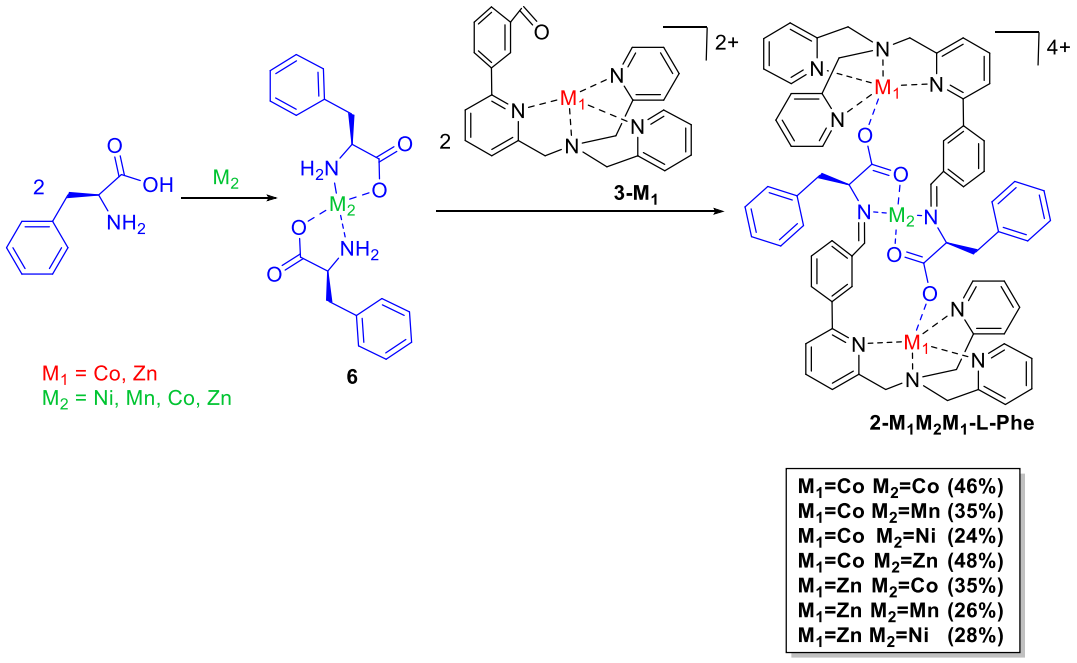

Scheme 3.1. Synthesis of the multimetallic structure. The counter anions are perchlorates.

As shown by the results obtained by ESI-MS, the initial formation of the amino acid complex core **6** is fundamental to avoid the scrambling of the metals within the metal coordination sites.

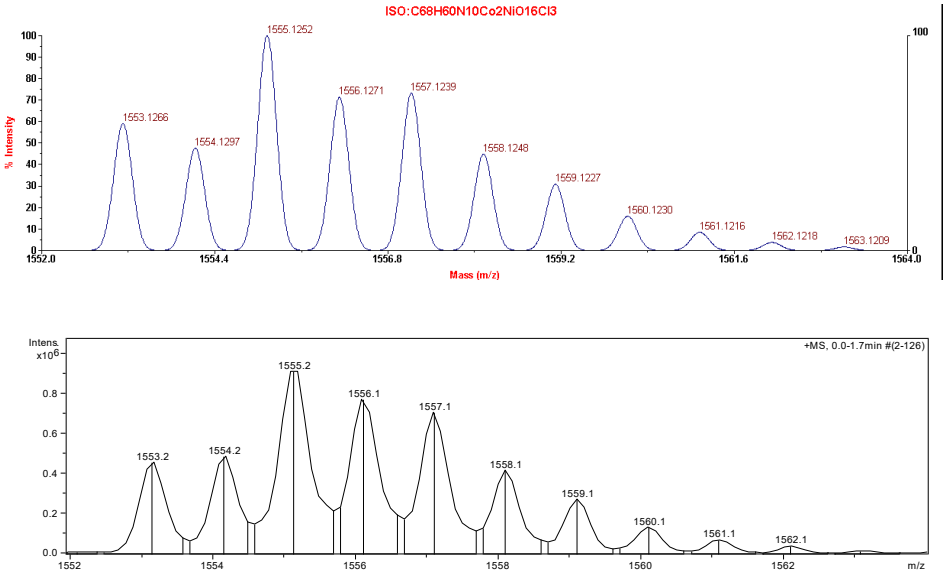

Figura3.2. ESI-MS Spectra of Compound **2-CoNiCo-L-Phe**, Calculated spectrum (top) Experimental spectrum (bottom)

Unlike the previous probes studied inside our research group, the multimetallic complexes **2-$M_1M_2M_1$-L-Phe** are formed without the presence of molecular sieves in the reaction mixture. Within the precipitated structures it has been possible to have crystals suitable for X-ray diffraction for the 2-Co-L-Phe system (Figure 3.3), the crystallographic study was done in collaboration with Prof. Klaus Wurst (University of Innsbruck). As expected the structures has three metal and an overall *C_2 symmetry*, with the two metal ions **M_1** (II) at the two ends of the complex in a trigonal bipyramidal geometry. The TPMA ligand adopts typical propeller-shape due to the orientation of the three pyridine rings. The structure of the coordination sphere around the metal atoms and in particular the helicity of the propeller motif is dictated by the stereochemistry of the amino acid. The geometry around the central metal atom **M_2** (II) is octahedral with two imine nitrogens, two carboxylates and two water molecules coordinated. In order to have the formation of a dimeric structure, the TPMA must adopt a trigonal bipyramidal geometry and this explains, while attempts to form this kind of structure with other metals like copper, that have a strong tendency to coordinate the ligand in an octahedral fashion, were unsuccessful.

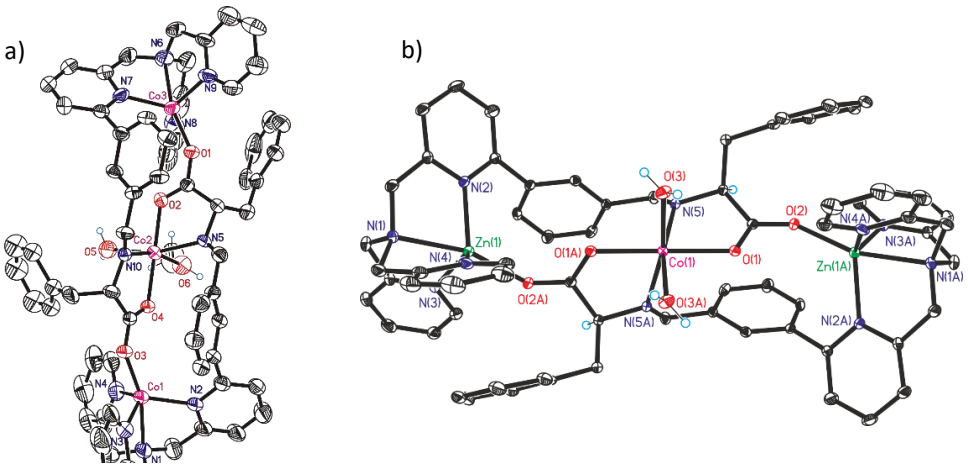

Figure 3.3. XRD structures of the trinuclear **2-Co-L-Phe** and **2-ZnCoZn-L-Phe** complexes

3.2.2. Optical studies

Our initial aim was to understand the effect that different metals can have on the chiroptical properties of this particular system. For this reason, CD measurements with the seven **2-$M_1M_2M_1$-L-Phe** complexes have been performed and we compared their g-value with the original ZnZnZn system. As it can be seen in Figure 3.4 the shape of the dichroic signal is similar for all the system. Two negative bands in the region before 300 nm are present for all the systems with some variation on the intensity. While it is difficult to find a clear cut correlation between the metal and the observed CD signal, compounds **2-CoM_2Co-L-Phe** shows in general a higher absorption intensity on the wavelength between 250 and 275nm. On the other hand, the compounds **2-ZnM_2Zn-L-Phe** shows a higher absorption intensity on the wavelength between 275 and 300nm. It should be noted that literature data on the UV absorption spectra of these metals in solution, only a few of the metal

solutions (Cu, Ni and Fe) have shown a characteristic absorbance on the studied region.[14] For these reasons, we can interpret the observed differences not in term of "special" effects of the metals, but to small differences in the final structure of the complexes which results in changed chromophores interactions. Indeed, in a previous study within the group theoretical calculations have shown that the CD absorbances are mainly associated to exciton coupling of the aromatic chromophores within the system. A phenomenon in which small variations in the geometry can have important effects in the final spectra.

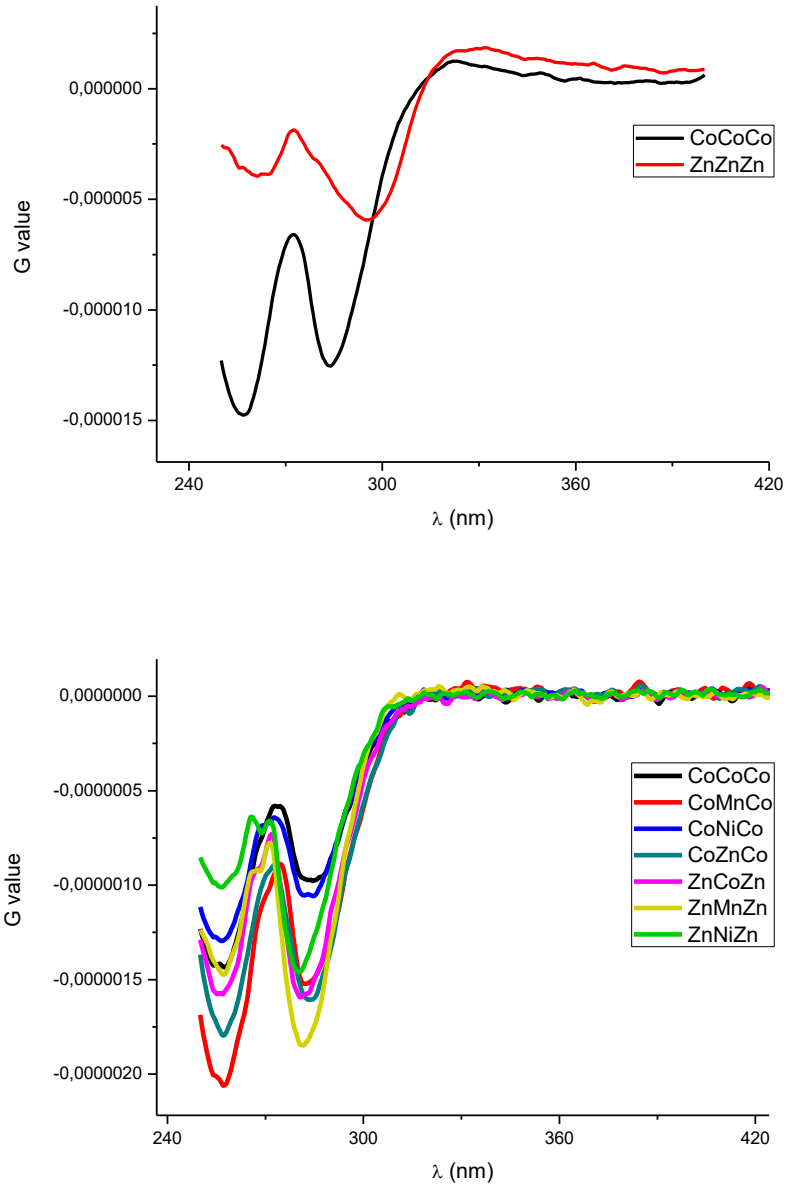

Figure 3.4. CD spectra of all **2-$M_1M_2M_1$-L-Phe** compounds

Within this studies, we had the possibility to study the chiroptical properties of some of **2-$M_1M_2M_1$-L-Phe** complexes with Vibrational CD technique in collaboration with the research group of Professor Lorenzo Di Bari (University of Pisa). Initially it was made a comparison between the previously published **2-Zn-L-Phe** and **2-Co-L-Phe** compounds (Figure 3.5). It was observed a massive contrast in the intensities of the VCD bands between monometallic Co(II) and Zn(II) complexes. The maximum intensity obtained for **2-Zn-L-Phe** was $\Delta\varepsilon$ = ±0.1 M^{-1} cm^{-1} after a considerable number of scans and a final analysis time of 1.5 hour, similar to the VCD spectra of several organic substances and most usual metal complexes. However, **2-Co-L-Phe** showed several absorption bands with $|\Delta\varepsilon|$ ten times higher than **2-Zn-L-Phe**, in the region between 1700 and 1500 cm^{-1} some signals reached two orders of magnitude stronger, including a maximum at around 1600 cm^{-1} with $\Delta\varepsilon$ = +3 M^{-1} cm^{-1}. Another considerable advantage of **2-Co-L-Phe** over **2-Zn-L-Phe** was the reduction of the measurement acquisition time to less than one minute even with a concentration 26.5 times lower.[15]

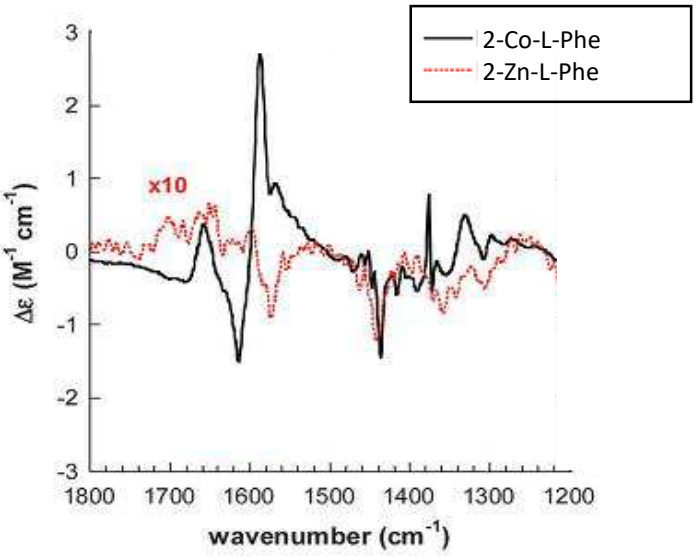

Figure 3.5. VCD spectra of compounds **2-Zn-L-Phe** and **2-Co-L-Phe.** Adapted from Ref. 15 with permission from The Royal Society of Chemistry

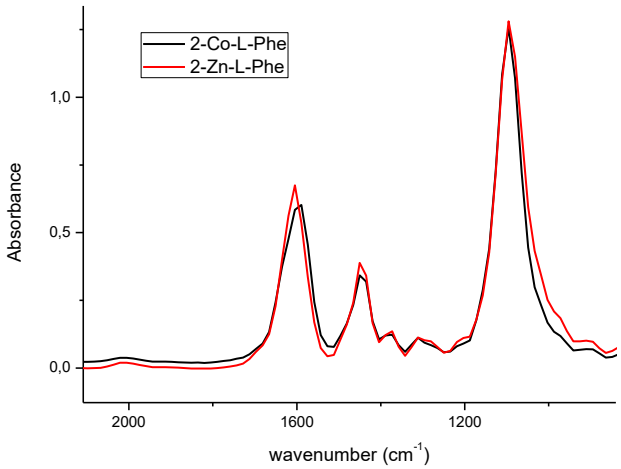

Figure 3.6 Absorption spectra of compounds **2-Zn-L-Phe** and **2-Co-L-Phe.**

In this case the observed differences between the confronted spectra are promoted by the metals present in the supramolecular architecture. It is well known in literature that the open-shell d^7 orbital system of Co (II) shows a low-lying d-d metal-centered electronic transitions that are not present on the closed-shell d^{10} orbital system of Zn (II). The enhancement of the VCD signal can be caused by these interferences between the metal-centered electronic state and the ligand-centered vibrational state, in other words, the presence of the open-shell transition metal amplifies the VCD signals of the functional groups on its surrounds because of the low-lying electronic exited state.[15]

3.3. Conclusions

In this chapter, it has been showed that it is possible to synthesize the dimeric trinuclear structure with combination of different metals with high reproducibility, as long as the structural requirements are respected, e.g. the trigonal pyramidal conformation of the complexes used to form the edge of the final chiroptical probe and the third metal that occupies the central position of the trimetallic architecture must present an octahedral coordination geometry. From the x-Ray diffraction measurements one can conclude that the compounds **2-$M_1M_2M_1$-L-Phe** have a similar conformation of the modified TPMA ligand in all structures independent from the metal present, therefore the position of the chromophore can be considered as almost constant thus the CD spectra show similar shapes. Complex **2-Co-L-Phe** exhibited a considerable enhancement of the VCD signal. This is beneficial, because allows fast measurements and it limits baseline variations successfully. The heterometallic compounds **2-CoZnCo-L-Phe** and **2-ZnCoZn-LPhe** were also studied, but the VCD absorption spectra did not showed a significant difference from the compound **2-Co-L-Phe**, leading to the preliminary conclusion that the amount of Co (II) ions in the structure has a low influence on the interferences between the metal-centered electronic state and the ligand-centered vibrational state.

3.4. Experimental Section

3.4.1. General Remarks

Chemicals were purchased from Aldrich, Fluka or Acros and used without further purification. ^{1}H and ^{13}C NMR spectra (referenced to the solvent residual peak) were recorded at 301 K with Bruker AC-300 or 250 MHz instruments. CD spectra were recorded with a Jasco J-715 or Jasco J-1500 instrument equipped with a Jasco MCB-100 circulation bath. ESI-MS experiments were carried out in positive mode with an Agilent Technologies LC/MSD Trap SL AGILENT instrument (mobile phase methanol). Microanalyses were performed with a Flash 2000 Thermo Scientific Analyser. For new compounds, satisfactory determinations were obtained: C±0.3, H±0.27.

3.4.2. Synthesis of 3-Co

0.300 g (0.761 mmol) of [6-(3-formylphenyl)-2-pyridylmethyl]bis(2-pyridylmethyl)-amine were dissolved in the minimum amount of anhydrous acetonitrile and 0.365 g (0.761 mmol) of $Co(ClO_4)_2*6H_2O$ were added. The solution was left at room temperature for 15 minutes and diethyl ether was added giving a light purple precipitate (0.364 g, 0.560 mmol, yield =73.6%) that was filtered and the residual solvent removed under reduced pressure. Caution! Perchlorate salts of metal complexes with organic ligands are potentially explosive. They should be handled in small quantity and with caution. IR (KBr, cm^{-1}): 3447, 1697, 1610, 1571, 1441, 1092. ESI+ MS(m/z): Calc. $C_{25}H_{22}N_4OCo$ 453.4, Found 226.5 ($M^{2+}/2$). Elem. $Anal._{Calc.}$ ($C_{25}H_{22}Cl_2N_4O_9Co$): C, 46.03; H, 3.40; N, 8.59. Found: C, 45.88; H, 3.21; N, 8.46. [12b]

3.4.3. Synthesis of 2-$M_1M_2M_1$-L-Phe

General Procedure: The amino acid L-Phe (0.033 mmol) was mixed with the desired perchlorate salt of the metal (M_2) (0.017 mmol) in 1 mL of anhydrous methanol. The mixture was heated and stirred at 60 °C for 10 minutes. To the resulting solution the desired tris-(pyridylmethyl)-amine metal complex (0.031 mmol) was added and the mixture stirred at 65 °C for 10 minutes. The solvent was slowly evaporated in a Dean Stark similar system to remove the formed water from the imination reaction. To the residue it was added 1 mL of anhydrous methanol. Leaving the resulting mixture 0.5 hour at room temperature results in the formation of a precipitate that is centrifuged and washed with dry methanol and diethyl ether.

2-Co-L-Phe (M_1=M_2= Co) Bright green (Yield 46 %). ESI-MS(m/z): Calc. $C_{68}H_{60}N_{10}O_4Co_3$. 3 ClO_4 1556.4, Found 1556.1 (M^+). Elemental analysis: Calc. $C_{68}H_{60}N_{10}O_{16}Co_3$. 4 $ClO_4 \cdot$ 5 H_2O: 46.78%, H = 4.04%, N = 8.02%, Found: C = 46.20%, H = 3.91%, N = 7.69%

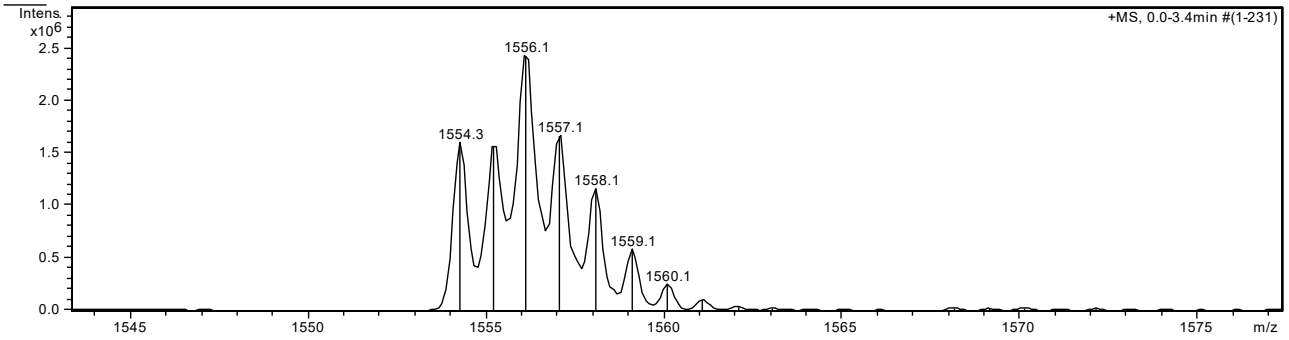

2-CoMnCo-L-Phe (M_1= Co M_2= Mn) Bright green (Yield 35 %). ESI-MS(m/z): Calc. $C_{68}H_{60}N_{10}O_4Co_2Mn$. 3 ClO_4 1552.4, Found 1552.2 (M^+).

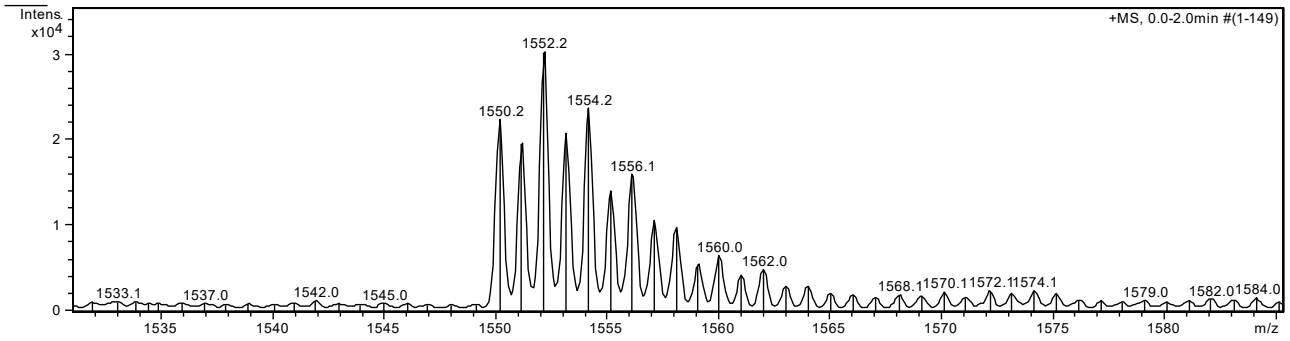

2-CoNiCo-L-Phe (M_1= Co M_2= Ni) Bright green (Yield 24 %). ESI-MS(m/z): Calc. $C_{68}H_{60}N_{10}O_4Co_2Mn$. 3 ClO_4 1555.1, Found 1555.4 (M^+).

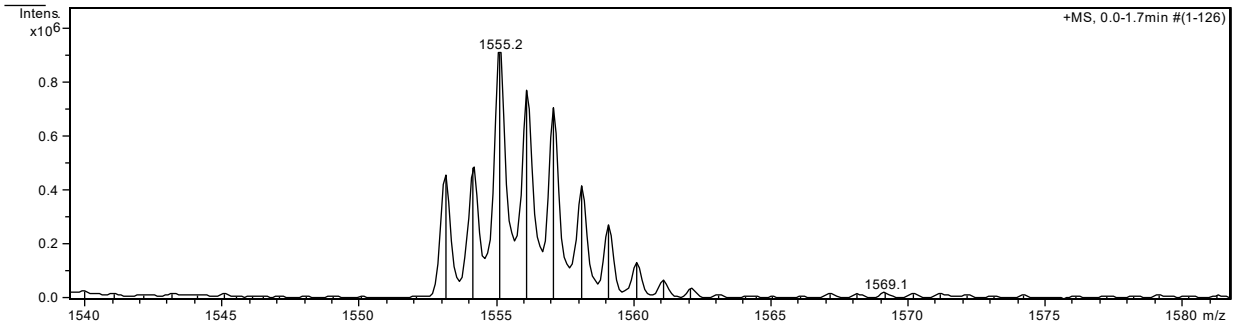

2-CoZnCo-L-Phe (M_1= Co M_2= Zn) Bright green (Yield 48 %). ESI-MS(m/z): Calc. $C_{68}H_{60}N_{10}O_4Co_2Mn$. 3 ClO_4 1559.1, Found 1556.5 (M^+).

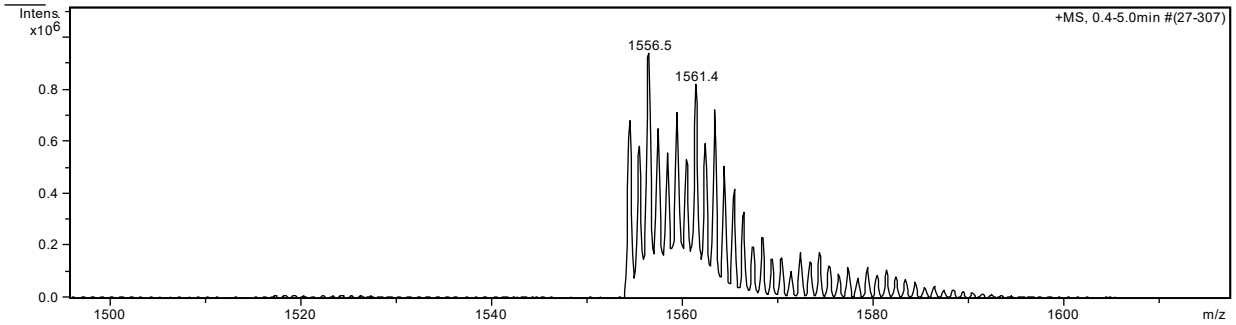

2-ZnCoZn-L-Phe (M_1= Zn M_2= Co) Light green (Yield 35 %). ESI-MS(m/z): Calc. $C_{68}H_{60}$ $N_{10}O_4$ Zn_2Co. 3 ClO_4 1566.4, Found 1568.5 (M^+).

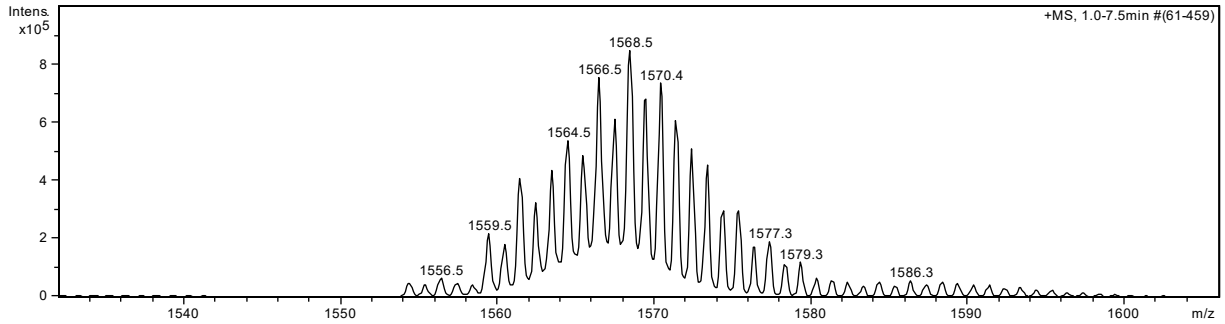

2-ZnMnZn-L-Phe (M_1= Zn M_2= Mn) Light gray (Yield 26 %). ESI-MS(m/z): Calc. $C_{68}H_{60}$ $N_{10}O_4$ Zn_2Mn. 3 ClO_4 1564.4, Found 1564.5 (M^+).

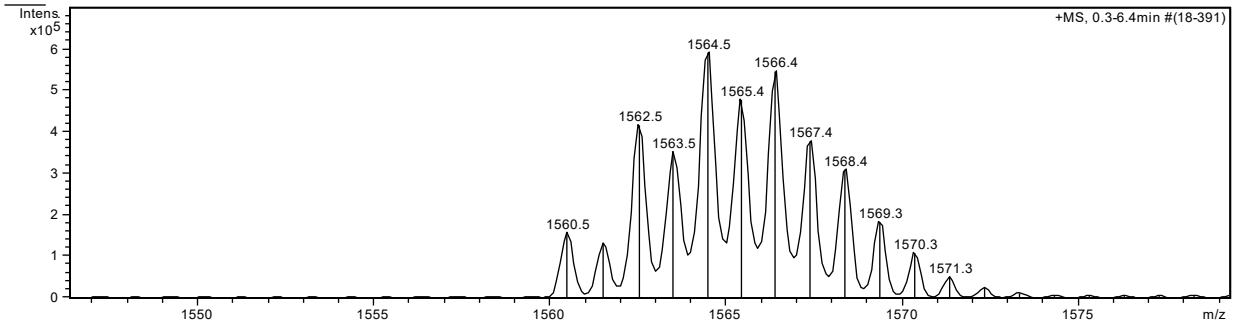

2-ZnNiZn-L-Phe (M_1= Zn M_2= Ni) Pale green (Yield 28 %). ESI-MS(m/z): Calc. $C_{68}H_{60}$ $N_{10}O_4$ Zn_2Ni. 3 ClO_4 1567.1, Found 1569.1 (M^+).

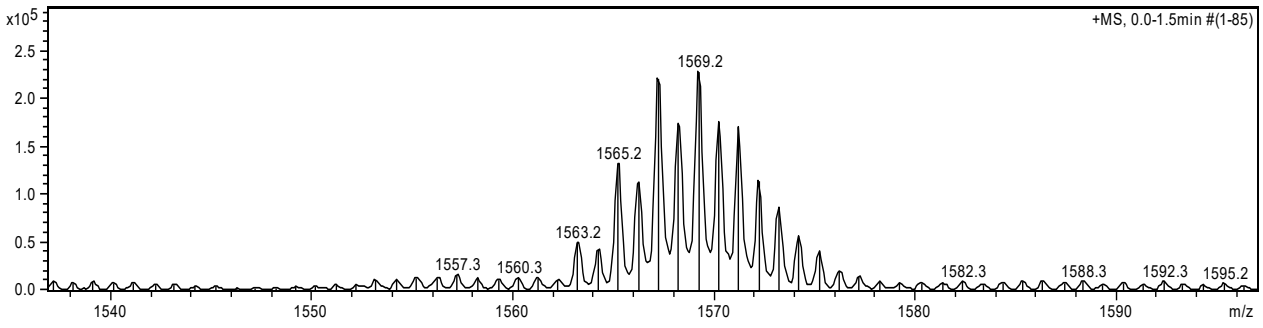

3.5. References

[1] S. M. King, S. L. Buchwald, *Org. Lett.* **2016**, *18*, 4128-4131.

[2] (a) H. H. Jo, C.-Y. Lin, E. V. Anslyn, *Acc. Chem. Res* **2014**, *47*, 2212-2221; (b) S. H. Shabbir, C. J. Regan, E. V. Anslyn, *Proc. Natl. Acad. Sci. U.S.A.* **2009**, *106*, 10487-10492.

[3] E. G. Shcherbakova, V. Brega, T. Minami, S. Sheykhi, T. D. James, P. Anzenbacher, *Chem. Eur. J.* **2016**, *22*, 10074-10080.

[4] (a) T. J. Wenzel, J. D. Wilcox, *Chirality* **2003**, *15*, 256-270; (b) F. Zinna, L. Di Bari, *Chirality* **2015**, *27*, 1-13; (c) G. Muller, *Dalton Trans.* **2009**, 9692-9707.

[5] (a) N. Berova, G. Pescitelli, A. G. Petrovic, G. Proni, *Chem. Commun.* **2009**, 5958-5980; (b) X. Huang, N. Fujioka, G. Pescitelli, F. E. Koehn, R. T. Williamson, K. Nakanishi, N. Berova, *J. Am. Chem. Soc* **2002**, *124*, 10320-10335; (c) S. Matile, N. Berova, K. Nakanishi, S. Novkova, I. Philipova, B. Blagoev, *J. Am. Chem. Soc* **1995**, *117*, 7021-7022; (d) G. Proni, G. Pescitelli, X. Huang, K. Nakanishi, N. Berova, *J. Am. Chem. Soc* **2003**, *125*, 12914-12927.

[6] (a) H. Gholami, M. Anyika, J. Zhang, C. Vasileiou, B. Borhan, *Chem. Eur. J.* **2016**, *22*, 9235-9239; (b) M. Anyika, H. Gholami, K. D. Ashtekar, R. Acho, B. Borhan, *J. Am. Chem. Soc* **2014**, *136*, 550-553; (c) X. Li, C. E. Burrell, R. J. Staples, B. Borhan, *J. Am. Chem. Soc* **2012**, *134*, 9026-9029; (d) M. Tanasova, M. Anyika, B. Borhan, *Angew. Chem. Int. Ed.* **2015**, *54*, 4274-4278.

[7] (a) S. Zahn, J. W. Canary, *Org. Lett.* **1999**, *1*, 861-864; (b) J. Zhang, A. E. Holmes, A. Sharma, N. R. Brooks, R. S. Rarig, J. Zubieta, J. W. Canary, *Chirality* **2003**, *15*, 180-189.

[8] (a) K. W. Bentley, Y. G. Nam, J. M. Murphy, C. Wolf, *J. Am. Chem. Soc* **2013**, *135*, 18052-18055; (b) K. W. Bentley, D. Proano, C. Wolf, **2016**, *7*, 12539; (c) Z. A. De los Santos, C. Wolf, *J. Am. Chem. Soc* **2016**, *138*, 13517-13520; (d) S. L. Pilicer, P. R. Bakhshi, K. W. Bentley, C. Wolf, *J. Am. Chem. Soc* **2017**, *139*, 1758-1761.

[9] (a) J. M. Dragna, A. M. Gade, L. Tran, V. M. Lynch, E. V. Anslyn, *Chirality* **2015**, *27*, 294-298; (b) L. A. Joyce, M. S. Maynor, J. M. Dragna, G. M. da Cruz, V. M. Lynch, J. W. Canary, E. V. Anslyn, *J. Am. Chem. Soc* **2011**, *133*, 13746-13752; (c) L. You, J. S. Berman, A. Lucksanawichien, E. V. Anslyn, *J. Am. Chem. Soc* **2012**, *134*, 7126-7134.

[10] X.-X. Chen, Y.-B. Jiang, E. V. Anslyn, *Chem. Commun.* **2016**, *52*, 12669-12671.

[11] (a) L. You, G. Pescitelli, E. V. Anslyn, L. Di Bari, *J. Am. Chem. Soc* **2012**, *134*, 7117-7125; (b) Y. Zhou, Y. Ren, L. Zhang, L. You, Y. Yuan, E. V. Anslyn, *Tetrahedron* **2015**, *71*, 3515-3521; (c) L. You, S. R. Long, V. M. Lynch, E. V. Anslyn, *Chem. Eur. J.* **2011**, *17*, 11017-11023.

[12] (a) E. Badetti, K. Wurst, G. Licini, C. Zonta, *Chem. Eur. J.* **2016**, *22*, 6515-6518; (b) F. A. Scaramuzzo, E. Badetti, G. Licini, C. Zonta, *European Journal of Organic Chemistry* **2017**, *2017*, 1438-1442; (c) F. A. Scaramuzzo, G. Licini, C. Zonta, *Chem. Eur. J.* **2013**, *19*, 16809-16813.

[13] (a) Y. Zhou, H. Ye, L. You, *JOC* **2015**, *80*, 2627-2633; (b) P. T. Corbett, J. Leclaire, L. Vial, K. R. West, J.-L. Wietor, J. K. M. Sanders, S. Otto, *Chem. Rev.* **2006**, *106*, 3652-3711; (c) J. Li, P. Nowak, S. Otto, *J. Am. Chem. Soc* **2013**, *135*, 9222-9239; (d) A. G. Orrillo, A. M. Escalante, R. L. E. Furlan, *Chem. Eur. J.* **2016**, *22*, 6746-6749.

[14] R. P. Buck, S. Singhadeja, L. B. Rogers, *Analytical Chemistry* **1954**, *26*, 1240-1242.

[15] R. Berardozzi, E. Badetti, N. A. Carmo dos Santos, K. Wurst, G. Licini, G. Pescitelli, C. Zonta, L. Di Bari, *Chem. Commun.* **2016**, *52*, 8428-8431.

CHAPTER 4

A Stereodynamic Fluorescent Probe for Amino-Acids. Circular Dichroism and Circularly Polarised Luminescence Analysis

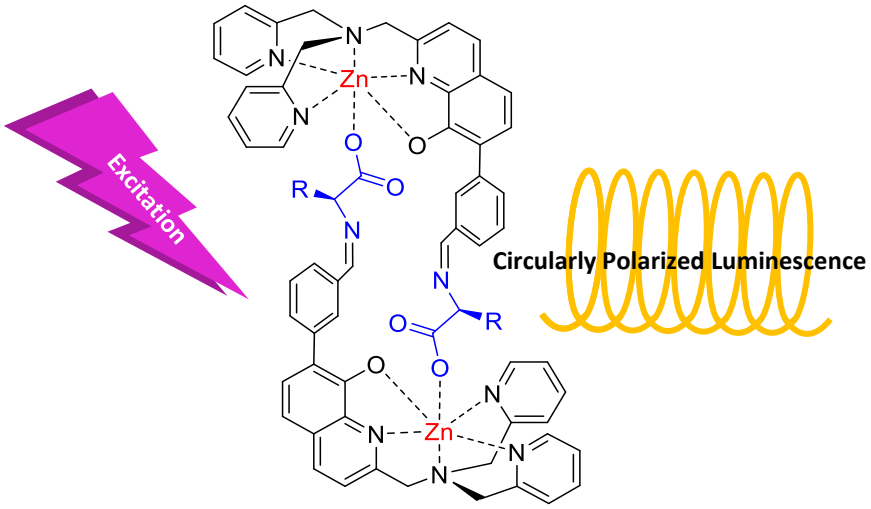

The use of stereodynamic probes is becoming one of the leading strategies for the fast and effective determination of enantiomeric excess. In the previous chapter, it was reported a series of novel molecular architectures based on a modified tris(2-pyridylmethyl)amine complex (TPMA) which are able to amplify the electronic CD, in the case of Zn(II) assemblies and vibrational CD, in the case of Co(II) assemblies. In this chapter, it is reported a structural modification of the ligand with the purpose to obtain a fluorescent chiral probe. The study deals with the synthesis of the novel ligand, the formation of the self-assembly system with amino acids and the study of the electronic CD and Circular Polarized Luminescence. The study reported herein was done in collaboration with the research group of Prof. Abbate and Prof Longhi from the University of Brescia, this Chapter was published with small modifications from N. A. Carmo dos Santos, E. Badetti, G. Licini, S. Abbate, G. Longhi, C. Zonta. *Chirality*, **2017**, 1-9. htpps://doi.org/10.1002/22780

4.1 Introduction

In the last few decades, several research groups have been studying chiral sensors due to the important applications that chiral molecules have in several fields of science, ranging from catalysis to materials. Under this respect, special attention has been paid to searching new methods and techniques for the determination of enantiomeric excess (*e.e.*), that are faster and cheaper than traditional chromatographic methods.[1] In this context, several supramolecular architectures have been developed in order to gather an optical signal that can be easily measured through the most common spectroscopic techniques, *i.e.* circular dichroism (CD).[2] Usually, these supramolecular sensors possess at least one labile stereogenic element which interconverts between two enantiomeric forms. The addition of a chiral analyte leads preferentially to the formation of one diasteroisomer which furnishes back the optical chiral information. Within these stereodynamic probes, tris(2-pyridylmethyl)amine (TPMA) based metal complexes have shown to be versatile chemical systems for the determination of *e.e.*[3] This ligand assumes a propeller-like arrangement around the metal center that in solution is in equilibrium between the two helical configurations (clockwise and anti-clockwise). In the presence of a suitable analyte, one configuration is preferred and the resulting diasteroisomer is able to provide a chiroptical signal.[4]

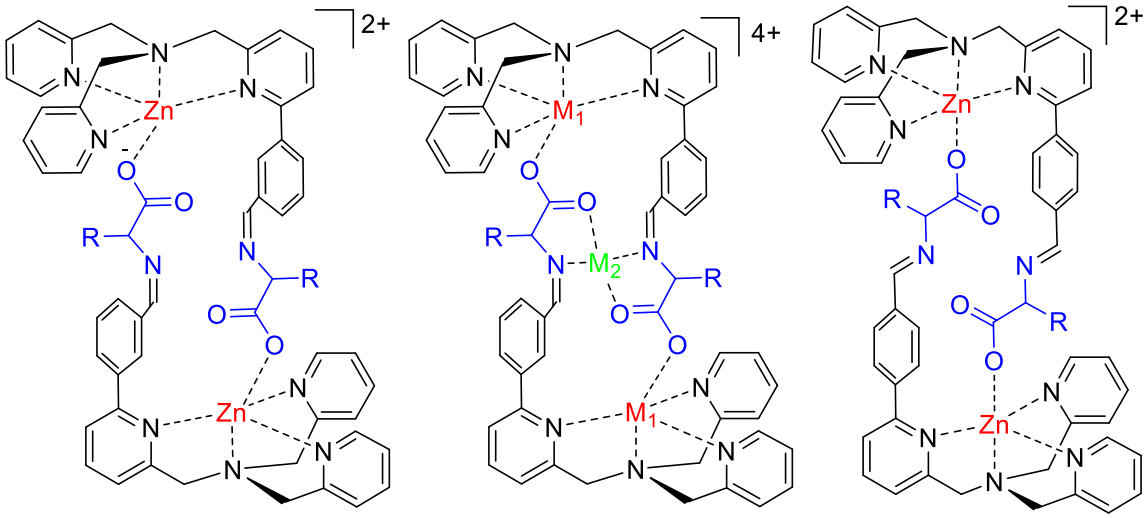

Scheme 4.1 TPMA based self-assembled architectures **1-Zn-aa**, **2-Zn-aa**, **2-Co-aa** and **7-Zn-aa** used for the determination of *e.e.* of amino acids (aa). In all of the structures anions are perchlorates.

Recently, we have started to combine the TPMA scaffold with dynamic covalent chemistry (DCC) of imines formation.[5] DCC[6] has already shown its fundamental role in the formation of new complex nano-architectures (Scheme 4.1). These systems have shown to perform as probes for amino acids,[7] furnishing

dichroic signals characteristic of the amino acidic side chain and proportional to the enantiomeric excess. While all systems are effective using electronic CD, the presence of cobalt(II) in **2-Co-aa**, induces additionally giant vibrational CD bands, allowing the measurement of a VCD spectrum in only a few seconds and/or minutes.

In this Chapter, it is reported a novel version of the TPMA based probe which has been designed to work as stereodynamic probe using circularly polarized luminescence (CPL). CPL is a relatively mature technique,[8] which has though recently met new success due to experimental and theoretical advancement.[9] CPL is finding numerous applications in material science[9,10] and in biochemistry.[10b] Within this context it is worth mentioning that CPL of specially prepared pyrene systems has also been used to monitor peptide systems.[10c,11] CPL probes geometry and electronic properties of the first excited state, which may be characteristically dependent on interactions not only with guest molecules,[10b,c,11] but also on concentration and solvent.[12]

4.2 Results and Discussion

4.2.1. Synthesis of the Fluorescent Ligand

In order to build a fluorescent version of the probes reported previously on chapter 2 and 3, we decide to introduce in one of the ligand arms a quinolinic moiety. The quinoline system is known to be fluorescent in basic conditions.[13] The synthesis of both the modified TPMA Zn(II) complex **13** and of the molecular probe **14-Zn-aa,** follows a procedure similar to those already described (Scheme 4.2). In detail, bromination of the commercially available 2-methyl-8-quinolinol *via* reaction with *N*-bromosuccinimide (NBS) in toluene and *t*-butylamine, gives 7-bromo-2-methylquinolin-8-ol **8**. This intermediate was oxidized with SeO_2 in dioxane, giving 7-bromo-8-hydroxyquinoline-2-carbaldehyde **9**. The subsequent step was the protection of the OH group with chloromethyl methyl ether (MOMCl). Ligand **12** was then obtained by reductive amination with di(2-picolyl)amine followed by a Suzuki coupling with 3-formylphenylboronic acid to add the aldehyde motif. Ligand **12** was solubilized in anhydrous acetonitrile to give a pale-yellow solution, and one equivalent of zinc perchlorate was added. After the addition of the metal salt, the solution acquires a darker shade of yellow and it was observed a fluorescence with the given excitation at 395 nm. The zinc complex was then precipitated with anhydrous diethyl ether to yield a yellow solid.

The supramolecular architecture **14-Zn-aa** was obtained by a reaction between complex **13** and the desired amino acid (**aa** = L-Ile, L-Phe, L-Trp) in anhydrous DMSO at 70 °C in presence of molecular sieves (Scheme 4.3). These three amino acids have been chosen in order to have one aliphatic, one aromatic and one fluorescent lateral chain residue. The formation of the product was confirmed by ^{1}H NMR analysis, indicating the imine

bond formation by the disappearance of the formyl proton at 10 ppm region after one hour. Further confirmations arise from ^{1}H-DOSY NMR which reveals the formation of a species with an experimental hydrodynamic radius of 9.1 Å (B3LYP/6-31G(d,p) calculated radius for **14-Zn-L-Phe** is 9.3 Å).[14]

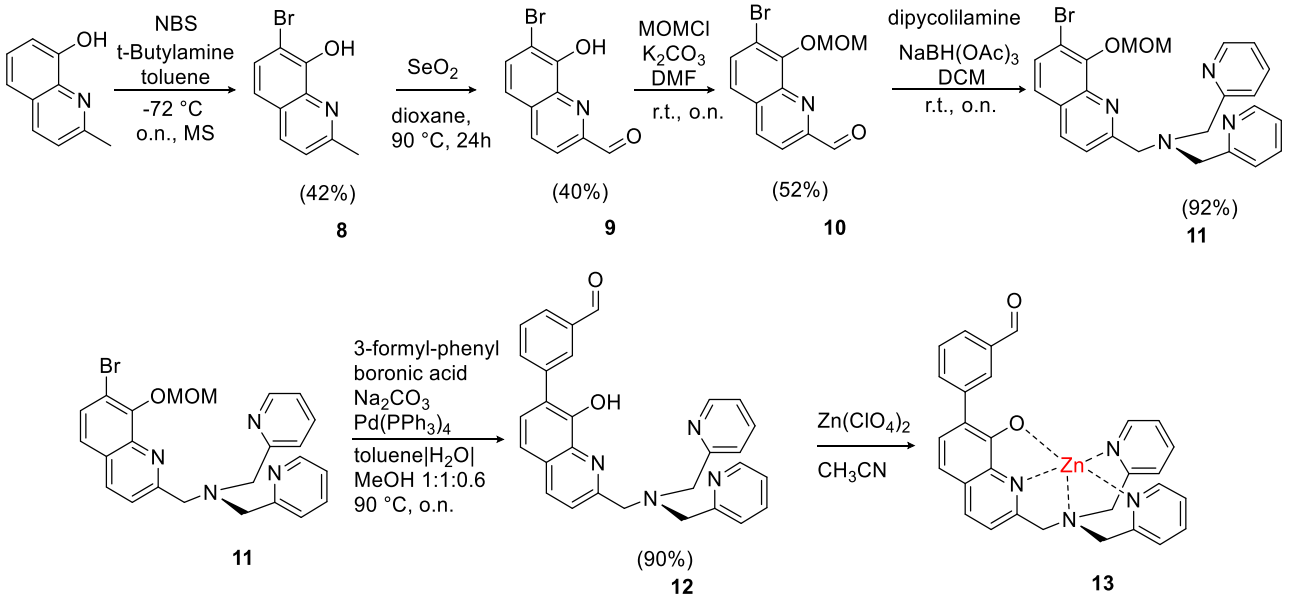

Scheme 4.2 Synthesis of the quinolinic complex **13**.

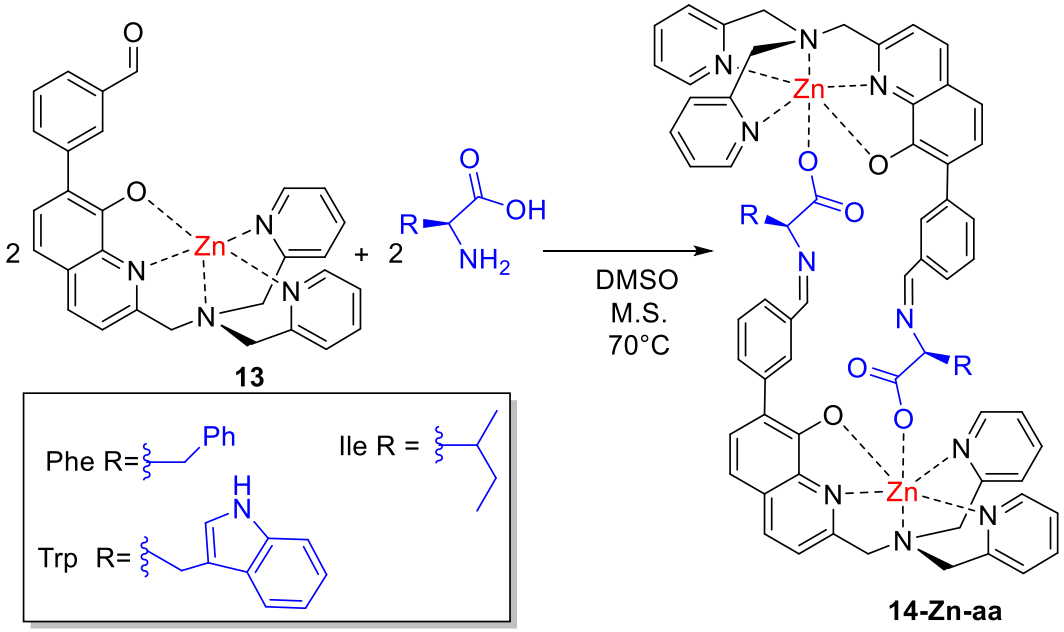

Scheme 4.3 Synthesis of the supramolecular optical active dinuclear zinc complex **14-Zn-aa**.

4.2.2. Optical Analysis

4.2.2.1 CD Measurements

The chiroptical properties of the new fluorescent probe were initially checked via CD. For the investigated supramolecular architectures **14-Zn-aa**, it was obtained a CD spectrum (Figure 4.1a) that is characteristic for each amino acid employed. This feature was already observed for the previously studied probes.[5a,d] In particular, the similarity of the CD spectra with the previously reported systems suggested that the origin of the signal is ascribable to the exciton coupling between the two chromophores, the quinoline and the phenyl group. Moreover, the natural L-amino-acids exhibit a negative sign in this region as in the previous probes.[5a,b,d] In Figure 4.1b the portion of the CD spectra in the 550-305 nm range for the systems **14-Zn-aa** (aa=L-Ile, L-Phe, L-Trp) have been reported and magnified. In all cases, there is a positive band at 375 nm and a negative large band at 420 nm. The dissymmetry factor $g_{abs} = \Delta\varepsilon/\varepsilon$ is quite low, about $2x10^{-4}$.

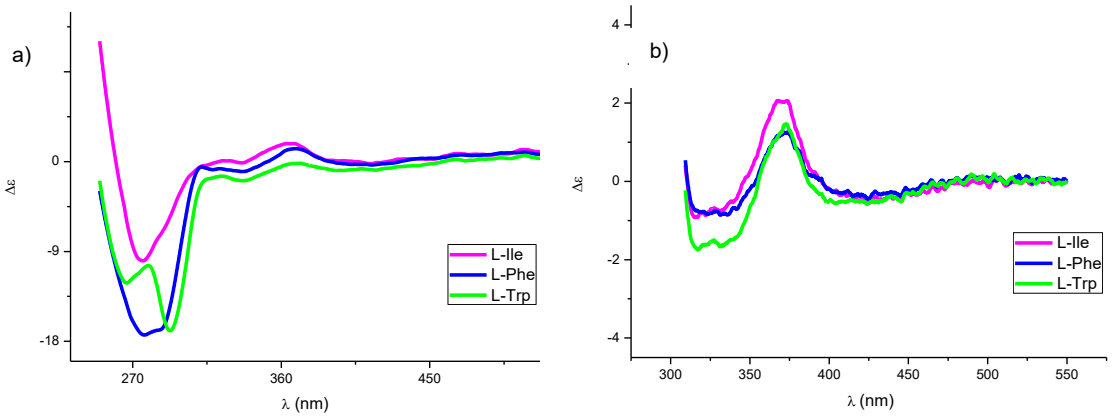

Figure 4.1 a) CD spectra of **14-Zn-aa** (aa = L-Ile, L-Phe, L-Trp). b) CD spectra of the molecular sensor zoomed between 305 and 550 nm.

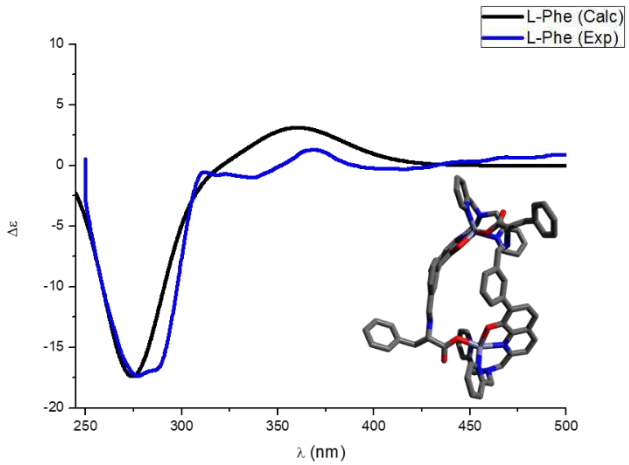

Figure 4.2 Comparison between the experimental (blue line) and calculated (black line) CD spectra for **14-Zn-Phe** (Gaussian exponential bandwidth,0.16 eV; wavelength shift, +70 nm) and inset of the structure.[54]

To further confirm the dimeric nature of the structure, a comparison between experimental and calculated CD spectra was carried out.[14a,15] Theoretical calculations with time-dependent DFT (TD-DFT) were conducted in DMSO (PCM) at the B3LYP/6-31G(d,p). The calculations have been performed on **14-Zn-L-Phe** starting from a geometry similar to reported crystal structure of **2-Zn-L-Phe**. It can be seen that the CD spectra is well reproduced confirming the dimeric nature of the structure.

4.2.2.2 Fluorescence Measurements

The emission spectra for all compounds (Figure 4.3) were obtained in the wavelength region between 300 and 850 nm, with the given excitation at 285 nm. All **14-Zn-aa** complex solutions in DMSO presented a dark yellow color. The fluorescence λ_{max} was observed in 560-600 nm region. The intrinsic tryptophan fluorescence λ_{max} was also detected, showing a shift from the values reported in the literature that are below 330 nm in apolar solvents and further than 330 nm in the presence of polar solvents.[16] Since the imination reaction between the aldehyde moiety of the probe and the amino acid forms water, the observed shift is explained.

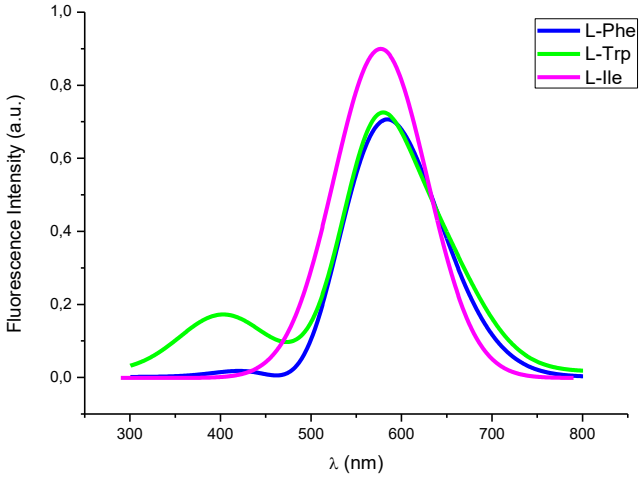

Figure 4.3 Fluorescence spectra of **14-Zn-aa** (aa = L-Ile, L-Phe, L-Trp).

4.2.2.3 CPL Measurements

In Figure 4.3 the CPL spectra are reported for all **14-Zn-aa** (**aa** = L-Ile, L-Phe, L-Trp) compounds. Measurements were calibrated with the procedure already described in literature.[9b] The sign of CPL resulted always negative and the CPL band was similar in the three cases. The g_{lum} value at the CPL maxima (maximum g_{lum} value is readable directly from Fig. 4.4, since the corresponding fluorescence spectra (not shown) were normalized) was about $-2x10^{-3}$ and it was larger (in absolute value) than the absorption dissymmetry ratio g_{abs}, either considering the positive g_{abs} value for the CD band at 370 nm or the negative one at about 420

nm. The electronic transition that gives origin to the CPL activity should be similar to the one responsible of the absorption, so it should be correlated with the negative CD band. Possible vibronic effects may contribute to the intensity and the shape of CD and CPL bands. [17] Despite the high noise level, one can see that the CPL band shape and bandwidth for the L-Phe case are slightly different from the other two cases. However, it should be noted that the intensity of the signal and the time required for the acquisition of these spectra make this approach less practical than CD.

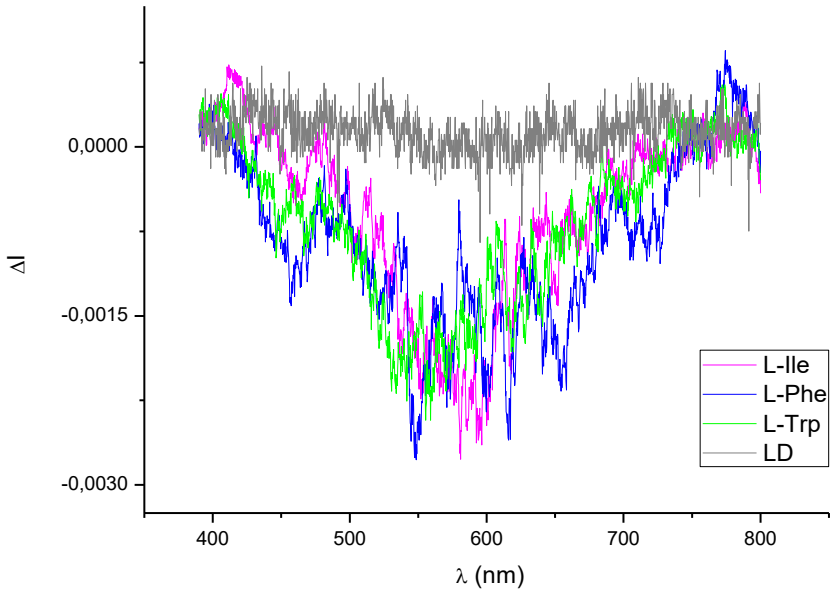

Figure 4.4 CPL spectra of **14-Zn-aa** (aa = L-Ile, L-Phe, L-Trp). Excitation wavelength 365nm. Linear dichroism components can be considered absent: as an example the analysis of the linear dichroism component of the emitted light by **14-Zn-L-Phe** is reported (gray trace labelled LD).

4.3 Conclusion

A novel ligand exhibiting fluorescence properties has been synthesized with the aim to exploit its capability to become an optical probe for the determination of enantiomeric excess, using either CD and/or CPL techniques. As per similar probes previously reported by the research group,[5] the CD spectrum shows sensitivity to the chosen amino acid at 270 nm, while at 400 nm it shows small variations and very low signal. Something similar had been observed in the case of simple carbo-helicenes[17c], namely CD was nearly forbidden bands and CPL was difficult to detect. In this case the observed CPL activity for **14-Zn-aa** systems has a dissymmetry factor that is not very low, but fluorescence is quite weak. Since CPL is associated to the CD features in longest wavelength region, CPL negative response correlates with negative weak CD. Moreover, the observed CPL is quite similar for all examined systems, within the limits of our detection; vibronic contributions may be different but they are hidden by the noise. Studies are under way to enhance luminescence and CPL and CD activities of long wavelength transitions, in the same way as done for helicens

4.4 Experimental Section

4.4.1. General Remarks

Chemicals were purchased from Aldrich, Fluka or Acros and used without further purification. CD spectra were recorded with a Jasco J-715 instrument. IR spectra were recorded with a Perkin–Elmer FTIR 1650. ^{1}H and ^{13}C NMR spectra (referenced to the solvent residual peak) were recorded at 301 K with Bruker AC-300 or 250 MHz instruments. ESI-MS experiments were carried out in positive mode with an Agilent Technologies LC/MSD Trap SL AGILENT instrument (mobile phase methanol).

4.4.2. General Procedure for CD and Fluorescence Measurements

For both CD and Fluorescence measurements, suitable dilutions were performed, to obtain a final concentration of the analyte in the cuvette equal to 1 x 10^{-4} M (**14-Zn-aa** of the desired amino acid) in anhydrous DMSO. All the CD and fluorescence spectra were taken using a 10 mm UV-quartz cell at room temperature. The CD spectra were measured in millidegrees, normalized for the concentration of the dimeric compound and are reported as $\Delta\varepsilon$. The fluorescence spectra were reported in fluorescence intensity (a.u.) and λ (nm).

4.4.3. General Procedure for CPL Measurements

CPL spectra were taken on a home-built apparatus described previously in literature,[18] with exciting radiation brought to the sample from a commercial fluorimeter Jasco FP8200 through a water-filled optical fiber. Solutions were contained in a 2 mm x 10 mm fluorescence cuvette, with a 90° collection geometry. Five scans were taken for each sample. Excitation bandwidth was 20 nm, emission bandpass 10 nm, scan velocity 30 nm/min. In all cases, excitation was at 365 nm, in correspondence of the major CD and absorption peak at longest wavelength.

4.4.4. Synthesis of The Ligand

4.4.4.1 Synthesis of 7-bromo-8-hydroxyquinoline-2-carbaldehyde (9)

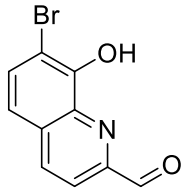

10.0 g (42 mmol) of 7-bromo-2-methylquinolin-8-ol [19] **8** were added to a suspension of 5.8 g (52.5 mmol) of selenium oxide in dioxane (150 mL), under nitrogen atmosphere. The mixture was heated at 90 °C for 24h and monitored by TLC (DCM). After this time, the mixture was cooled at room temperature, filtered over celite and the solvent was removed under reduced pressure. The obtained red oil was purified by column chromatography on silica gel,

by using dichloromethane as eluent, giving the desired aldehyde as a yellow solid. Yield: 40%. ^{1}H NMR (200 MHz, $CDCl_3$): δ (ppm) = 10.27 (s, 1H, CHO), 8.52 (s, 1H, OH), 8.35 (d, 1H, HAr), 8.15 (d, 1H, HAr), 7.80 (d, 1H, HAr), 7.41 (d, 1H, HAr). ^{13}C NMR (75.4 MHz, CD_3CN): δ (ppm)= 194.29, 152.52, 139.54, 135.26, 131.24, 120.50, 119.37, 106.91. ESI-MS m/z_{calc}: 250.96 Found $[MH]^+$ m/z: 252.0.

ESI+ MS (m/z):

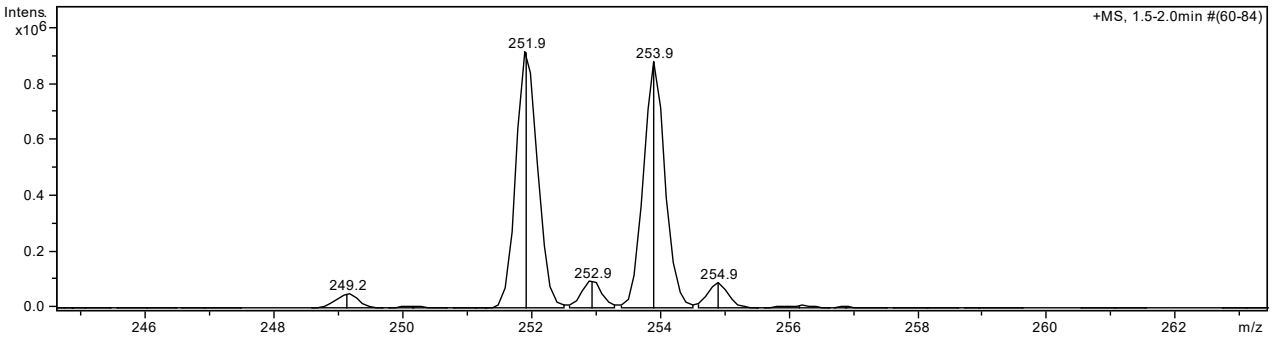

^{1}H NMR (200 MHz, CD_3CN):

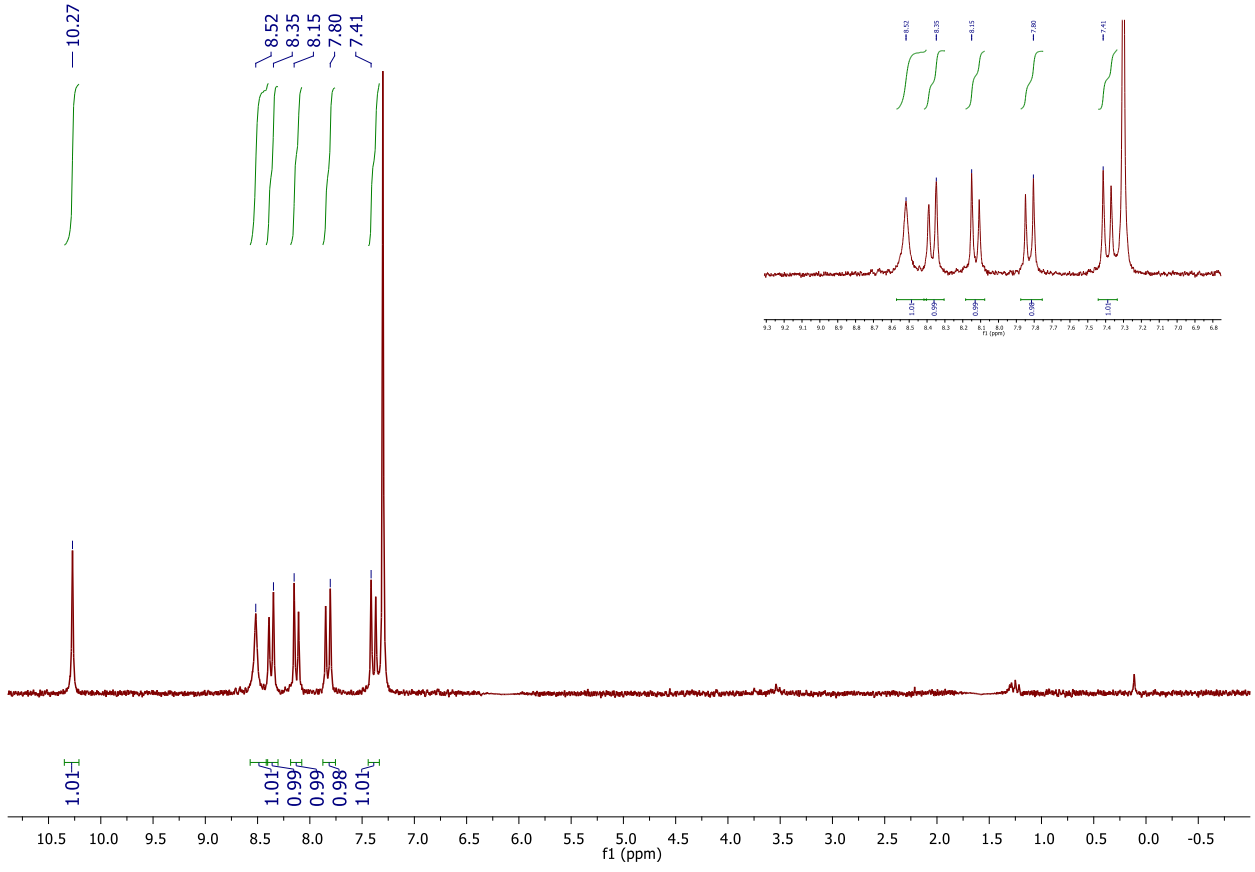

^{13}C NMR (300 MHz, $CDCl_3$):

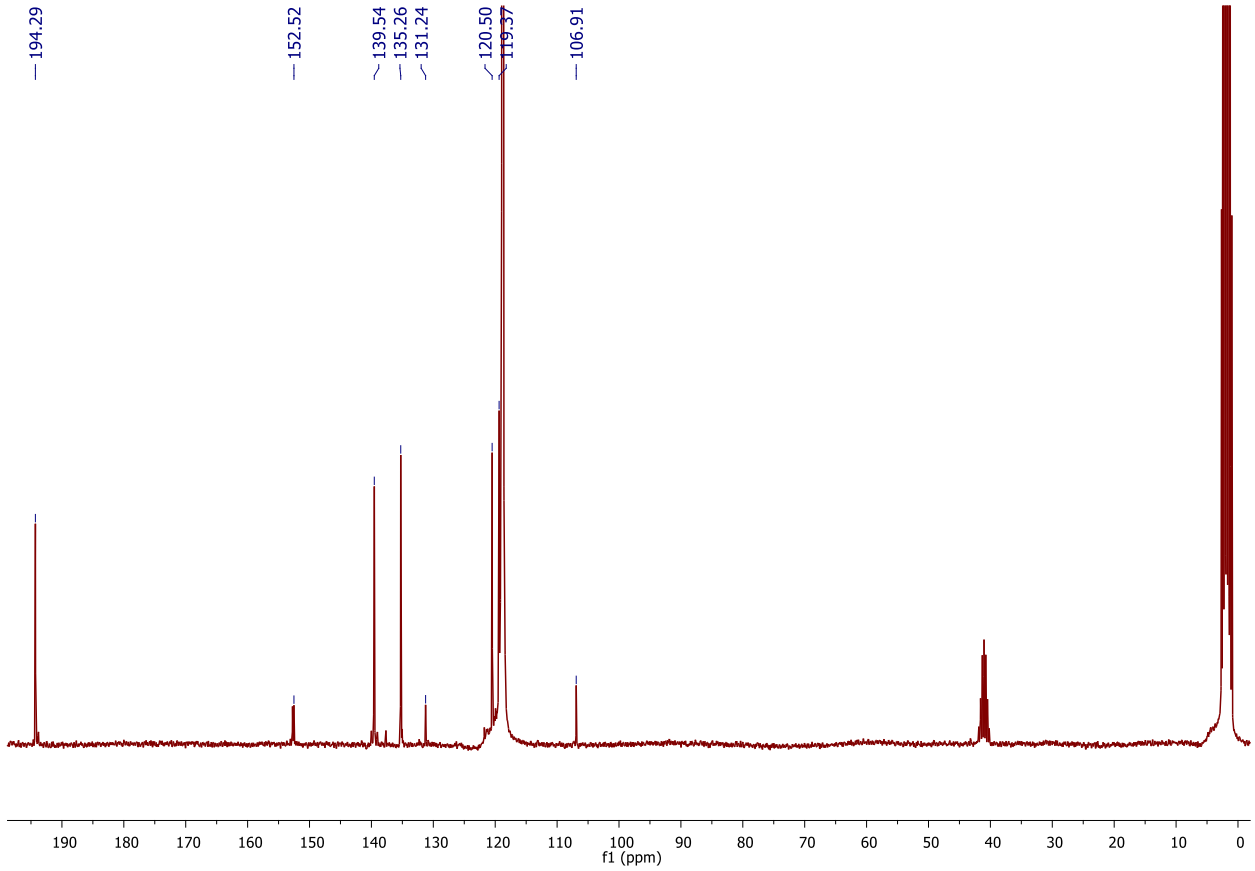

4.4.4.2 Synthesis of 7-bromo-8-(methoxymethoxy)quinoline-2-carbaldehyde (10)

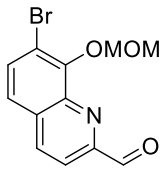

3.1 g (22.4 mmol) of K_2CO_3 were added to a solution of 4.7 g (18.7 mmol) of 7-bromo-8-hydroxyquinoline-2-carbaldehyde **9** in 200 mL of anhydrous DMF. After 20 minutes, 1.7 mL (22.4 mmol.) of methyl chloromethyl ether were added to the suspension. The reaction was kept under nitrogen flow overnight at room temperature. The reaction mixture was poured in water and the aqueous layer was extracted with ethyl acetate. The combined organic extracts were washed with distilled water and dried over Na_2SO_4. The solvent was evaporated, giving an oil which was purified by column chromatography on silica gel using dichloromethane as eluent. The desired product was obtained as a yellow solid. Yield: 52%.%. ^{1}H NMR (300 MHz, $CDCl_3$): δ (ppm) = 10.18 (s, 1H, CHO), 8.27 (d, 1H, HAr), 8.04 (d, 1H, HAr), 7.80 (d, 1H, HAr), 7.53 (d, 1H, HAr), 5.76 (s, 2H, CH_2), 3.77 (s, 3H, CH_3). ^{13}C NMR (75.4 MHz, CD_3CN): δ (ppm) = 194.57, 153.41, 144.19, 139.30, 135.19, 132.22, 125.21, 119.12, 101.89, 59.80. ESI-MS m/z_{calc}: 294.98 Found $[MH]^+$ m/z: 296.0.

ESI+ MS (m/z):

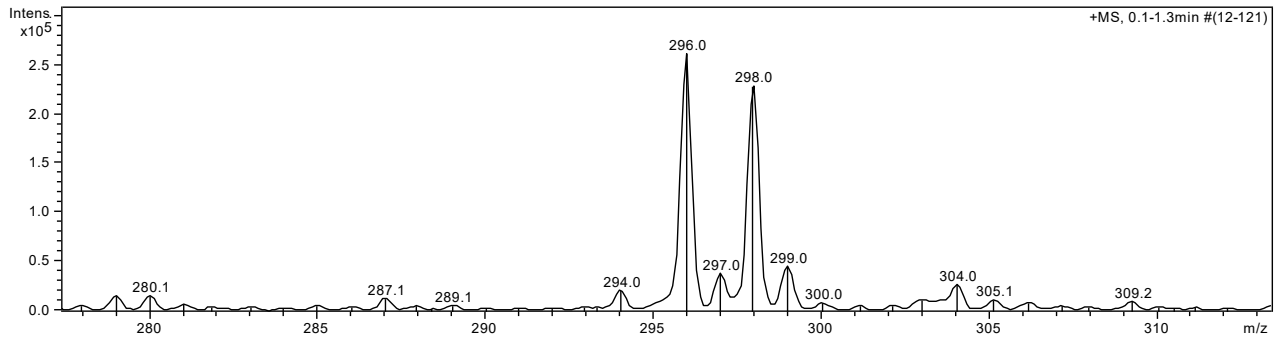

^{1}H NMR (200 MHz, CD_3CN):

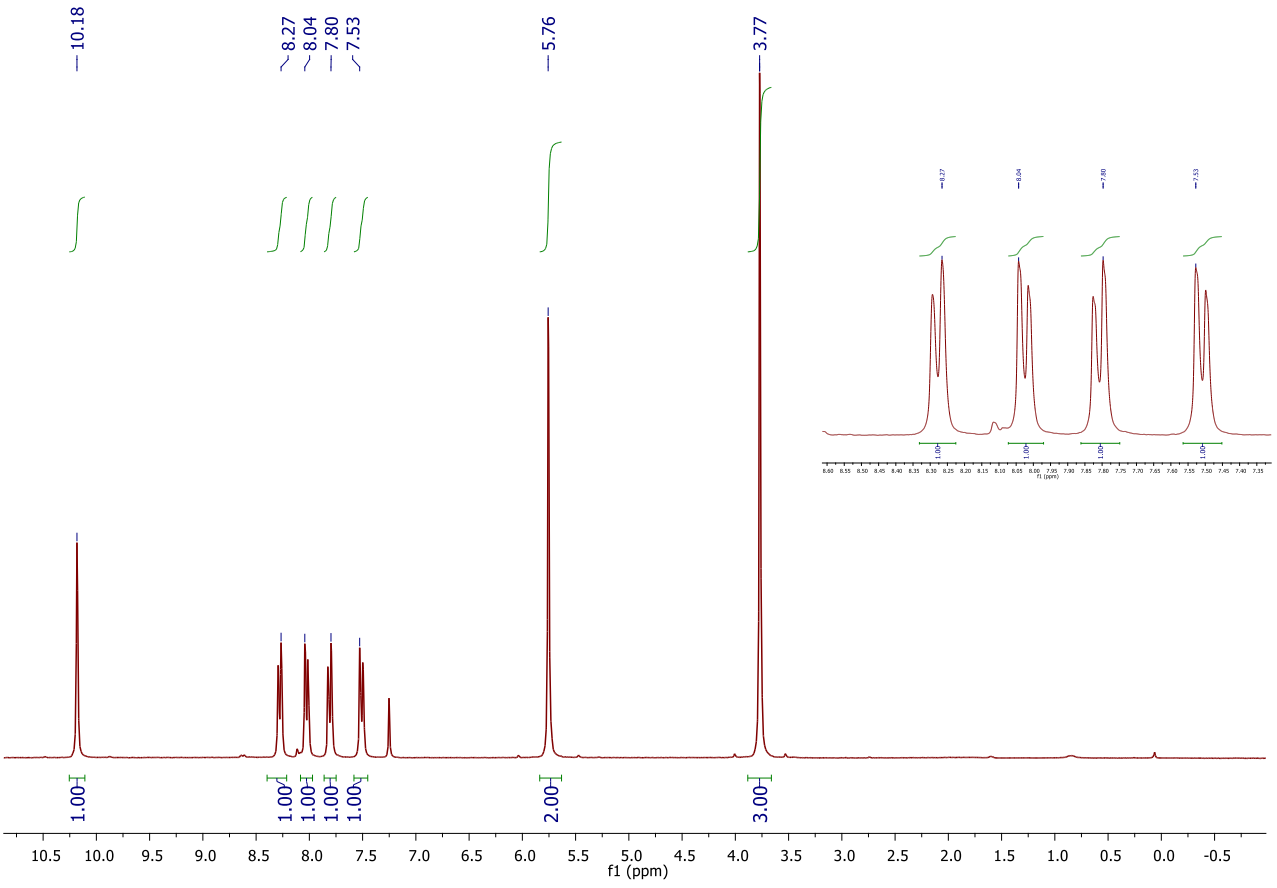

^{13}C NMR (300 MHz, $CDCl_3$):

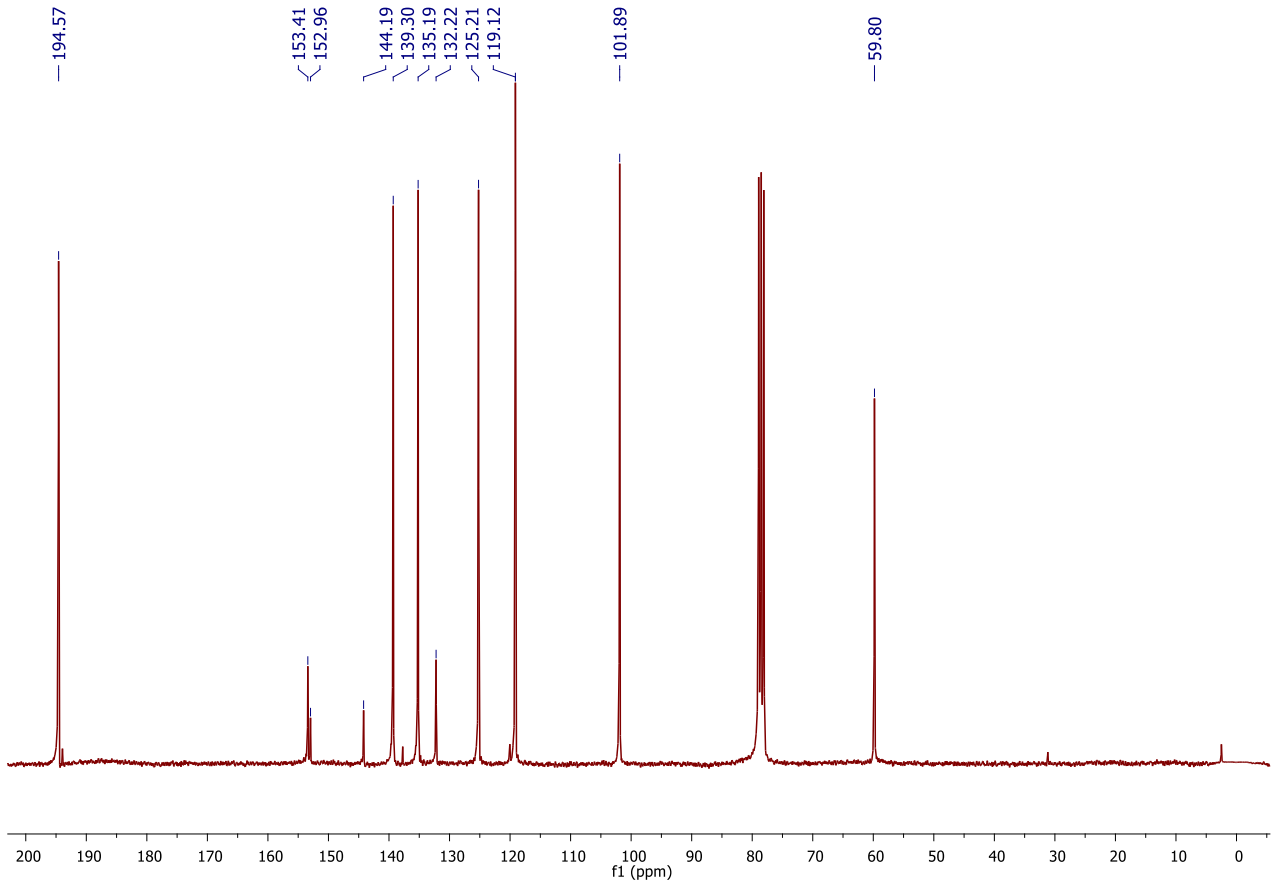

4.4.4.3 Synthesis of 1-(7-bromo-8-(methoxymethoxy)quinolin-2-yl)-N,N-bis(pyridin-2-ylmethyl)methanamine (11)

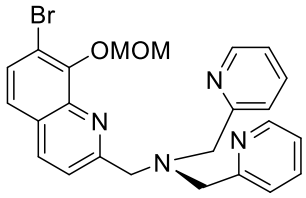

0.553 mL (3.1 mmol) of di-(2-picolyl)amine and 1.0 g (3.4 mmol) of 7-bromo-8-(methoxymethoxy)quinoline-2-carbaldehyde **10** were stirred in anhydrous dichloromethane (34 mL) under nitrogen atmosphere for 3 hours. To this solution, 0.85 g (4.0 mmol) of sodium triacetoxy borohydride were added and the mixture was stirred overnight at room temperature. The resulting mixture was washed with saturated $NaHCO_3$ solution and the organic phase was dried over Na_2SO_4. The solvent was removed under reduced pressure to furnish the desired product as a light-yellow solid. Yield: 92%. ^{1}H NMR (200 MHz, $CDCl_3$): δ (ppm) = 8.56 (d, 2H, HAr), 8.09 (d, 1H, HAr), 7.63 (m, 6H, HAr), 7.45 (d, 1H, HAr), 7.18 (t, 2H, HAr), 5.71 (s, 2H, CH_2), 4.07 (s, 4H, CH_2), 3.96 (s, 4H, CH_2), 3.77 (s, 3H, CH_3). ^{13}C NMR (50 MHz, $CDCl_3$): δ (ppm) = 159.89, 159.23, 150.41, 149.16, 142.21, 136.51, 136.36, 130.42, 128.07, 123.53, 123.05, 122.04, 121.39, 116.46, 60.78, 60.43, 58.19. ESI-MS m/z_{calc}: 478.1 Found $[MH]^+$ m/z: 478.1.

ESI+ MS (m/z):

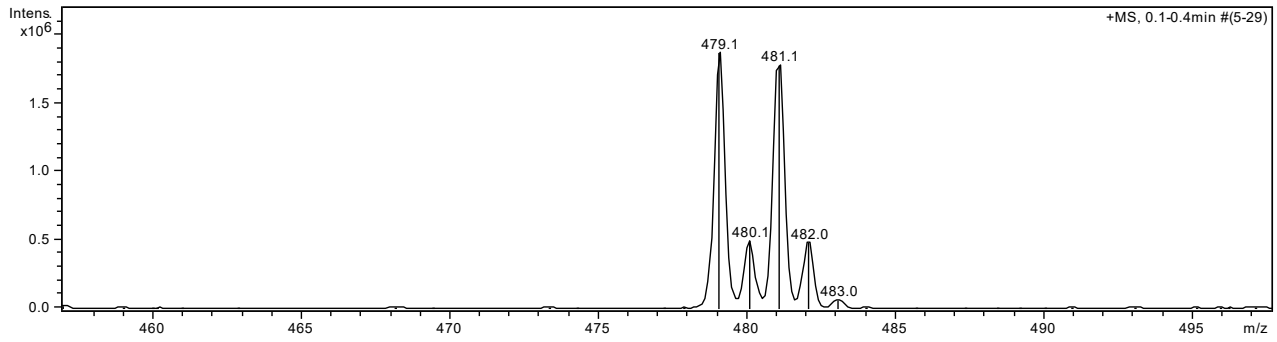

^{1}H NMR (200 MHz, CD_3CN):

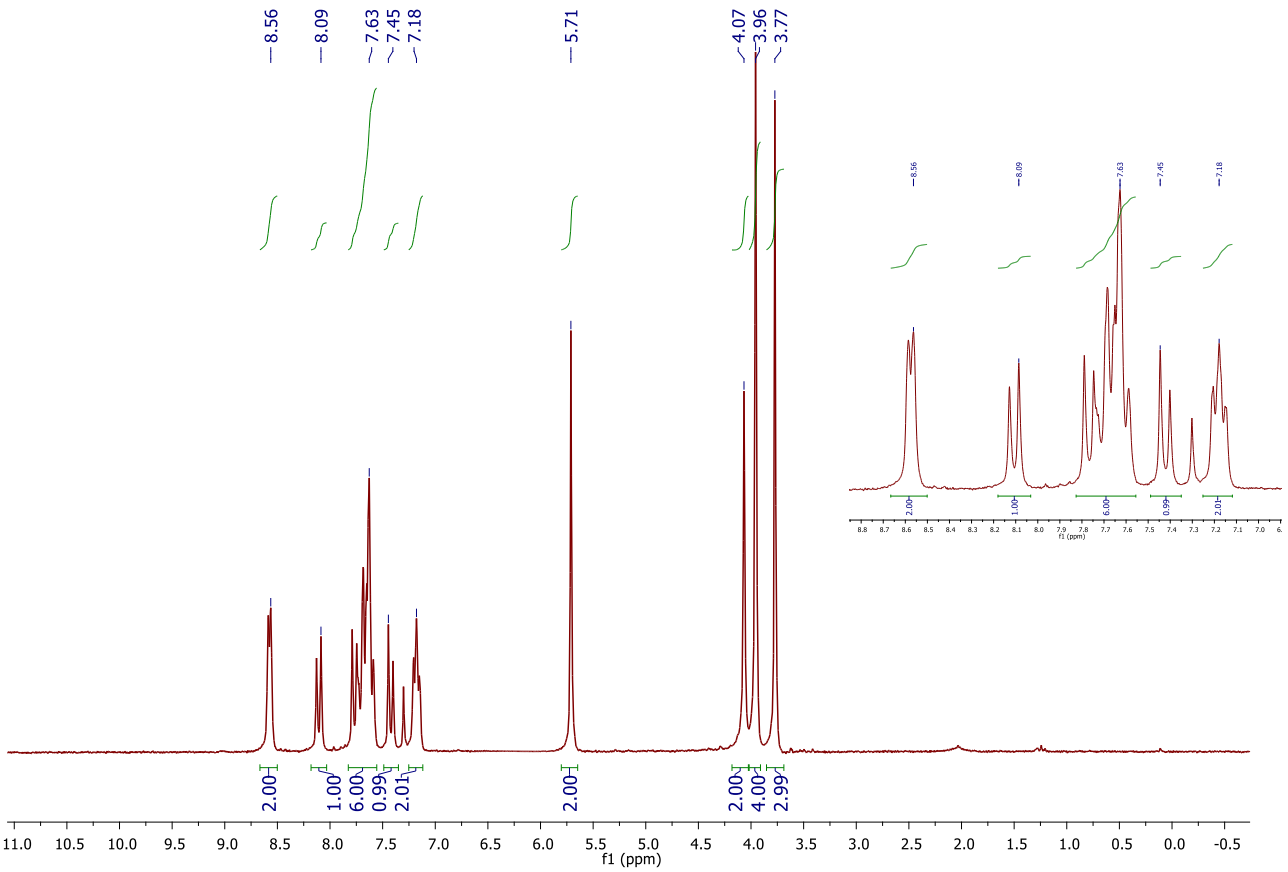

^{13}C NMR (300 MHz, $CDCl_3$):

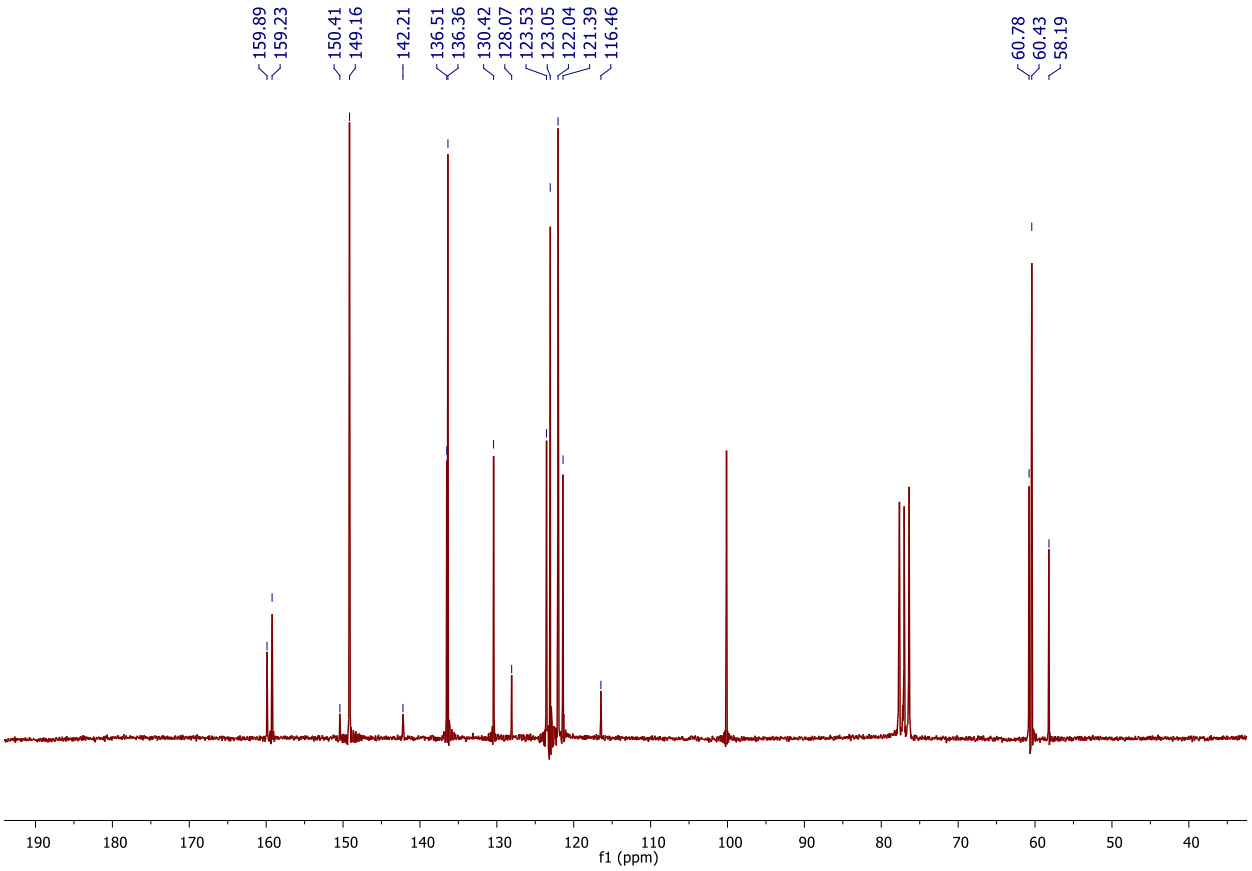

4.4.4.4 Synthesis of 3-(2-((bis(pyridin-2-ylmethyl)amino)methyl)-8-hydroxyquinolin-7-yl)benzaldehyde (12)

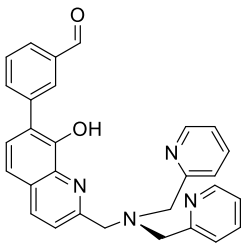

1.7 g (3.55 mmol) of 1-(7-bromo-8-(methoxymethoxy)quinolin-2-yl)-N,N-bis(pyridin-2-ylmethyl)methanamine **11**, 0.8 g (5.32 mmol) of 3-formylphenylboronic acid, 0.9 g (8.87 mmol) of Na_2CO_3 and 0.4 g (0.36 mmol) of $Pd(PPh_3)_4$ were dissolved in 60 mL of degassed H_2O/toluene/CH_3OH (1:1:0.6) mixture under nitrogen atmosphere. The mixture was stirred at 90°C overnight. The solvent was removed under reduced pressure and the residue was dissolved in $CHCl_3$. The organic phase was stirred with a 5% HCl water solution for 1 hour. The aqueous phase was then separated from the organic phase, basified with NaOH and extracted with $CHCl_3$. The remaining organic solution was dried over Na_2SO_4 and then the solvent was removed under low pressure to give the pure desired product as oil. Yield: 90%.^{1}H NMR (300 MHz, $CDCl_3$): δ (ppm) = 10.11 (s, 1H, CHO), 8.57 (d, 2H, HAr), 8.32 (s, 1H, OH), 8.11 (m, 2H, HAr), 7.86 (d, 1H, HAr), 7.65 (m, 6H, HAr), 7.40 (d, 2H, HAr), 7.16 (t, 2H, HAr), 6.96 (d, 6H, CH_2). ^{13}C NMR (75.4 MHz, $CDCl_3$): δ (ppm) = 194.04, 159.16, 157.87, 150.55, 140.36, 139.21, 138.32, 138.00, 136.90, 133.49, 132.36, 130.47, 130.09, 130.02, 129.93, 129.51, 128.40, 125.12, 124.03, 123.32, 122.91, 119.14, 61.34, 60.71. ESI-MS m/z_{calc}: 460.2 Found $[MH]^+$ m/z: 461.

ESI+ MS (m/z):

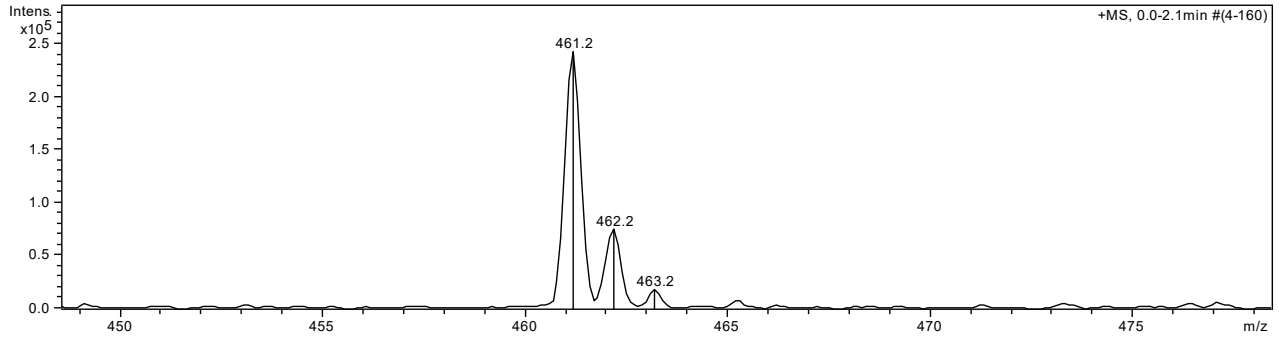

^{1}H NMR (200 MHz, $CDCl_3$):

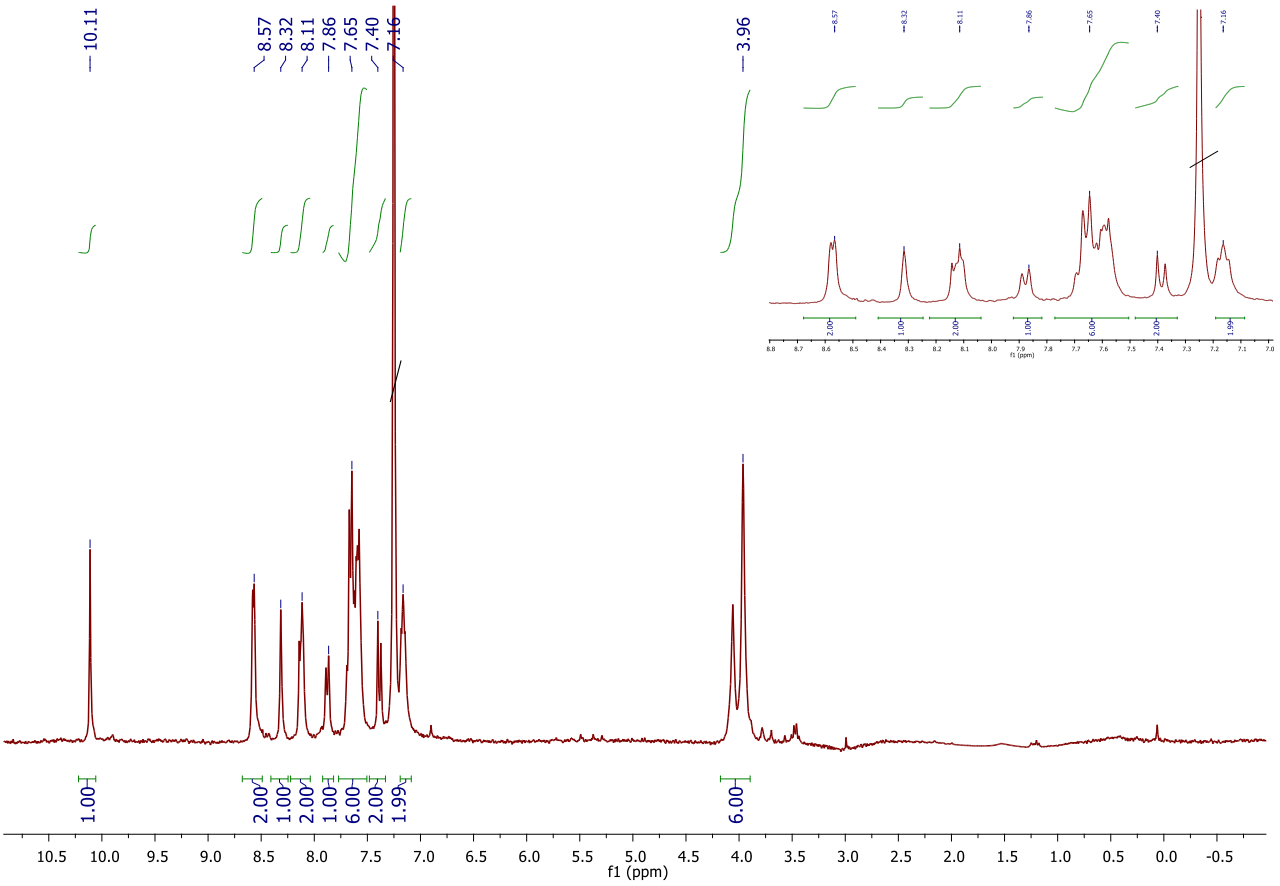

^{13}C NMR (75.4 MHz, $CDCl_3$):

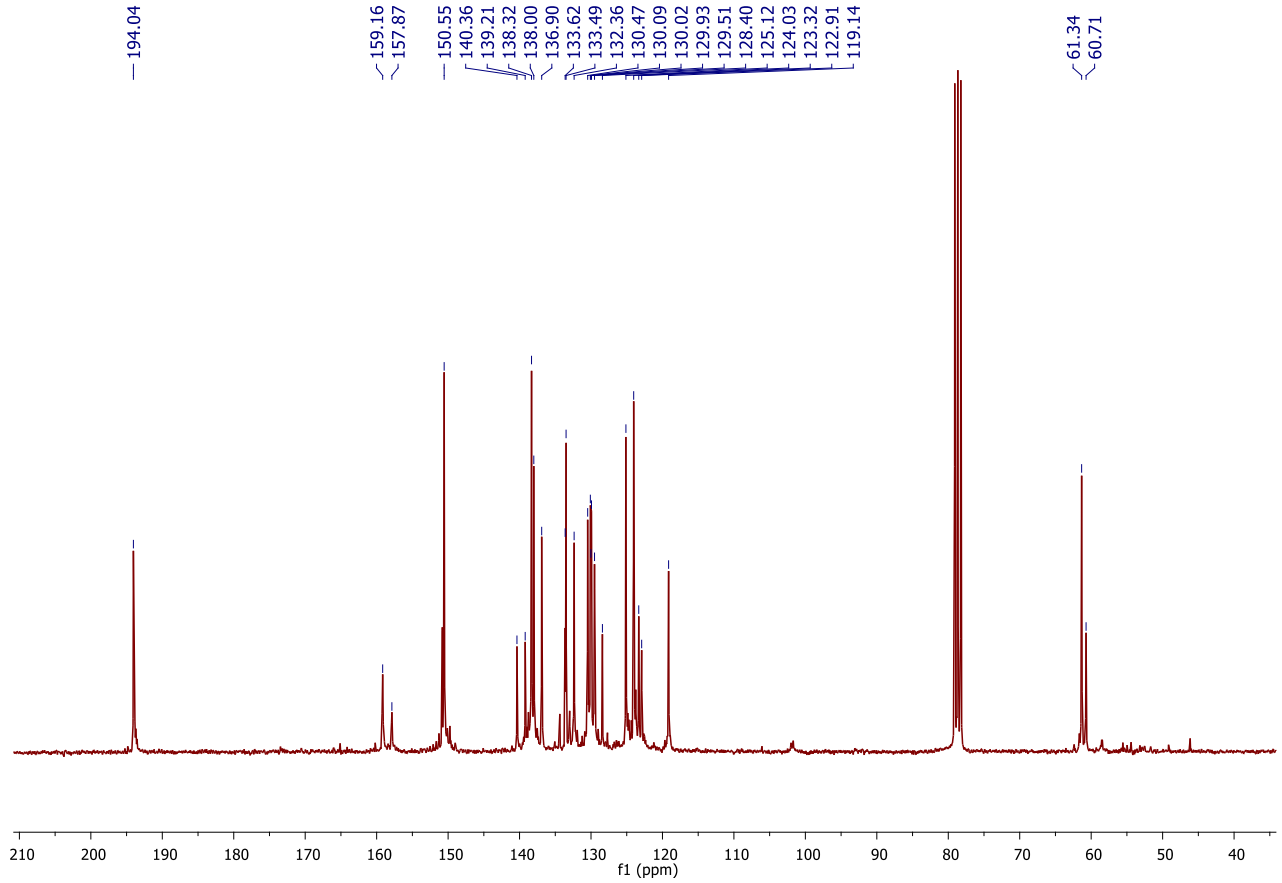

4.4.5. Synthesis of the Fluorescent Zinc Complexes

4.4.5.1 Synthesis of the monomeric complex (13)

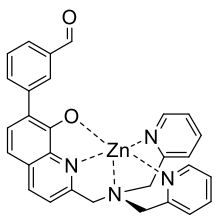

0.2 g (0.45 mmol) of 3-(2-((bis(pyridin-2-ylmethyl)amino)methyl)-8-hydroxyquinolin-7-yl)benzaldehyde **12** were dissolved in 5 mL of anhydrous acetonitrile and 0.17 g (0.45mmol) of zinc perchlorate hexahydrate were added, and the solution was left stirring at room temperature for 15 min. Diethyl ether was then slowly added to induce precipitation of the desired product as a bright yellow powder. Yield: 97%. Caution! Perchlorate salts of metal complexes with organic ligands are potentially explosive. They should be handled in small quantities and with caution. ^{1}H NMR (300 MHz, CD_3CN): δ (ppm) = 10.19 (s, 1H, CHO), 8.76 (d, 2H, HAr), 8.52 (d, 1H, HAr), 8.26 (s, 1H, HAr), 8.08 (m, 4H, HAr), 7.85 (t, 1H, HAr), 7.71 (q, 2H, HAr), 7.60 (m, 5H, HAr), 4.43 (d, 6H, CH_2). ESI-MS m/z_{calc}: 523.1 Found $[M]^+$ m/z: 523.1.

ESI+ MS (m/z):

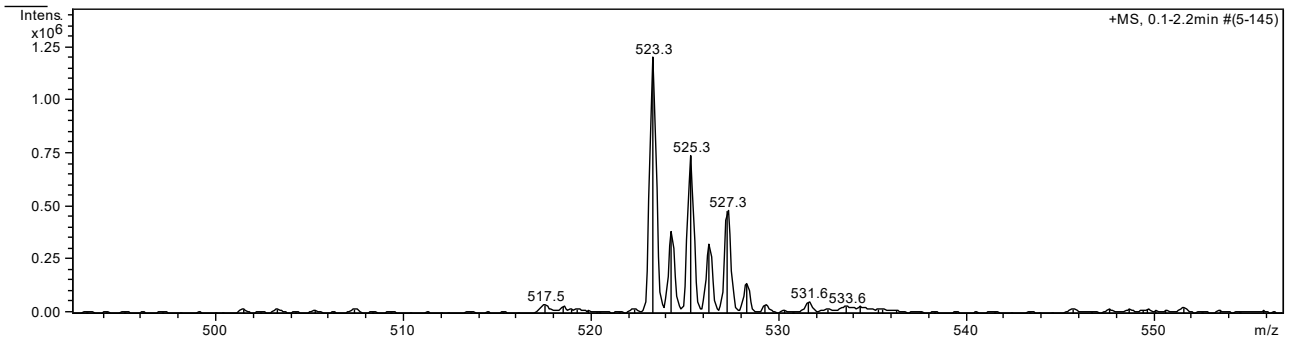

^{1}H NMR (200 MHz, CD_3CN):

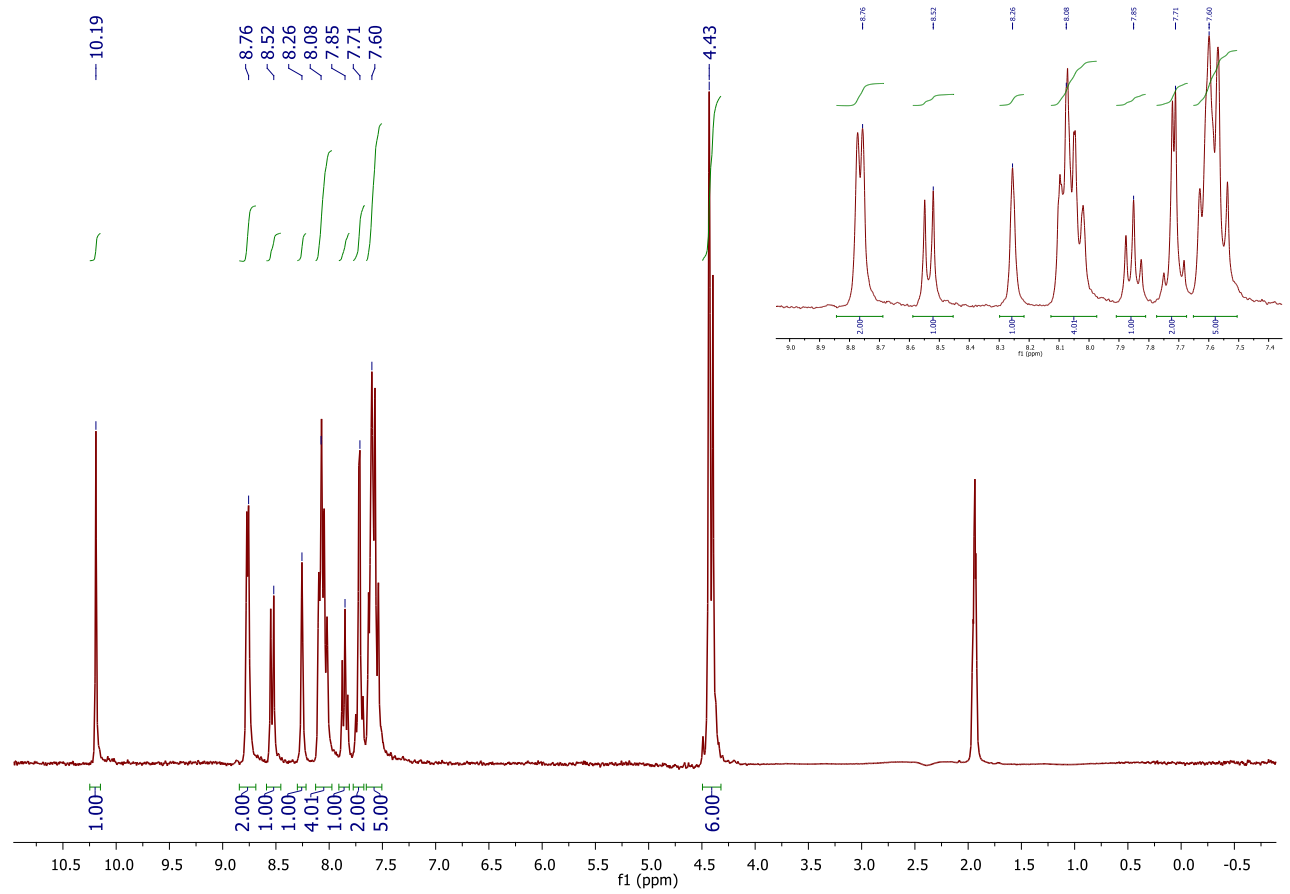

4.4.5.2 General procedure for CD and CPL measurements

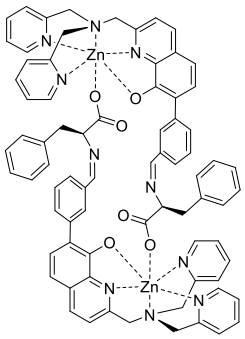

37,8 mg (0.06 mmol) of **13** were solubilized in 0.6 mL of anhydrous DMSO, molecular sieves and the desired amino acid (1 eq.) were added. The solution was let stirring at 70 °C for 1 hour. The compounds were used without further purification for CD measurements after suitable dilutions. ^{1}H NMR for **14-Zn-Phe** (300 MHz, DMSO): δ (ppm)= 8.17 (m, 7H, HAr), 7.23 (m, 16H, HAr), 4.48 (s, 4H, CH_2), 4.25 (s, 2H, CH_2), 3.03 (t, 1H, CH_2), 2.82 (t, 1H, CH_2).

^{1}H NMR (200 MHz, CD_3CN):

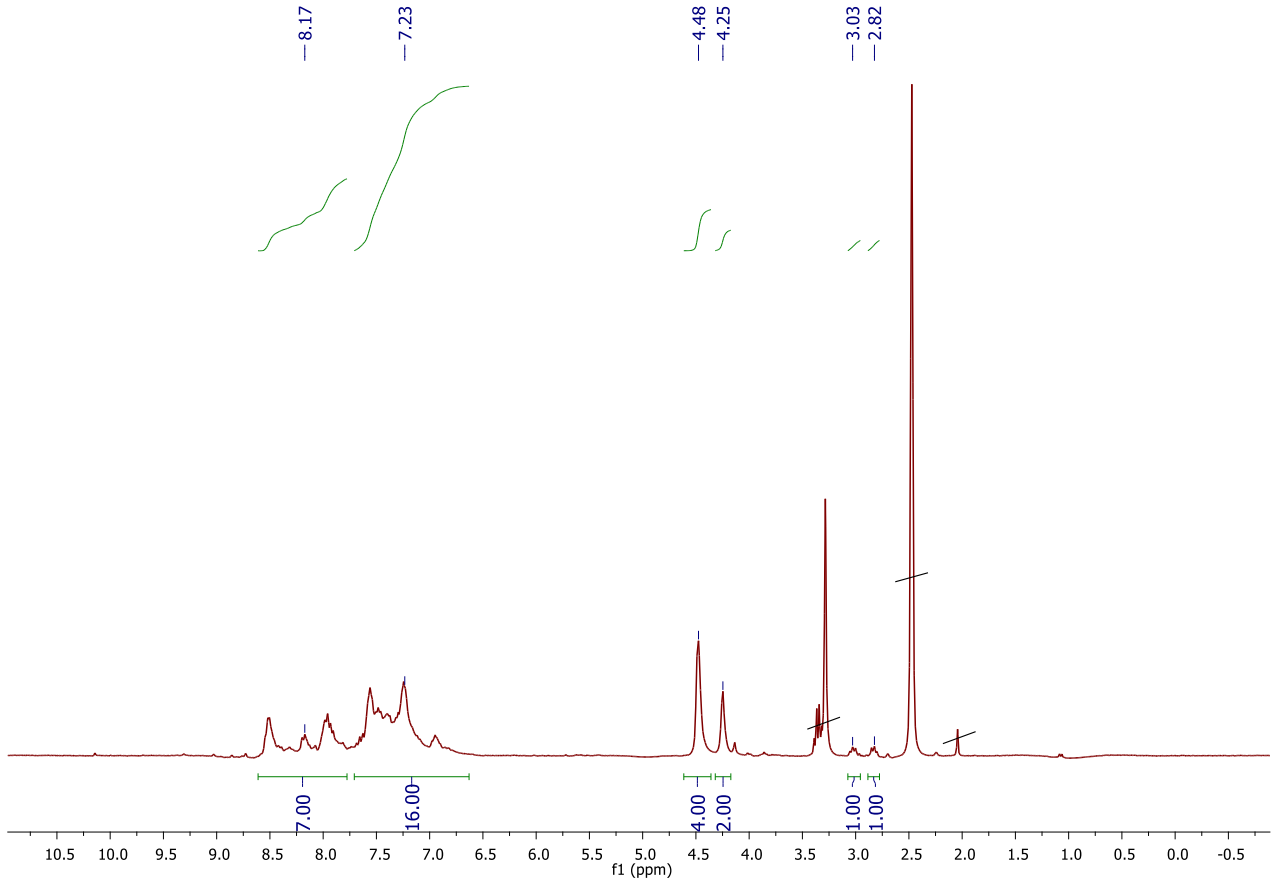

4.5 References

[1]. (a) D. Leung, S.O. Kang, E.V. Anslyn. *Chem Soc Rev* **2012**, 41,448-479; (b) N. Berova, L. Di Bari, G. Pescitelli, *Chem Soc Rev* **2007**, 36, 914–931; (c) G. Pescitelli, L. Di Bari, N. Berova, *Chem Soc Rev* **2014**, 43, 5211-5233; (d) Z. Chen, Q. Wang, X. Wu, Z. Li, Y.-B. Jiang, *Chem Soc Rev* **2015**, 44, 4249-4263.

[2] (a) M. Liu, L. Zhang, T. Wang, *Chem Rev* **2015**, 115, 7304−7397; (b) H.G. Jeon, M.J. Kim, K.S. Jeong, *Org Biomol Chem* **2014**, 12, 5464-5468; (c). L. González-Mendoza, J. Escorihuela, B. Altava, M.I. Burguete, S.V. Luis, *Org Biomol Chem* **2015**, 13, 5450-5459; (d). S. Hayashi, M. Yotsukura, M. Noji, T. Takanami, *Chem Commun* **2015**, 51, 11068-11071; (e) J. Zhang, H. Gholami, X. Ding, M. Chun, C. Vasileiou, T. Nehira, B. Borhan, *Org Lett* **2017**, 19, 1362−1365; (f). M. Anyika, H. Gholami, K.D. Ashtekar, R. Acho, B. Borhan, *J Am Chem Soc* **2014**, 136, 550−553; (g). H. Gholami, M. Anyika, J. Zhang, C. Vasileiou, B. Borhan, *Chem Eur J* **2016**, 22, 9235–9239; (h). Z.A. De los Santos, C. Wolf, *J Am Chem Soc* **2016**, 138, 13517−13520; (i). K. Wen, S Yu, Z. Huang, L. Chen, M. Xiao, X. Yu, L. Pu, *J Am Chem Soc* **2015**, 137, 4517–4524; (j). J.M. Dragna, G. Pescitelli, L. Tran, V.M. Lynch, E.V. Anslyn, L. Di Bari, *J Am Chem Soc* **2012**, 134, 4398-4407; (k) L.L. Wang, Z. Chen, W.-E. Liu, H. Ke, S.-H. Wang, W. Jiang, *J Am Chem Soc* **2017**, 139, 8436–8439.

[3] (a) L. You, G. Pescitelli, E.V. Anslyn, L. Di Bari, *J Am Chem Soc* **2012**, 134, 7117–7125; (b) Y. Zhou, Y. Ren, L. Zhang, L. You, Y. Yuan, E.V. Anslyn, *Tetrahedron* **2015**, *71*, 3515-3521; (c). L. You, R. Long, V.M. Lynch, E.V. Anslyn, *Chem Eur J* **2011**, 17*,* 11017–11023; (d). L. You, J.S. Berman, E.V. Anslyn, *Nature Chem* **2011**, 3*,* 943–948; (e). C.Y. Lin, M.W. Giuliano, B.D. Ellis, S.J. Miller, E.V. Anslyn, *Chem Sci* **2016**, 7, 4085-4090; (f) H.H. Jo, X. Gao, L. You, E.V. Anslyn, M.J. Krische, *Chem Sci* **2015**, 6, 6747-6753; (g). L.A. Joyce, M.S. Maynor, J.M. Dragna, G.M. da Cruz, V.M. Lynch, J.W. Canary, E.V. Anslyn, *J Am Chem Soc* **2011**, 133*,* 13746–13752.

[4] (a) J. Crassous, *Chem Commun* **2012**, 48, 9684–9692; (b) B. Irfanoglu, C. Wolf, *Chirality* **2014**, 26, 379–384.

[5] (a) F.A. Scaramuzzo, G. Licini, C. Zonta, *Chem Eur J* **2013**, 19, 16809-16813; (b) E. Badetti, K. Wurst, G. Licini, C. Zonta, *Chem Eur J* **2016**, 22, 6515-6518; (c). R. Berardozzi, E. Badetti, N.A. Carmo dos Santos, K. Wurst, G. Licini, G. Pescitelli, C. Zonta, L. Di Bari, *Chem Commun* **2016**, 52, 8428-8431; (d) F.A. Scaramuzzo, E. Badetti, G. Licini, C. Zonta,. *Eur J Org Chem* **2017**, 11, 1438-1442; (e). C. Bravin, E. Badetti, F.A. Scaramuzzo, G. Licini, C. Zonta,. *J Am Chem Soc* **2017**, 139, 6456−6460.

[6] P.T. Corbett, J. Leclaire, L. Vial, K.R. West, J.-L. Wietor, J.K.M. Sanders, S. Otto *Chem Rev* **2006**, 106, 3652–3711; (b) J. Li, P. Nowak, S. Otto, *J Am Chem Soc* **2013**, 135*,* 9222−9239; (c) I. Alfonso, *Chem Commun* **2016**, 52, 239-250.

[7] (a) F. Biedermann, W.M. Nau, *Angew Chem Int Ed* **2014**, 53, 5694–5699; (b) N. Kameta, M. Masuda, T. Shimizu, *Chem Commun* **2015**, 51, 11104-11107; (c) E.G. Shcherbakova, V. Brega, T. Minami, S. Sheykhi, T.D. James, P. Anzenbacher Jr., *Chem Eur J* **2016**, 22, 10074-10080; (d) Z.A. De los Santos, N.M. Legaux, C. Wolf, *Chirality* **2017**, DOI, 10.1002/chir.22765.

[8] Emeis CA, Oosterhoff LJ. Emission of circularly-polarized radiation by optically-active compounds. *Chem Phys Lett* **1967**, 1,129–132.

[9] (a) E. Sànchez-Carnerero, A.R. Agarrabeitia, F. Moreno, B.L. Maroto, G. Muller, M.J. Ortiz, S. de la Moya, *Chem Eur J* **2015**, 21, 13488–13500; (b) G. Longhi, E. Castiglioni, J. Koshoubu, G. Mazzeo, S. Abbate, *Chirality* **2016**, 28, 696-707.

[10] (a) N. Saleh, B. Moore, M. Srebro, N. Vanthuyne, L. Toupet, J.A.G. Williams, C. Roussel, K.K. Deol, G. Muller, J. Autschbach, J. Crassous, *Chem Eur J* **2015**, 21, 1673–1681; (b) A. Rybicka, G. Longhi, E. Castiglioni, S. Abbate, W. Dzwolak, V. Babenko, M. Pecul, *Chem Phys Chem* **2016**, 17, 2931-2937; (c) T. Nishikawa, N. Tajima, M. Kitamatsu, M. Fujiki, Y. Imai, *Org Biomol Chem* **2015**, 13, 11426-11431.

[11] (a) Y. Mimura, T. Nishikawa, R. Fuchino, S. Nakai, N. Tajima, M. Kitamatsu, M. Fujiki, Y. Imai, *Org Biomol Chem* **2017**, 15, 4548-4553.

[12] (a) J.L. Lunkley, D. Shirotani, K. Yamanari, S. Kaizaki, G. Muller, *Inorg. Chem.* **2011**, 11, 12724-12732; (b) Y. Mimura, S. Kitamura, M. Shizuma, M. Kitamatsu, M. Fujiki, Y. Imai, *Chem. Select* **2017**, 2, 7759-7764; (c) S. Ito, K. Ikeda, S. Nakanishi, Y. Imai, M. Asami, *Chem. Comm.* **2017**, 53, doi 10.10391/c7cc01351.

[13] (a) J. Kawakami, M. Ohta, Y. Yamauchi, K. *Anal Sci* **2003**, 19, 1353-4; (b) E Sapelli, T.A.S. Brandão, H.D. Fiedler, F. Nome, *J. Colloid Interface Sci* **2007**, 314, 214–222.

[14] (a) M.J. Frisch *et al.* Gaussian 09 (Gaussian Inc., 2009); (b) The minimised structure has a C_2 symmetry and the zinc metal has an octahedral geometry. The distance between the hydrogens in para of the phenyl rings of the amino acid residues is 18.7 Å.

[15] T. Bruhn, A. Schaumlöffel, Y. Hemberger, G. Bringmann, *Chirality* **2013**, 25, 243–249.

[16] (a) A.B.T. Ghisaidoobe, S.J. Chung, *Int J Mol Sci* **2014**, 15, 22518-22538; (b). J.T. Vivian, P.R. Callis *Biophys. J.* **2001**, 80, 2093–2109.

[17] (a) S. Abbate, G. Longhi, F. Lebon, E. Castiglioni, S. Superchi, L. Pisani, F. Fontana, F. Torricelli, T. Caronna, C. Villani, R. Sabia, M. Tommasini, A. Lucotti, D. Mendola, A. Mele, D.A. Lightner, *J Phys Chem C* **2014**, 118, 1682-1695; (b) G. Longhi, E. Castiglioni, C. Villani, R. Sabia, S. Menichetti, C. Viglianisi, F. Devlin, S. Abbate, *J Photobiol Photochem A Chem* **2016**, 331, 138-145; (c) Y. Liu, J. Cerezo, G. Mazzeo, N. Lin, X. Zhao, G. Longhi, S. Abbate, F. Santoro, *J Chem Theor Comp* **2016**, 12, 2799-2819.

[18] (a) E. Castiglioni, S. Abbate, G. Longhi, *Appl Spectrosc* **2010**, 64, 1416–1419; (b) E. Castiglioni, S. Abbate, F. Lebon, G. Longhi, *Methods Appl Fluoresc* **2014**, 2, 024006.7p.

[19] C. Deraeve, C. Boldron, A. Maraval, H. Mazarguil, H. Gornitzka, L. Vendier, M. Pitié, B. Meunier, *Chem Eur J* 2008, 14, 682-696.

CHAPTER 5

Ligands for Catalysis

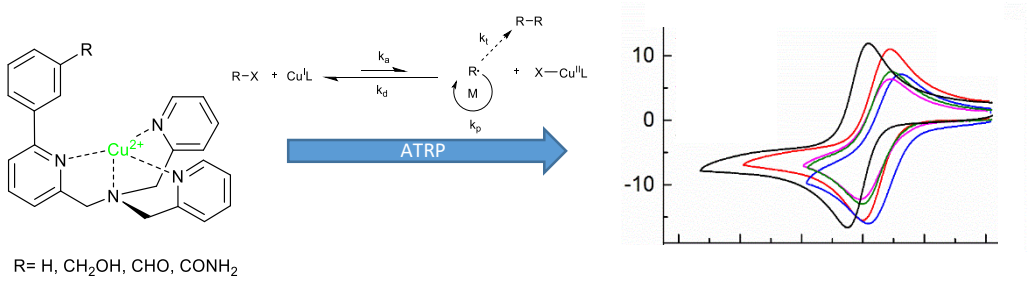

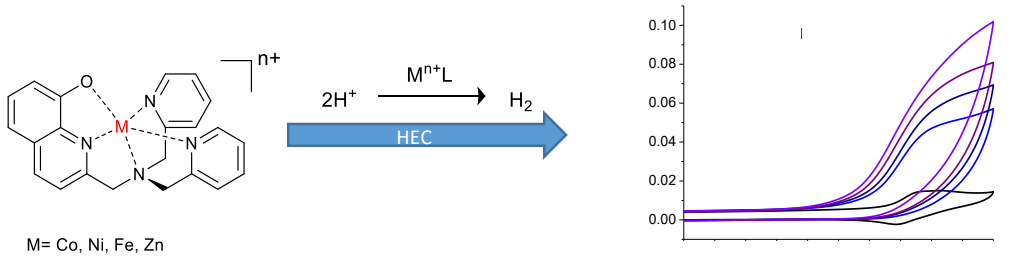

The work carried out along this thesis has offered the possibility to prepare also metal complexes suitable for catalysis. The first part of this chapter reports the synthesis of eight novel copper tris(2-methylpyridyl)amine (TPMA) based complexes, and the evaluation of the catalytic activity for electrochemically mediated atom transfer radical polymerization ATRP in both organic and aqueous media. This study has been conducted in collaboration with the group of Prof. Isse at the University of Padova and it has been published in *Polymer*, **2017**, 128, 169-176.

In the second part is reported the synthesis and characterization of cobalt, nickel, and iron complexes based on the pentadentate 8-hydroxyquinoline-di(2-picolyl)amine ligand and the study of these metal complexes as potential hydrogen evolving catalysts (HECs) under both electrochemical and light-driven conditions. This study has been conducted in collaboration with the group of Dr. Natali at the University of Ferrara. It has been published in *Dalton Transactions*, **2017**, 46, 16455 - 16464.

Section 5A – Copper complexes bearing TPMA based ligands on ATRP

5A.1 Introduction

Over the past years, atom transfer radical polymerization (ATRP) strongly impacted the world of polymer sciences thanks to its capability to generate macromolecules with predictable architectures, functionalities and compositions.[1] This versatile process was successfully applied to a large variety of monomers,[2] showing great flexibility towards solvents, functional groups and potential impurities. ATRP is a controlled radical polymerization technique catalyzed by transition metal complexes, mainly copper with polyamine ligands. The process is initiated by the transfer of a halogen atom from an alkyl halide initiator (R-X) to the active form of the catalyst, $[Cu^{I}L]^{+}$. This generates a free radical and the metal complex at a higher oxidation state, $[XCu^{II}L]^{+}$(Scheme 5A.1).[3] The radical propagates for a short period, adding only to few monomer units, before it is converted back to a dormant state (P_n-X) by a deactivation reaction with $[XCu^{II}L]^{+}$. ATRP equilibrium is strongly shifted towards the dormant species,[4] so that the concentration of the propagating radicals is very low and radical-radical termination events are predominantly suppressed. Therefore, the key-feature of the process is the continuous activation-(propagation)/fast deactivation cycle, which enables concurrent growth of all chains and hence very low molecular weight dispersity.

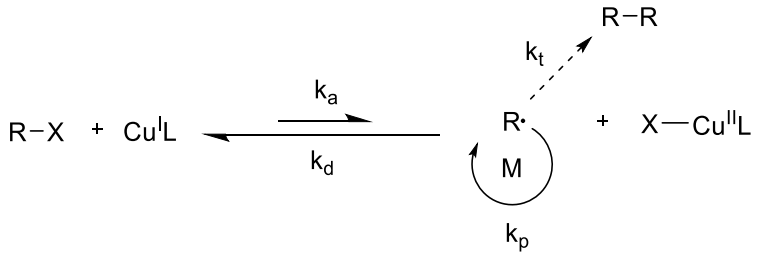

Scheme 5A.1. General ATRP mechanism (k_a = activation rate constant, K_d = deactivation rate constant, k_p = propagation rate constant, k_t = termination rate constant, R-X = alkyl halide (or dormant polymer chain), R· = alkyl (or polymeric) radical, M = monomer, L = ligand, X = Cl, Br)

The catalyst plays a fundamental role, regulating the equilibrium between dormant and active species along the whole process. A considerable disadvantage of ATRP, as it was originally conceived, was the large amount of copper catalyst needed. Recently, several methods using low ppm levels of copper catalysts have been developed. These include activators regenerated by electron transfer (ARGET) ATRP,[5] initiators for continuous activator regeneration (ICAR) ATRP,[5b,6] supplemental activator and reducing agent (SARA) ATRP,[7] also known as SET-LRP,[8] photochemically mediated ATRP[9] and electrochemically mediated ATRP (*e*ATRP).[10] Besides these advanced techniques, the quest to decrease the quantity of copper led to the synthesis of novel ligands for the preparation of highly active copper catalysts. Copper complexes with ligands based on tris(2-methylpyridyl)amine (TPMA) are among the most active catalysts.[11] In particular, Cu/TPMA is the best performing catalyst in aqueous media.[10c]

The reactivity of ATRP catalysts can be related to the standard reduction potential ($E^{\ominus}$) of the Cu(II)/Cu(I) couple. Both the activation rate constant and the equilibrium constant of ATRP increase by enhancing the reducing power of the catalyst, *i.e.* diminishing $E^{\ominus}$.[11c,12] In this context, the ligand plays a fundamental role in regulating the catalyst activity; it can modify the charge density on the metallic center, influencing the relative stability of Cu(II) and Cu(I). Therefore, the ligand structure can be modified in order to tune the electronic properties of the metallic center. Copper complexes with TPMA bearing methyl and methoxy groups on one or more pyridine rings have recently been prepared to enhance catalyst activity in ATRP.[11a,b] In this study, we report four novel TPMA copper complexes in which the second coordination sphere of the copper center has been varied. These modifications have been performed by adding functionalized phenyl substituents to the TPMA skeleton. The redox properties of these complexes in the absence and presence of halide ions were analyzed by cyclic voltammetry and compared with Cu/TPMA system in order to predict their reactivity in ATRP systems. Among the low-ppm techniques, *e*ATRP is receiving a growing interest, mainly because it allows to gain a deep understanding of the process besides introducing addition tools for control.[13] Herein, is described the use of *e*ATRP on various monomers with $[Cu^{II}L]^{2+}$ as catalyst, where L = TPMA or modified TPMA. By comparing redox and synthetic features, it was possible to identify systems in which the use of phenyl-substituted TPMA can be successful and even beneficial.

5A.2 Results and Discussion

Tris(2-methylpyridyl)amine complexes are widely used in catalysis and molecular recognition. This is due to their polydentate nature, which allows the formation of stable metal complexes also under turnover conditions. In the recent years, this research group has been interested in the study of the catalytic and molecular recognition properties of this class of complexes [14]. In particular, Co(II) complexes in which the ligand bears different functional groups have been synthesized and studied as hydrogen evolving catalysts, in light-assisted conditions.[15] The initial findings on the catalytic properties of these newly developed systems have driven our interest to study *e*ATRP activity of a series of Cu(II) complexes. Our investigation was directed to evaluate if the phenyl substitution and/or the presence of extra functionalities in the ligand backbone were affecting the catalytic properties of the complexes. This goal has been achieved by *i*) synthetizing and studying the Cu(II) coordination chemistry of a series of ligands having different functionalities, *ii*) studying their electrochemistry in solution and *iii*) performing *e*ATRP in organic and aqueous solvents.

5A.2.1 Coordination Chemistry

Ligands **15a-d,** as well as the corresponding copper complexes **16a-d** and **17a-d** (Scheme 5A.1), have been prepared using a previously reported methodology [15]. The method consists in the synthesis of

a bromo derivative via reductive amination of commercially available 6-bromo-2-pyridinecarboxaldehyde and di(2-picolyl)amine, followed by a Suzuki coupling with appropriate boronic acid. The general procedure for the synthesis of Cu(II) complexes requires the mixing of an equimolar amount of copper salt with the corresponding ligand **15a-d** in acetonitrile. The solution is stirred at room temperature for 10 min and the desired compounds are obtained as crystalline powders or by recrystallization with diethyl ether.

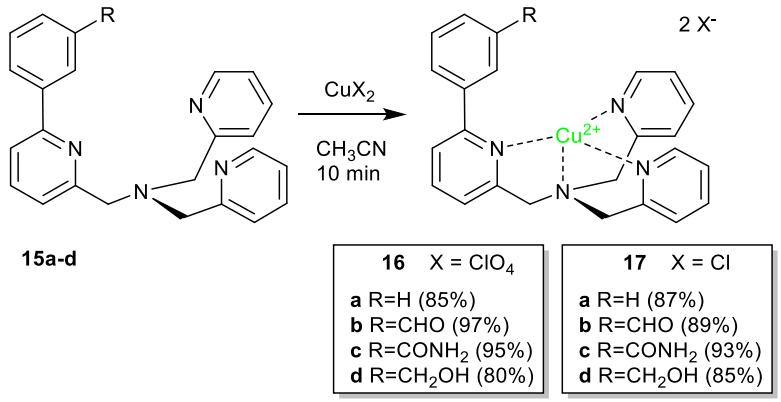

Scheme 5A.1. General synthetic procedures for compounds **16a-d** and **17a-d**.

The obtained complexes have been characterized by ESI-MS, FT-IR spectroscopy and/or elemental analysis, confirming the purity of the desired compounds (see supporting information). Among the different structures, it was possible to obtain crystals suitable for X-ray diffraction of complexes **16a,d** and **17a,c**, the crystallographic study was done in collaboration with Prof. Klaus Wurst (University of Innsbruck). All the monocationic structures (Fig. 5A.2) show a distinctive Jahn-Teller effect with a strong distorted octahedral coordination for the Cu(II) centre. The four short bonds of **16a,d** and **17a,c**, arranged in a square planar manner, come from the amino group N(1) in the range between 203 and 206 pm, the two unsubstituted pyridine moieties N(3), N(4) with bond lengths between 197 and 202 pm and finally from acetonitrile N(5) at **16a,d** with equal distances of 198 pm and Cl anions at **17a,c** around 225 pm, respectively. The elongated bonds at complexes **16a** and **16d** (N(2): 234, O(1): 281 and N(2): 249, O(2): 254 pm) are comparable to well described Cu(II) complexes of pentadentate bispiridine ligands with two amino groups and three pyridine moieties, and a coordinated acetonitrile [16]. The molecules of **17a,c** form a dimer, whereas the chloride anions generate additional elongated bonds to the other Cu(II) centre with lengths of 295 at **17c** and 328 pm at **17a.** The distances of the nitrogen atoms are elongated to 245 and 250 pm (N(2) and N(7)) at **17c** and 252 pm at N(2) of **17a**. The dimerization could be favoured by additive π-π interactions between the pyridine rings with carbon-carbon distances of 342 (**17c**) and 354 pm at (**17a**).

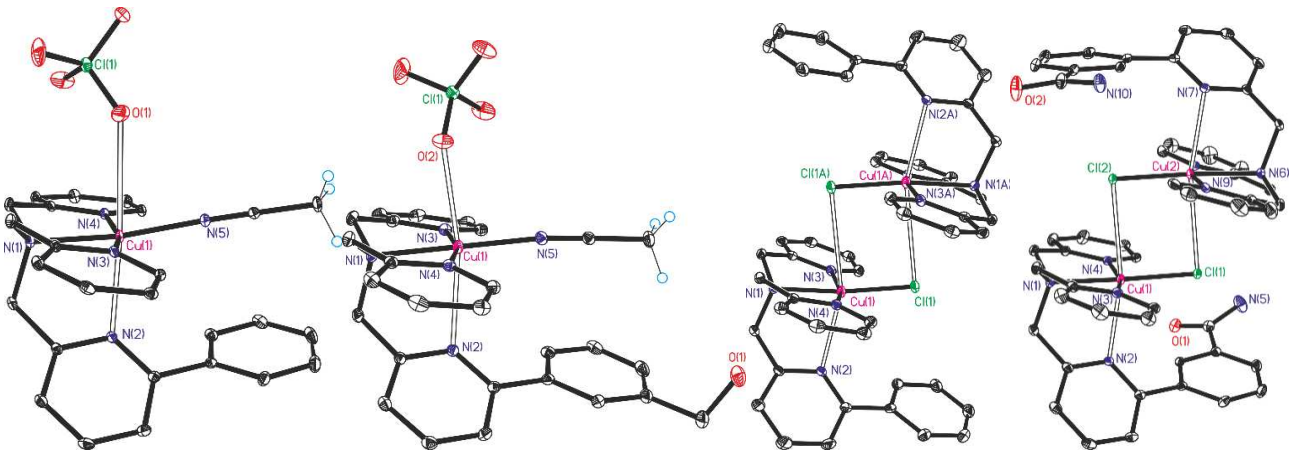

16a R = H; X = ClO_4 **16d** R = CH_2OH; X = ClO_4 **17a** R = H; X = Cl **17c** R = $CONH_2$ X = Cl

Fig. 5A.2. X-ray crystal structures of complexes **16a,d** and **17a,c**.

Table 5A.1

Thermodynamic data for Cu(II) and Cu(I) complexes in CH_3CN + 0.1 M $(C_2H_5)_4NBF_4$ at 25 °C.

			$[Cu^{II}L]^{2+}$ [a]		$[ClCu^{II}L]^{+}$ [b]		$[BrCu^{II}L]^{+}$ [c]	
Entry	L	R	$E^{\ominus}$ (V *vs.* SCE)	β^{II}/β^{I} [d]	$E^{\ominus}$ (V *vs.* SCE)	K^{II}_{Cl}/K^{I}_{Cl} [e]	$E^{\ominus}$ (V *vs.* SCE)	K^{II}_{Br}/K^{I}_{Br} [e]
1	- [f]	-	1.056					
2	**TPMA**	-	-0.019	1.49×10^{18}	-0.363	6.53×10^{5}	-0.282	2.79×10^{4}
3	**15a**	H	0.043	1.33×10^{17}	-0.197	1.14×10^{4}	-0.130	8.40×10^{2}
4	**15b**	CHO	0.071	4.48×10^{16}	-0.203	4.28×10^{4}	-0.157	7.15×10^{3}
5	**15c**	$CONH_2$	0.039	1.56×10^{17}	-0.218	2.21×10^{4}	-0.136	9.08×10^{2}
6	**15d**	CH_2OH	0.045	1.23×10^{17}	-0.200	1.39×10^{4}	-0.131	9.44×10^{2}

[a] Obtained by dissolving the crystalline complexes in acetonitrile. [b] Obtained by dissolving crystalline complexes **16a-d** in acetonitrile, followed by the addition of 2 equivalents of $(C_2H_5)_4NCl$. [c] Obtained by dissolving crystalline complexes **16a-d** in acetonitrile, followed by the addition of 2 equivalents of $(C_2H_5)_4NBr$. [d] β^{II} and β^{I} are the stability constants of $[Cu^{II}L]^{2+}$ and $[Cu^{I}L]^{+}$, respectively. [e] K^{II}_{X} and K^{I}_{X} are the association constants of X^- with $[Cu^{II}L]^{2+}$ and $[Cu^{I}L]^{+}$, respectively. [f] No added ligand, $E^{\ominus}$ of $Cu^{II}(OTf)_2$ taken from ref. 17.

It should be noted that while the reported complexes display octahedral geometries in the solid state, and in two cases are dinuclear, previous solution studies of related complexes suggest a monomeric character and C_3 trigonal-bypiramidal symmetry [11b].

5A.2.2 Cyclic voltammetry of copper complexes

The voltammetric studies were done in collaboration with the research group of Prof. Isse from the University of Padova. The redox properties of the overall complexes were investigated in acetonitrile by cyclic voltammetry. Examples of typical voltammetric pattern for binary $[Cu^{II}L]^{2+}$ and ternary $[XCu^{II}L]^{+}$ complexes are reported in Figure 5A.3. A reversible peak couple, corresponding to one electron transfer was observed for each complex.

$[Cu^{II}L]^{2+} + e^- \rightleftharpoons [Cu^{I}L]^{+}$ (1)

$[XCu^{II}L]^{+} + e^- \rightleftharpoons [XCu^{I}L]$ (2)

The peak-to-peak separation, ΔE_p, was greater than the typical value for a fast or Nernstian electron transfer (ΔE_p = 60 mV) and increased with the scan rate. These results agree with previous reports on the electrochemical behaviour of copper-amine complexes employed as catalysts for ATRP, confirming that electron transfer is accompanied by significant reorganizations.[12] The standard potential ($E^\ominus$) of the Cu(II)/Cu(I) couple was determined as $E^\ominus \approx E_{1/2} = (E_{pc} + E_{pa})/2$, where E_{pc} and E_{pa} are the cathodic and anodic peak potentials, respectively. The average of $E_{1/2}$ values measured with scan rates ranging from 0.02 V/s to 0.2 V/s is reported in **Table 5A.1** as an estimate of $E^\ominus$ for each complex.

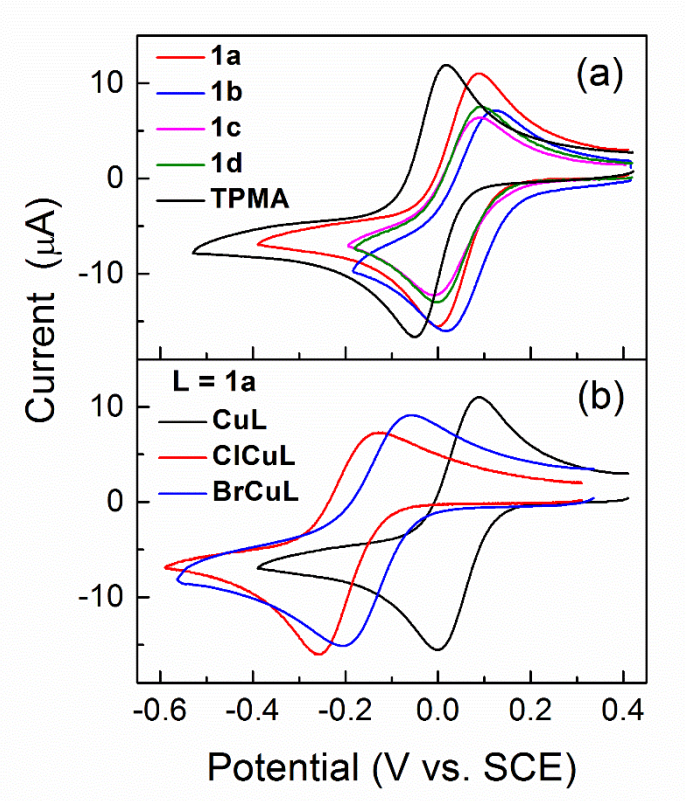

Figure 5A.3. Cyclic voltammetry of 1 mM Cu(II) complexes in CH_3CN + 0.1 M $(C_2H_5)_4NBF_4$, recorded on a GC electrode at a scan rate of 100 mV s^{-1}.

As reported in **Figure 5A.3a** and **Table 5A.1**, small differences on $E^\ominus$ values were observed within the class of compounds formed by Cu(II) and ligands **15a-d**. $E^\ominus$ is weakly affected by the substituent on the phenyl ring probably because of the large distance separating it from the metallic centre. Crystal structures (Fig. 5A.2) support this statement, evidencing that the biarylic system can rotate, increasing the distance between the substituent and the metal.

Although the substituent effect is small, $E^{\ominus}$ of these compounds is 58-90 mV more positive than the redox potential of $[Cu^{II}\mathbf{TPMA}]^{2+}$. It appears that the presence of the phenyl ring significantly decreases the charge density on the metal centre, making it more easily reducible. The reactivity of Cu(I) complexes with these ligands is also expected to be smaller in comparison to $[Cu^{I}\mathbf{TPMA}]^{+}$.

When halide ions were added to a solution of $[Cu^{II}L]^{2+}$, ternary complexes $[XCu^{II}L]^{+}$ were readily formed. Cyclic voltammetry of these compounds (Figure 5A.3b) showed a negative shift of the Cu(II)/Cu(I) peak couple (Eq. 2). $E^{\ominus}$ values calculated from the peak potentials as previously described are reported in **Table 5A.1**. The trend of $E^{\ominus}$ values is quite similar to that observed for the binary complexes: all $[ClCu^{II}L]^{+}$ complexes have similar $E^{\ominus}$ values that are 145-163 mV more positive than $E^{\ominus}$ of $[ClCu^{II}\mathbf{TPMA}]^{+}$. Analogously, $E^{\ominus}$ values of $[BrCu^{II}L]^{+}$ are 125-152 mV more positive than $E^{\ominus}$ of $[BrCu^{II}\mathbf{TPMA}]^{+}$. Nonetheless, the standard potentials of $[XCu^{II}L]^{+}$ are more negative (by 0.18-0.34 V) than those of the corresponding binary complexes $[Cu^{II}L]^{2+}$.

With all ligands **15a-d**, Cu(II) shows much better affinity than Cu(I) for halide ions. This is a fundamental prerequisite for a good ATRP catalyst: Cu(II) must be predominantly present in the deactivator form, $[XCu^{II}L]^{+}$, while Cu(I) is desired to give less stable $[XCu^{I}L]$ complex that readily dissociates to regenerate the activator $[Cu^{I}L]^{+}$ [3a].

5A.2.3 Copper-Catalysed Electrochemically Mediated ATRP

All the copper-catalyzed *e*ATRP reactions were done by the research group of Prof. Isse in the University of Padova. Since the author of this dissertation had a very small contribution to this part of the study the results are going to be briefly discussed in this section, for more information refer to the publication: "Tuning the reactivity and efficiency of copper catalysts for atom transfer radical polymerization by synthetic modification of tris(2- methylpyridyl)amine" N. A. Carmo dos Santos, F. Lorandi, E. Badetti, K. Wurst, A. A. Isse, A. Gennaro, G. Licini, C. Zonta *Polymer*, **2017**, 128, 169-176.

All polymerizations were performed with only one catalyst, the copper complex obtained from ligand **15a** was chosen as model catalyst for the described series of copper complex on *e*ATRP reactions, because, as showed in Table 5A.1, all copper complexes **16a-d** had small differences on $E^{\ominus}$ values, therefore it was assumed that the new complexes have comparable reactivity. Electrochemically mediated atom transfer radical polymerization (*e*ATRP) of different monomers was tested in both organic solvents and water.

The first polymerization trials used methyl acrylate (MA) as monomer in CH_3CN and DMF and the results were similar in both solvents: after 6h of reaction no polymer was formed, however when commercial TPMA was used in the same conditions, the results were positive, the polymerization was achieved with high conversion

and well-controlled. This initial comparison confirmed the lower activity of the new ligands compared with the commercial one. Therefore, the following trials using compound **15a** as ligand for *e*ATRP were done under conditions in which polymerization with TPMA is not well-controlled.

A fourth *e*ATRP experiment was run in DMF using methyl methacrylate (MMA) in place of MA and ethyl 1-phenyl-1-bromoacetate (EBPA) as initiator. Homopolymerization of MMA by *e*ATRP catalyzed by Cu complexes has never been reported before this work. This time good results were obtained: a well-controlled process with 83% conversion in 14 h. *e*ATRP of MMA using Cu/TPMA was also performed, however the higher activity of $[Cu^{I}\ TPMA]^{+}$ resulted in a poor controlled polymerization and lower conversion under analogous conditions.

The polymerization of oligo(ethylene glycol) methyl ether methacrylate (OEOMA) in water using ligand **15a** was well-controlled, the reaction reached 88% conversion in 3 h. While using $[Cu^{II}TPMA]^{2+}$ as catalyst it was obtained a conversion of 95% in 4 h, both results are in agreement. The final polimerirization experiment was performed using MMA as monomer in water, the polymerization of MAA using TPMA as ligand presented 96% conversion in 4 h, when using ligand **15a** instead of TPMA a comparable result was obtained with 83% conversion in 5 h. These results indicate that the copper complex with **15a** ligand is a suitable catalyst for aqueous *e*ATRP, even in acidic conditions, providing a catalytic efficiency comparable to the one observed with copper/TPMA in identical conditions.

5A.3 Conclusion

Eight novel copper complexes with modified TPMA ligands were synthesized and fully characterized. Electrochemical studies have shown a small influence of the substituents in the phenyl ring on the redox properties of the catalyst and hence on its reactivity, the dominant effect being the electron-withdrawing nature of the phenyl substituent itself. The small influence of the substituents can be explained considering that the possible rotation of the biarylic system moves the substituents away from the metal center. Surprisingly, the presence of one phenyl ring on the TPMA backbone reduced significantly the activity of $[Cu^{I}\ L]^{+}$, while substituents on that ring had virtually no effect on catalyst activity. Nevertheless, the novel copper complexes are robust and suitable catalysts for *e*ATRP in organic solvents with reactive monomers such as methyl methacrylate or in aqueous media. Although the new catalysts are less reactive than the parent TPMA complex, their lower catalytic activity may be exploited to gain easy control of extremely reactive systems, where the activation rate is not an issue.

5A.4 Experimental Section

5A.4.1. General Remarks

Acetonitrile (VWR) was distilled over CaH_2 and stored under N_2. Milli-Q ultrapure water was used to prepare aqueous solutions. Tetraethylammonium tetrafluoroborate ($(C_2H_5)4NBF_4$, Alfa Aesar, 99%), used as supporting electrolyte, was recrystallized from ethanol and dried in a vacuum oven at 70 C for 48 h. Tetraethylammonium bromide ($(C_2H_5)4NBr$, Sigma-Aldrich, 99%) and tetraethylammonium chloride ($(C_2H_5)_4NCl$, SigmaAldrich, 98%), used as a source of halide ions, were recrystallized from ethanol and ethanol/acetone (2/1 v/v), respectively, and dried at 70 °C under vacuum for 48 h. All other commercial products were used without further purification.

^1H and $^{13}C\{^1H\}$ NMR spectra were recorded at 301 K on a Bruker AC-400, AC-300, and AC-200 MHz instruments. The ^1H NMR spectra were referenced to the solvent residual peak of MeOD-d_4 (3.31 ppm) or CD_3CN-d_3 (1.94 ppm); the ^{13}C NMR spectra (50 MHz) were referenced to MeOD (49.00 ± 0.02 ppm) or CD_3CN peaks (1.32 ± 0.02 and 118.26 ± 0.02 ppm). Monomer conversion was determined by ^1H NMR at room temperature. Spectra of samples collected in organic solvents were recorded in $CDCl_3$, whereas D_2O was used for water-soluble monomers. Cyclic Voltammetry (CV) and polymerization experiments were carried out in a three-electrode cell by means of an Autolab PGSTAT 30 potentiostat/ galvanostat (EcoChemie, The Netherlands) run by a PC with Autolab GPES 4.9 software. In CV experiments, a Pt ring was used as counter electrode, whereas the working electrode was a glassy carbon (GC) disk, fabricated from a 3 mm diameter GC rod (Tokai GC-20). Before each experiment, the GC surface was cleaned by polishing with a 0.25-mm diamond paste, followed by ultrasonic rinsing in ethanol for 5 min. In *e*ATRP experiments, a Pt mesh and a Pt foil were used as working and counter electrodes, respectively. The working electrode was electrochemically activated by cycling the potential between -0.7 and 1 V vs. Hg/Hg_2SO_4 in 0.5 M H_2SO_4, for 30 min at a scan rate of 0.05 V/s. The counter electrode was separated from the cathodic compartment through a glass frit and a methylcellulose gel saturated with $(C_2H_5)_4NBF_4$. In aqueous media, the reference electrode was a saturated calomel electrode (SCE), whereas Ag|AgI|0.1 M n-Bu_4NI in DMF was used as a reference electrode in organic solvents. In the latter case, the reference electrode was calibrated versus the ferrocenium/ferrocene couple (Fc^+/Fc) after each experiment and potentials were converted to the SCE scale by using the known values of E^o (Fc^+/Fc) vs. SCE: -0.390 in CH_3CN and- 0.476 V in DMF [18]. During electrolysis, the cathodic compartment was maintained under vigorous magnetic stirring and Ar atmosphere. The cell had a double wall jacket through which water was circulated from a thermostatic bath (Thermo Scientific, HAAKE SC100), to keep the temperature constant at 25 °C. The structures of the ligands were characterized by ESI-MS experiments, carried out in positive mode with an Agilent Technologies LC/MSD Trap SL AGILENT instrument. The mobile phase was either methanol or acetonitrile. MS peaks are reported as monoisotopic

mass. Microanalyses were performed with a Flash 2000 Thermo Scientific Analyser. X-ray analysis of each structure was performed, and supplementary crystallographic data were deposited as CCDC-1542046- 49 (**16a** 1542046, **16d** 1542047, **17a** 1542048 and **17c** 1542049). Copies of the data can be obtained, free of charge, at the Cambridge Crystallographic Data Centre.

5A.4.2. General synthetic procedures of copper complexes

0.25 mmol of ligand **15a-d** were dissolved in anhydrous acetonitrile (15 mL) and 43 mg (0.25 mmol) of the desired copper salt ($Cu(ClO_4)_2$*$6H_2O$ or $CuCl_2$*$2H_2O$) were added. The solution was left at room temperature for 15 min, then diethyl ether was added to give a precipitate that was filtered off. The residual solvent was then removed under reduced pressure to give the desired copper complex. Caution! Perchlorate salts of metal complexes with organic ligands are potentially explosive. They should be handled in small quantity and with caution.

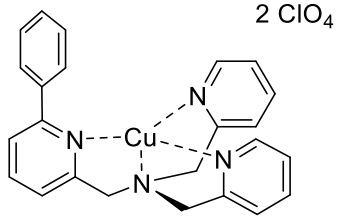

16a Dark blue crystal (85%). IR (KBr, cm^{-1}): 3057, 2333, 1605, 1449, 1074, 769, 619. ESI-MS (m/z) Calc. $C_{24}H_{22}N_4CuClO_4$ 528.1, Found 528.0 (M^+). Elemental analysis Calc. $C_{24}H_{22}N_4Cu$. 2 ClO_4. CH_3CN: C = 46.61%, H = 3.76%, N = 10.45%, Found: C = 46.25%, H = 3.93%, N = 10.45%.

IR (KBr, cm^{-1})

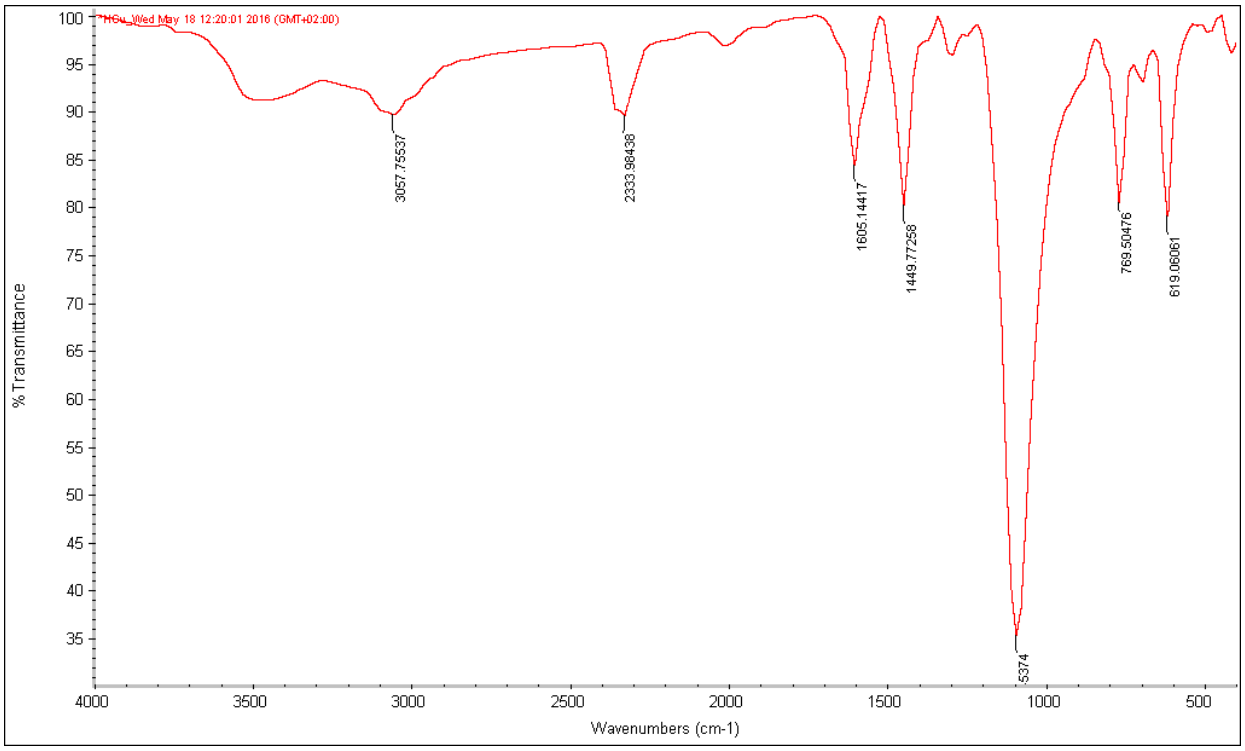

ESI+ MS (m/z)

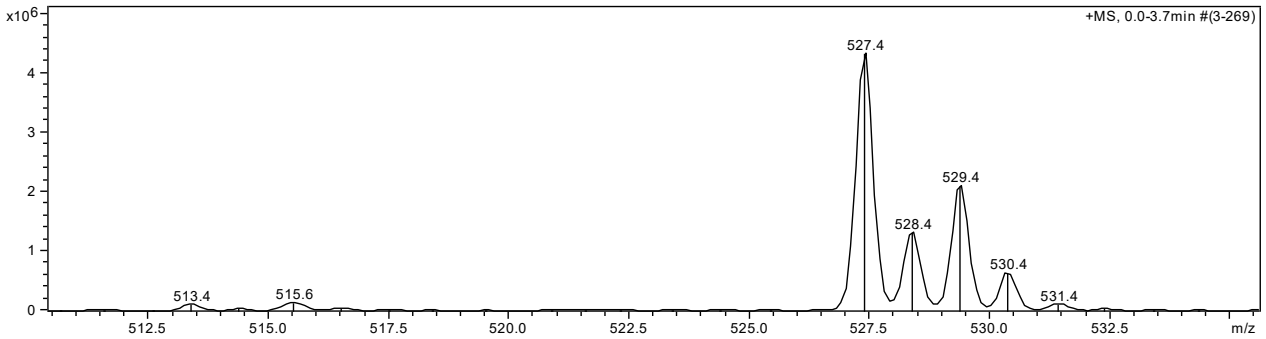

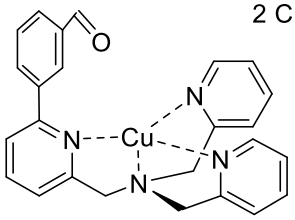

2 ClO_4 **16b** Dark green solid (97%). IR (KBr, cm^{-1}): 3482, 2353, 1693, 1606, 1448, 1172, 776, 622. ESI-MS (m/z) Calc. $C_{25}H_{22}N_4CuClO_5$ 556.1, Found 556.1 (M^+). Elemental analysis Calc. $C_{25}H_{22}N_4Cu$. 2 ClO_4. $6H_2O$: C = 45.7%, H = 3.38%, N = 8.53%, Found: C = 45.26%, H = 3.66%, N = 8.79%.

IR (KBr, cm^{-1})

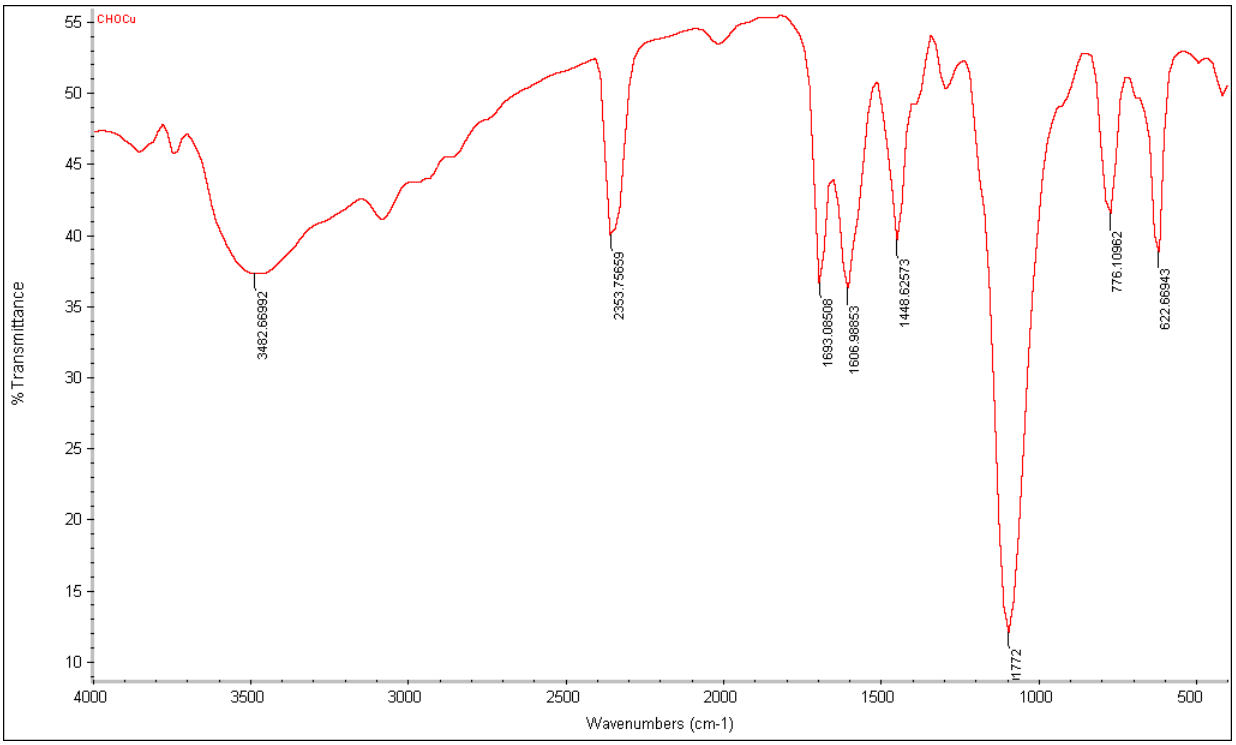

ESI+ MS (m/z)

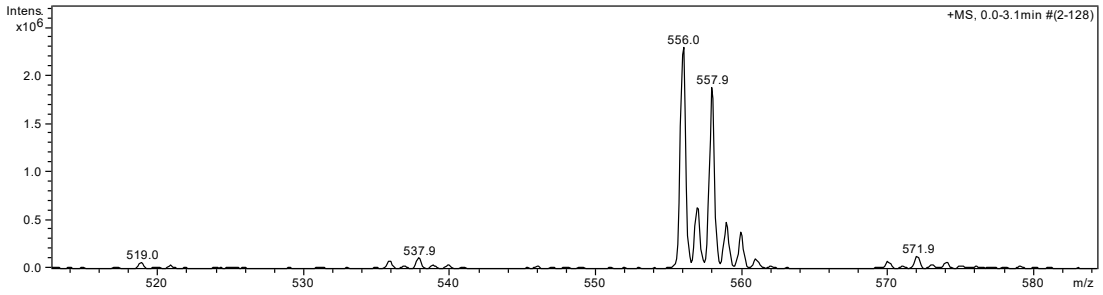

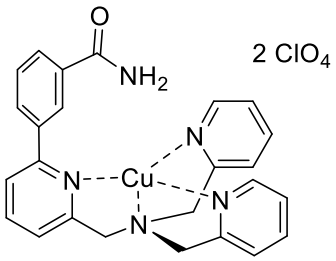

16c Blue solid (95%). IR (KBr, cm^{-1}): 3357, 2354, 1660, 1610, 1572, 1442, 1082, 764, 620. ESI-MS (m/z) Calc. $C_{25}H_{23}N_5CuClO_5$ 571.1, Found 571.0 (M^+). Elemental analysis Calc. $C_{25}H_{23}N_5OCu$. 2 ClO_4. $3H_2O$: C = 41.36%, H = 4.03%, N = 9.65%, Found: C = 41.71%, H = 3.60%, N = 9.98%.

IR (KBr, cm^{-1})

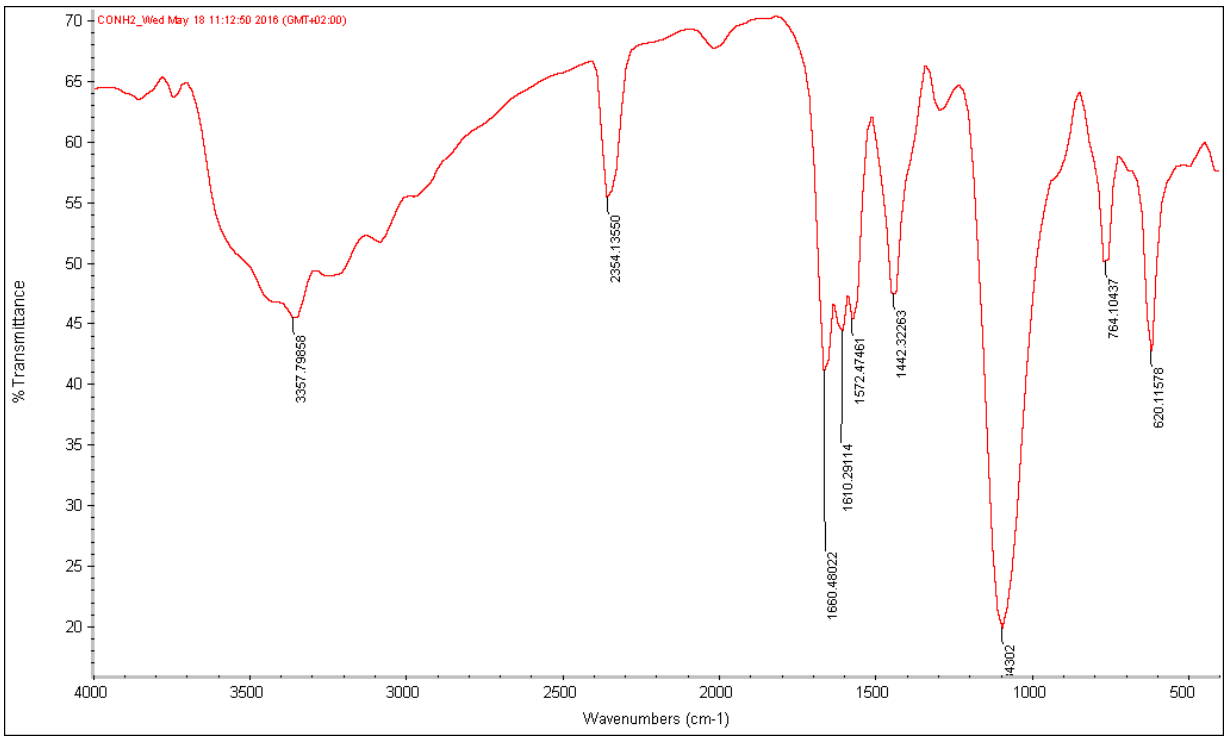

ESI+ MS (m/z)

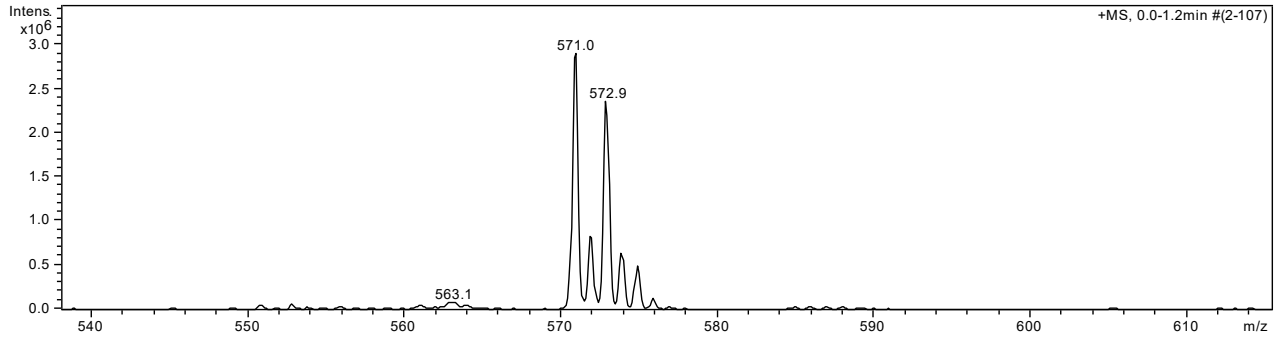

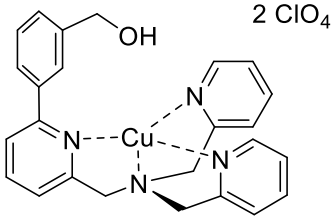

16d Dark blue solid (80%). IR (KBr, cm^{-1}): 3467, 3086, 1601, 1449, 1094, 786, 619. ESI-MS (m/z) Calc. $C_{25}H_{24}N_4CuClO_5$ 558.1, Found 558.0 (M^+). Elemental analysis Calc. $C_{25}H_{24}N_4OCu$. 2 ClO_4. CH_3CN: C = 46.33%, H = 3.89%, N = 10.01%, Found: C = 46.07%, H = 4.07%, N = 10.27%.

IR (KBr, cm^{-1})

ESI+ MS (m/z)

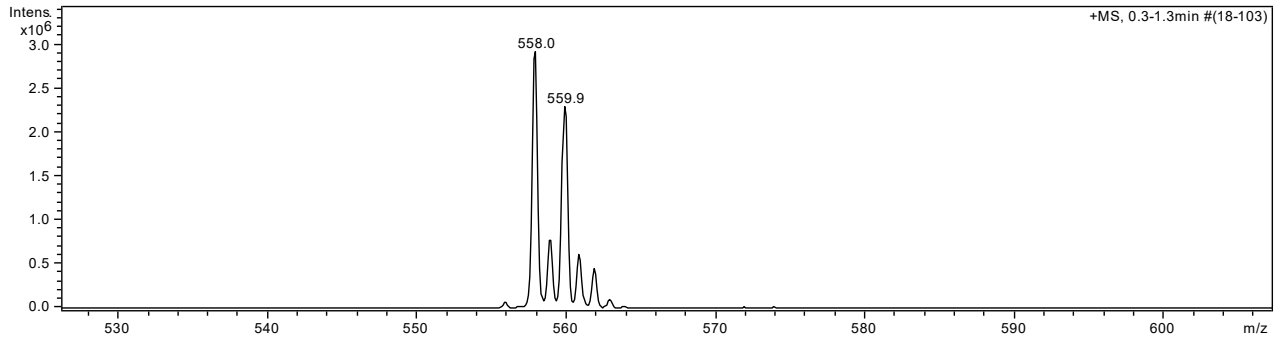

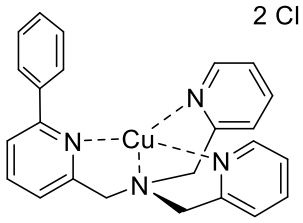

17a Green crystals (87%). IR (KBr, cm^{-1}): 1583, 1445, 765, 692. ESI-MS (m/z) Calc. $C_{24}H_{22}N_4CuCl$ 464.1, Found 464.1 (M^+). Elemental analysis Calc. $C_{24}H_{22}N_4CuCl_2$: C = 57.55%, H = 4.43%, N = 11.19%, Found: C = 57.82%, H = 4.59%, N = 11.42%

. IR (KBr, cm^{-1})

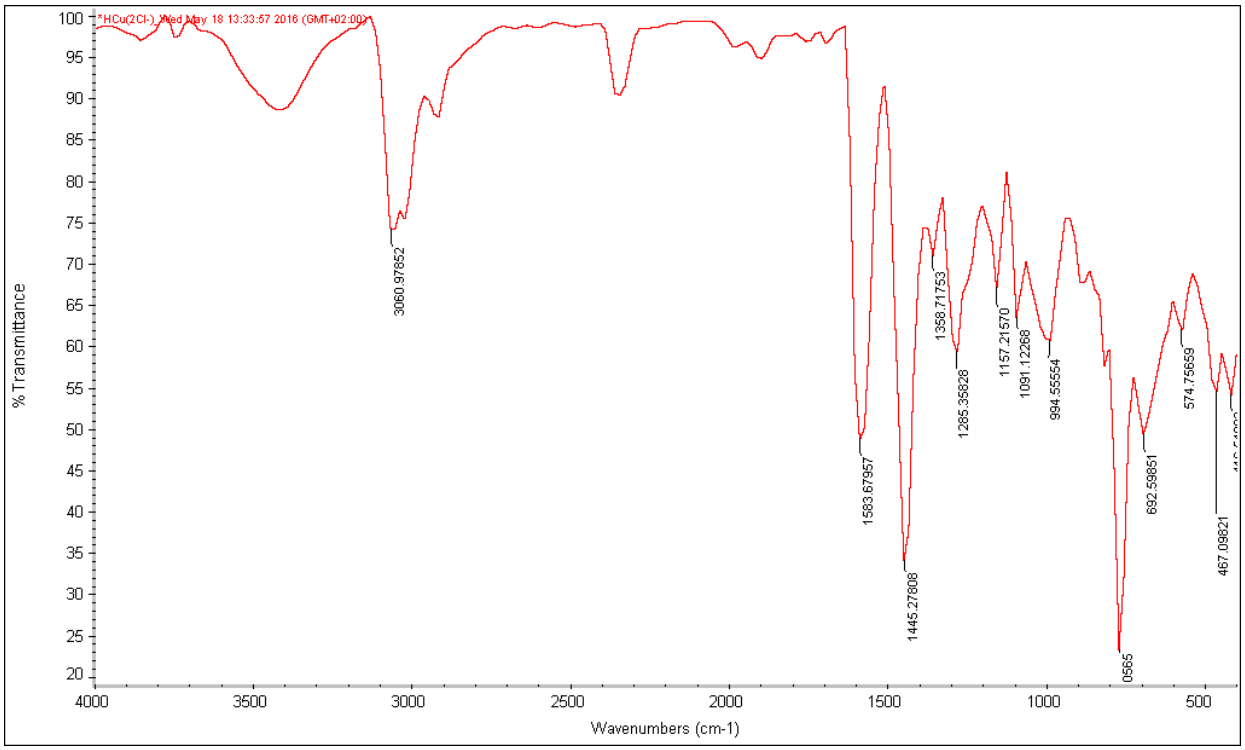

ESI+ MS (m/z)

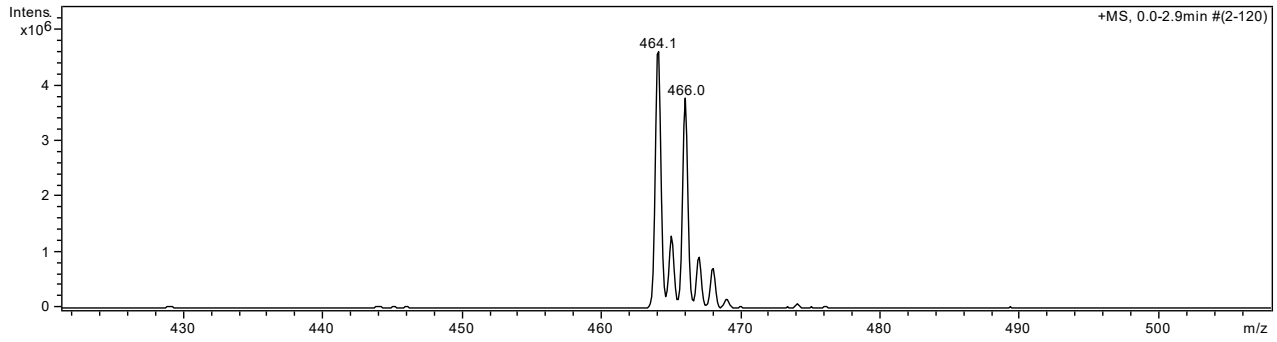

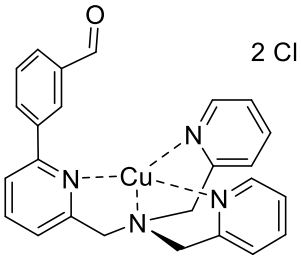

2 Cl

17b Green solid (89%). IR (KBr, cm^{-1}): 3401, 3065, 1662, 1573, 1448, 801, 771. MS (m/z) ESI-MS (m/z) Calc. $C_{25}H_{22}N_4OCuCl$ 492.1, Found 492.1 (M^+). Elemental analysis Calc. $C_{25}H_{22}N_4OCuCl_2$. CH_3CN: C = 56.77%, H = 4.19%, N = 10.59%, Found: C = 55.97%, H = 4.27%, N = 10.57%.

IR (KBr, cm^{-1})

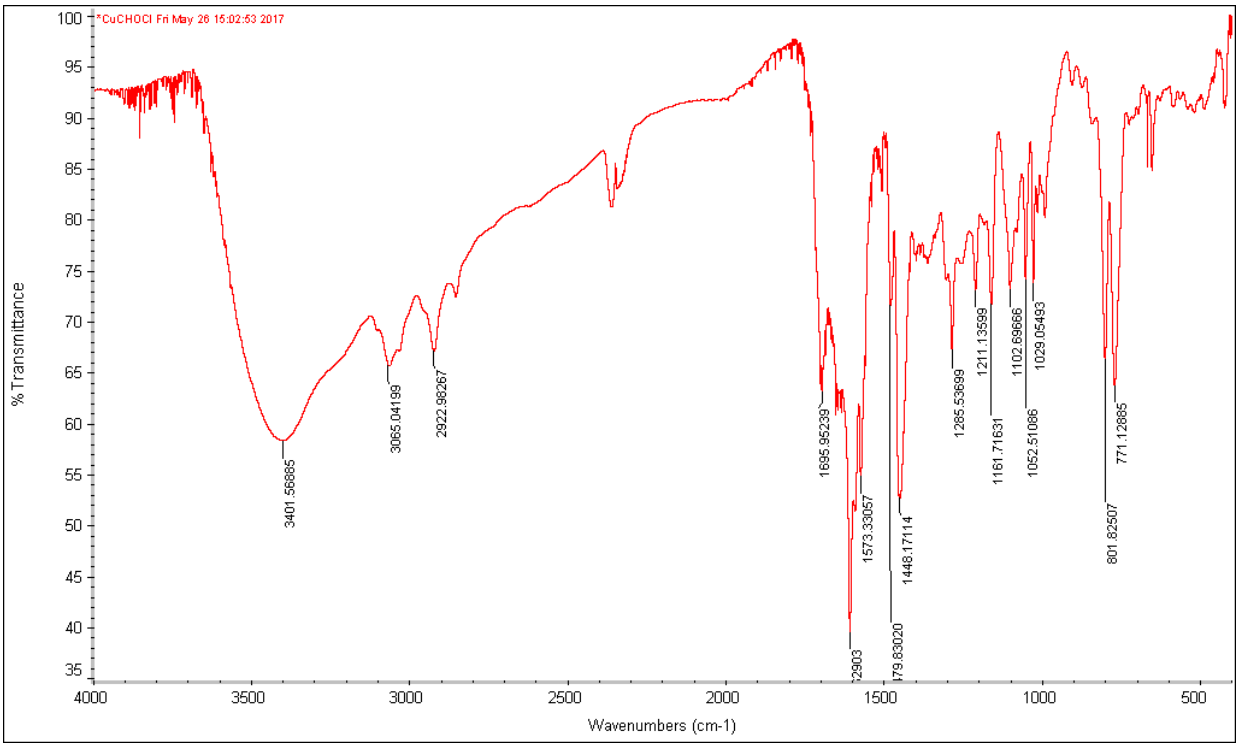

ESI+ MS (m/z)

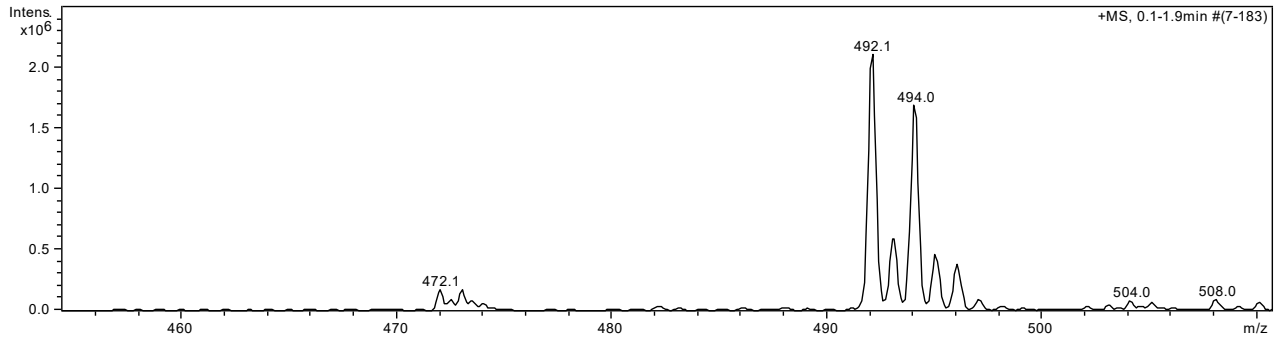

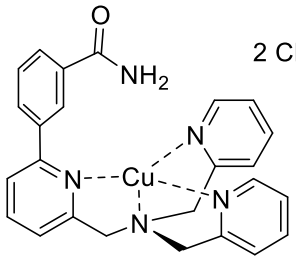

2 Cl

17c Light green needle shape crystal (93%). IR (KBr, cm^{-1}): 3404, 3064, 2353, 1601, 1439, 1382, 763. ESI-MS (m/z) Calc. $C_{25}H_{23}N_5OCuCl$ 507.1, Found 507.0 (M^+). Elemental analysis Calc. $C_{25}H_{23}N_5OCuCl_2$. CH_3CN: C = 55.44%, H = 4.48%, N = 14.37%, Found: C = 55.54%, H = 4.52%, N = 14.57%.

IR (KBr, cm^{-1})

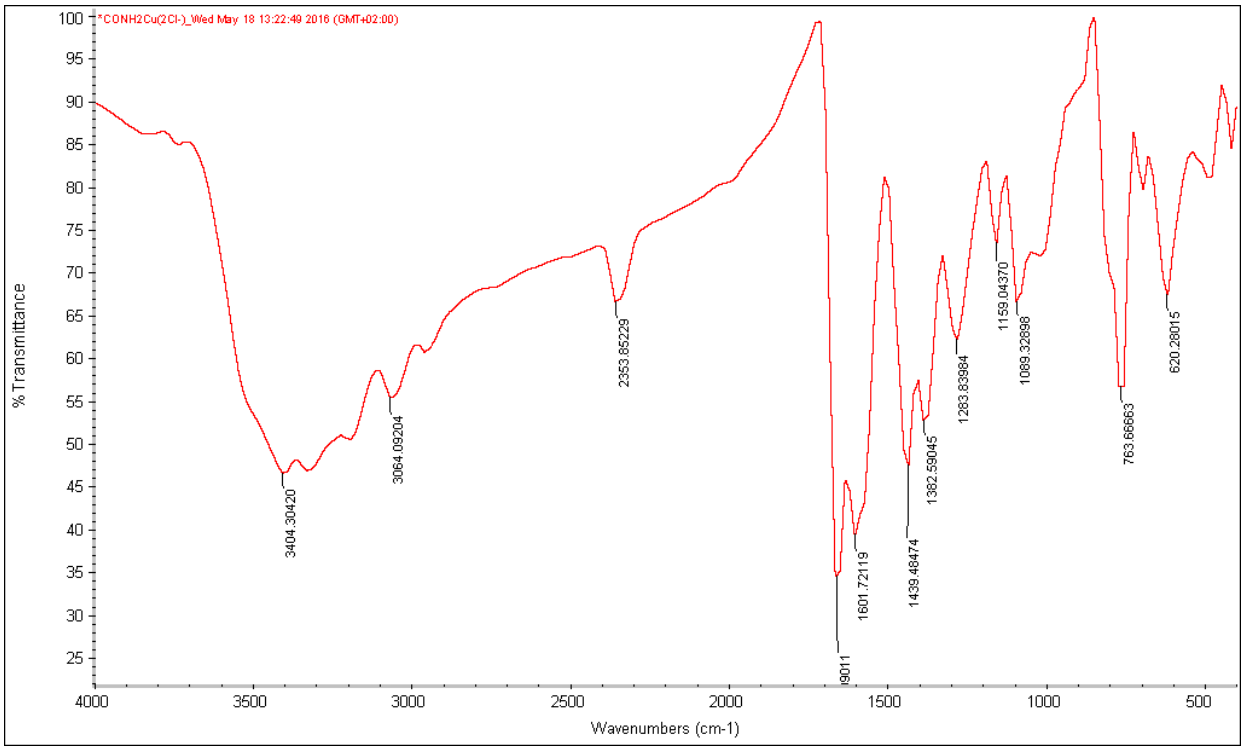

ESI+ MS (m/z)

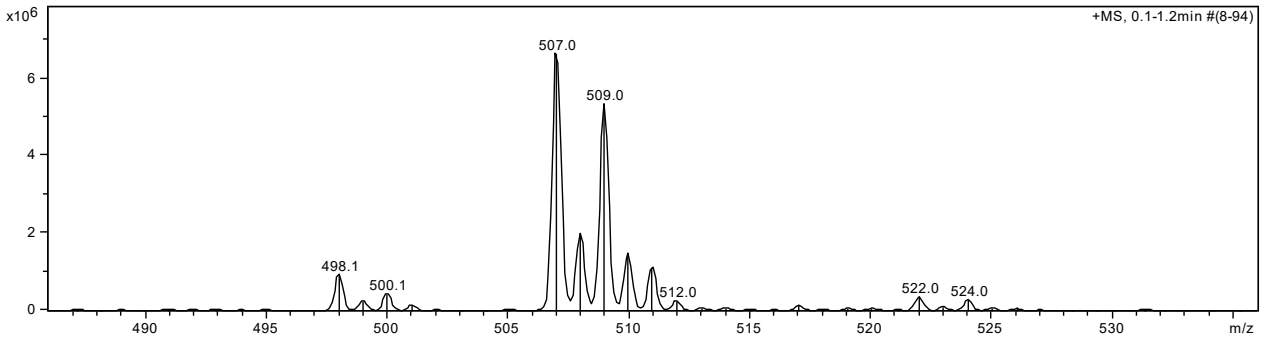

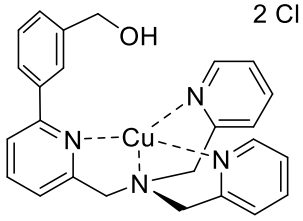

17d Dark green crystal (85%). IR (KBr, cm^{-1}): 3382, 3020, 2915, 1589, 1439, 1288, 1186, 1005, 799. ESI- MS (m/z) Calc. $C_{25}H_{24}N_4OCuCl$ 494.1, Found 494.0(M^+). Elemental analysis Calc. $C_{25}H_{24}N_4OCuCl_2$: C = 56.56%, H = 4.56%, N = 10.55%, Found: C = 56.33%, H = 4.78%, N = 10.72%.

IR (KBr, cm^{-1})

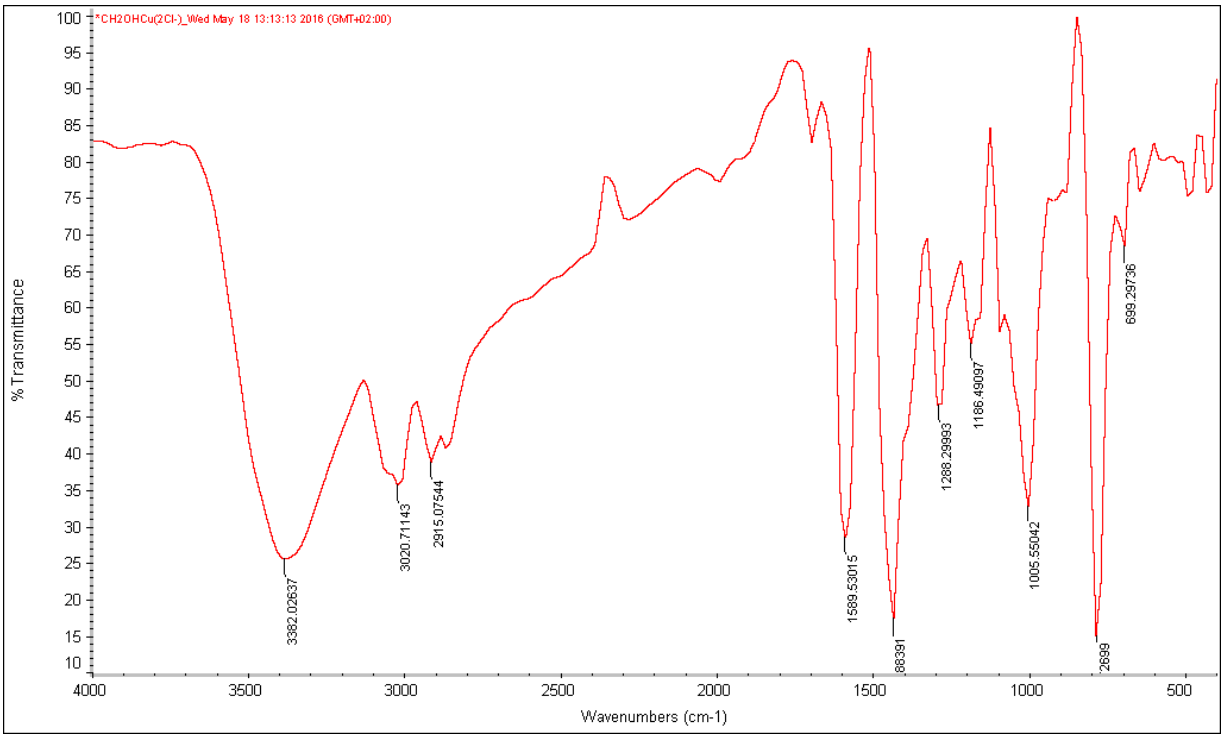

ESI+ MS (m/z)

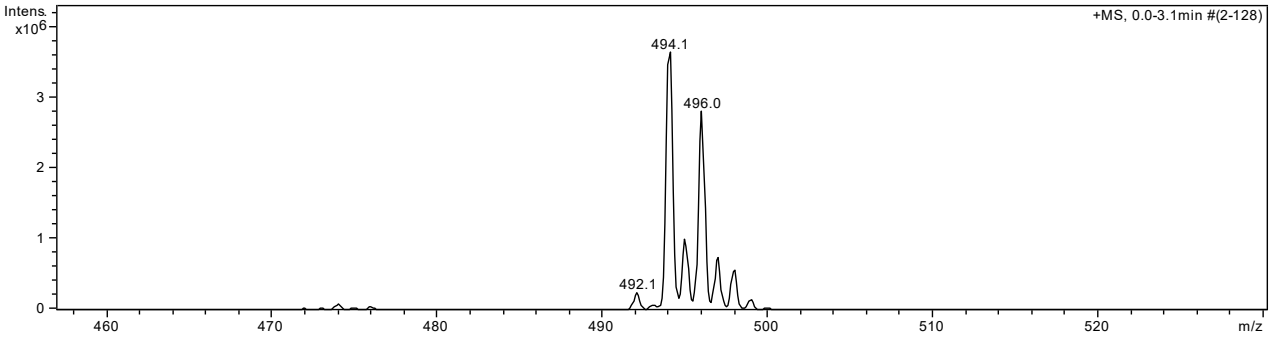

5A.5 References

[1] (a) K. Matyjaszewski, *Macromolecules* **2012**, 45, 4015-4039. (b) K. Matyjaszewski and N. V. Tsarevsky, *J. Am. Chem. Soc.*, **2014**, 136, 6513-6533; (c) C. Boyer, N. A. Corrigan, K. Jung, D. Nguyen, T.-K. Nguyen, N. N. M. Adnan, S. Oliver, S. Shanmugam and J. Yeow, *Chem. Rev.* **2016**, 116, 1803–1949.

[2] K. Matyjaszewski, and J. Xia, *Chem. Rev.* **2001**, 101, 2921.

[3] P. De Paoli, A. A. Isse, N. Bortolamei and A. Gennaro, *Chem. Commun.*, **2011**, 47, 3580-3582; (b) A. A. Isse, N. Bortolamei, P. De Paoli, A. Gennaro, *Electrochim. Acta* **2013**, 110, 655−662.

[4] W. Tang, Y. Kwak, W. Braunecker, N. V. Tsarevsky, M. L. Coote and K. Matyjaszewsk, *J. Am. Chem. Soc.*, **2008**, 130, 10702-10713.

[5] (a) W. Jakubowski and K. Matyjaszewski, *Angew. Chem. Int. Ed.*, 2006, 45, 4482−4486; (b) K. Matyjaszewski, W. Jakubowski, K. Min, W. Tang, J. Huang, W. A. Braunecker and N. V. Tsarevsky, *Proc. Natl. Acad. Sci. U. S. A.* **2006**, 103, 15309−15314.

[6] D. Konkolewicz, A. J. D. Magenau, S. E. Averick, A. Simakova, H. He and K. Matyjaszewski, *Macromolecules*, **2012**, 45, 4461-4468.

[7] D. Konkolewicz, Y. Wang, P. Krys, M. Zhong, A. A. Isse, A. Gennaro and K. Matyjaszewski, *Polym. Chem.*, **2014**, 5, 4396−4417.

[8] B. M. Rosen and V. Percec, *Chem. Rev.*, **2009**, 109, 5069−5119.

[9] (a) A. Anastasaki, V. Nikolaou, Q. Zhang, J. Burns, S. R. Samanta, C. Waldron, A. J. Haddleton, R. McHale, D. Fox, V. Percec, P. Wilson and D. M. Haddleton, *J. Am. Chem. Soc.*, **2014**,

136, 1141-1149; (b) X. Pan, C. Fang, M. Fantin, N. Malhotra, W. Y. So, L. A. Peteanu, A. A. Isse, A. Gennaro, P. Liu and K. Matyjaszewski, *J. Am. Chem. Soc.*, **2016**, 138, 2411-2425.

[10] (a) A. J. D. Magenau, N. C. Strandwitz, A. Gennaro and K. Matyjaszewski, *Science*, **2011**, 332, 81−84; (b) N. Bortolamei, A. A. Isse, A. J. D. Magenau, A. Gennaro and K. Matyjaszewski, *Angew. Chem. Int. Ed.* **2011**, 50, 11391−11394; (c) M. Fantin, A. A. Isse, A. Gennaro and K. Matyjaszewski, *Macromolecules*, **2015**, 48, 6862-6875; (d) F. Lorandi, M. Fantin, A. A. Isse and A. Gennaro, *Polym. Chem.*, **2016**, 7, 5357-5365.

[11] (a) K. Schröder, R. T. Mathers, J. Buback, D. Konkolewicz, A. J. D. Magenau and K. Matyjaszewski, *ACS Macro Lett.*, **2012**, 1, 1037−1040; (b) A. Kaur, T. G. Ribelli, K. Schröder, K. Matyjaszewski and T. Pintauer, *Inorg. Chem.*, **2015**, 54, 1474-1486; (c) M. Fantin, A. A. Isse, N. Bortolamei, K. Matyjaszewski and A. Gennaro, *Electrochim. Acta*, **2016**, 222, 393–401.

[12] J. Qiu, K. Matyjaszewski, L. Thouin, C. Amatore, *Macromol. Chem. Phys.*, **2000**, 201, 1625-1631.

[13] P. Chmielarz, M. Fantin, S. Park, A. A. Isse, A. Gennaro, A. J.D. Magenau, A. Sobkowiak and K. Matyjaszewski, Prog. Polym. Sci. **2017**, 69, 47-78.

[14] (a) C. Bravin, E. Badetti, F. A. Scaramuzzo, G. Licini and C. Zonta, *J. Am. Chem. Soc.*, **2017**, 139, 6456-6460; (b) F. A. Scaramuzzo, G. Licini and C. Zonta *Chem. Eur. J.*, **2013**, 19, 16809-16813; (c) E. Badetti, K. Wurst, G. Licini and C. Zonta, *Chem. Eur. J.*, **2016**, 22, 6515–6518; (d) R. Berardozzi, E. Badetti, N. A. Carmo dos Santos, K. Wurst, G. Licini, G. Pescitelli, C. Zonta and L. Di Bari, *Chem. Commun.*, **2016**, 52, 8428-8431.

[15] M. Natali, E. Badetti, E. Deponti, M. Gamberoni, F. A. Scaramuzzo, A. Sartorel and C. Zonta, *Dalton Trans*., **2016**, 45, 14764-14773.

[16] P. Comba, A. Hauser, M. Kerscher and H. Pritzkow, *Angew. Chem. Int. Ed.*, **2003**, 42, 4536-4540.

[17] N. Bortolamei, A.A. Isse, V.B. Di Marco, A. Gennaro, K. Matyjaszewski, *Macromolecules* **2010**, 43, 9257-9267.

[18] L. Falciola, A. Gennaro, A.A. Isse, P.R. Mussini, M. Rossi, *J. Electroanal.Chem.* **2006**, 593, 47-56.

5B.1. Introduction

The research for renewable energy sources that are cheap, abundant and wide-ranging is a current concern in modern society.[1] The production of hydrogen gas as a clean fuel by solar-driven water splitting is considered a viable solution, however it presents some challenges.[2] In the last years, great attention has been paid to the preparation and characterization of molecular hydrogen evolving catalysts (HECs),[3] specially on their implementation into light-driven photoreaction schemes.[4] The study of HECs based on first-row transition metals receives special attention in this research field,[4,6,7,8] because when compared to noble-metals these transition metals are cheaper, more abundant, and less toxic, therefore compatible with a sustainable energy approach.[3c] Due to the synthetic simplicity and flexibility, metal complexes based on polydentated-pyridine ligands have broad usage among the HECs investigations,[9] these compounds present efficient catalytic activity in purely aqueous solutions, and enhanced stability under turnover conditions. With the recent interest within the research group in the molecular recognition and catalytic properties of these systems[9l,10] it was decided to give some attention toward the synthesis and characterization of four metal complexes **20a-d** obtained by coordination of the pentadentate ligand **19**, the 8-hydroxyquinoline-di(2-picolyl)amine, with first-row transition metals such as cobalt, nickel, iron, and zinc (Scheme 5B.1).

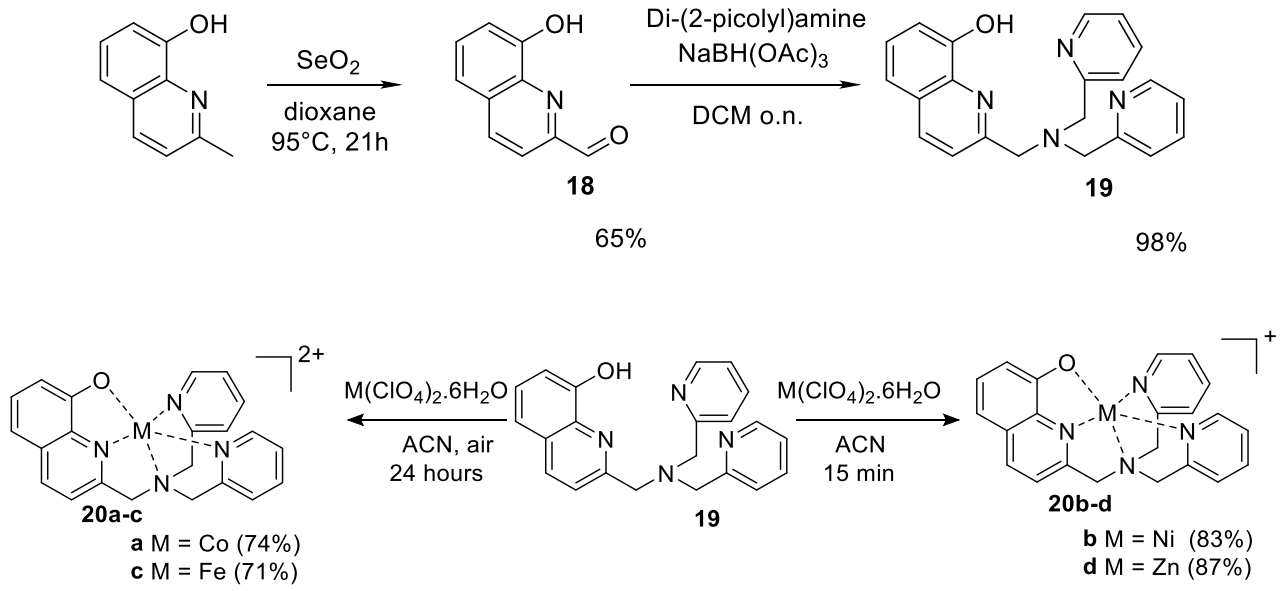

Scheme 5B.1. General synthetic procedure for the preparation of ligand **19** and metal complexes **20a-d**.

The described complexes have been evaluated as possible HEC catalysts and tested under photoactivated conditions within two different photochemical systems, namely (i) a aqueous solution (1 M acetate buffer, pH 5) with $Ru(bpy)_3Cl_2 \cdot 6H_2O$ (where bpy = 2,2'-bipyridine) as the sensitizer and ascorbic acid as the sacrificial electron donor and (ii) a 50/50 acetonitrile/water mixture (pH 10) using $Ir(ppy)_2(bpy)PF_6$ (where ppy = 2-

phenylpyridine and bpy = 2,2'-bipyridine) as the chromophore and triethylamine (TEA) as the sacrificial reagent.

5B.2. Results and discussion

5B.2.1. Synthesis and Coordination Chemistry

Ligand **19** has been prepared in two steps by oxidation of commercially available 2-methyl-8-quinolinol with selenium dioxide in dioxane for 21 hours at 95°C to give 8-hydroxyquinoline-2-carboxaldehyde,[11] followed by reductive amination with di(2-picolyl)amine (Scheme 5B.1, left). The compound is a light yellow oil and can be obtained in good yield. The general procedure for the synthesis of the metal complexes requires the mixing of an equimolar amount of ligand **19** to the corresponding dicationic perchlorate salt (Co^{2+}, Ni^{2+}, Fe^{2+}, or Zn^{2+}) in acetonitrile. The solution was stirred at room temperature (15 minutes for the nickel and zinc cases, 24 hours for both cobalt and iron) and the desired compounds were obtained either as crystalline powders or by recrystallization with diethyl ether (Scheme 5B.1, right). While in the case of the nickel and zinc metal centers the complexes are stable in their original oxidation state (i.e., +2), in the case of cobalt and iron the crystallization process in air leads to the formation of the cobalt(III) and iron(III) complexes. The obtained products have been characterized by ESI-MS and Elemental Analysis. In the case of complexes **20a** and **20c** it was also possible to obtain crystals suitable for X-ray diffraction, the crystallographic study was done in collaboration with Prof. Klaus Wurst (University of Innsbruck). The molecular structure of both complexes are displayed in Figure 5B.1, while relevant crystallographic data are reported in Table 5B.1. In the crystal structure of complex **20a** (Figure 5B.1, left; relevant bond lengths and angles are gathered in Table 5B.2 and 5B.3, respectively), the central cobalt ion is observed to be six-coordinated with a distorted octahedral geometry wherein the pentadentate 8-hydroxyquinoline-di(2-picolyl)amine ligand is shown to chelate the metal center and an acetonitrile solvent molecule is placed in the apical position to complete the pseudo-octahedral coordination motif. The distortion with respect to the ideal octahedral geometry is expected to be largely imparted by the structural constrain of the chelating ligand, as demonstrated by the bond angles between the cobalt center and the nitrogen atoms which result systematically lower than 90° (see Table 5B.3). Importantly, the average Co-N bond length is 1.907(4) Å and falls within the range typically observed for related cobalt(III) polypyridine complexes,[12] thus confirming the occurrence of a Co(II)-to-Co(III) oxidation during the crystallization process under air-equilibrated conditions.¥ Interestingly, the shortest length is observed for the Co-N(2) bond (1.734 Å, see Table 5B.2) which might be related to both the better σ-donation and π-back-bonding abilities of the quinoline moiety with respect to the amine and pyridine ligands.[13] These enhanced electronic effects exerted by the quinoline moiety on the cobalt center are also seen to remarkably influence the length of the bond between the metal and the acetonitrile solvent molecule, resulting in the elongation of the Co-N bond (2.012 Å, see Table 5B.2) with respect to the average

distance. Importantly, this latter observation may be potentially relevant in order to enable those processes (namely ligand detachment and proton coordination) which are typically expected in the catalytic HER mechanism by a six-coordinated metal complex.[5,9]

Table 5B.1. Relevant crystallographic data obtained from X-ray diffraction on crystals of complexes **20a** and **20c**.

	20a	**20c**
Space Group	I 4_1/a	P -1
Cell Lengths (Å)	a 11.8893(5) b 11.8893(5) c 42.742(2)	a 12.5578(4) b 12.6591(5) c 18.4393(6)
Cell Angles (°)	α 90 β 90 γ 90	α 86.2019(14) β 83.5197(14) γ 68.4545(13)
Cell Volume (Å^3)	6041.81	2708.09
Z, Z’	Z: 8 Z': 0	Z: 2 Z': 0

Table 5B.2. Relevant bond lengths of complex **20a**.

Atom 1	**Atom 2**	**Length (Å)**
Co(1)	**N(1)**	1.939
Co(1)	**N(3)**	1.926
Co(1)	**N(3A)**	1.926
Co(1)	**N(2)**	1.734
Co(1)	**O(1)**	1.928
Co(1)	**N(4)**	2.012

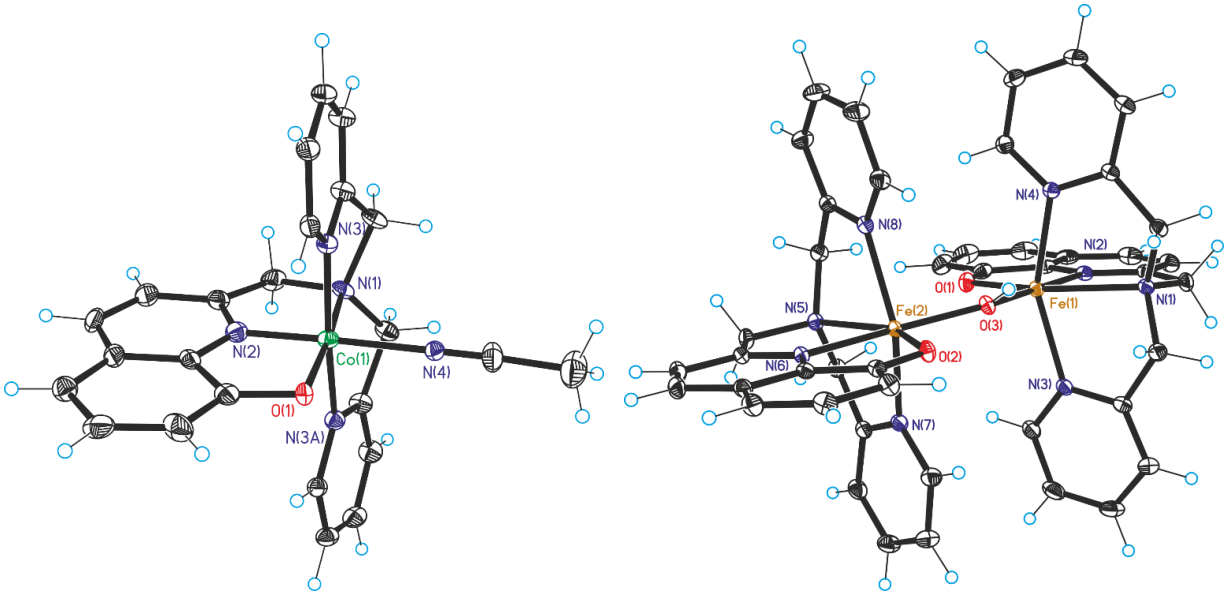

Figure. 5B.1. Crystal structure of complexes **20a** (left) and **20c** (right) with selected atom labeling.

Table 5B.3. Relevant bond angles of complex **20a**.

Angle	(°)
N(1)-Co(1)-N(2)	88.24
N(1)-Co(1)-N(3)	83.02
N(1)-Co(1)-N(3A)	86.42
N(1)-Co(1)-N(4)	95.44
N(2)-Co(1)-O(1)	87.64
N(2)-Co(1)-N(3)	89.57
N(2)-Co(1)-N(3A)	91.93
N(3)-Co(1)-O(1)	96.64
N(3)-Co(1)-N(4)	90.13
N(3A)-Co(1)-O(1)	94. 02
N(3A)-Co(1)-N(4)	89.05
N(4)-Co(1)-O(1)	88.68

Interestingly, in the case of the iron analogue **20c**, the crystallization process leads to the formation of a dinuclear structure as determined by X-ray diffraction (Figure 5B.1, left; relevant bond angles are collected

in Table 5B.4 of the ESI). Both iron centers are surrounded by one 8-hydroxyquinoline-di(2-picolyl)amine ligand and a hydroxo group *trans* to the quinolinic nitrogen, with the latter acting as a bridging ligand and completing a six-coordinating environment around the metal centers in a distorted pseudo-octahedral geometry. The two hydroxyquinoline moieties are oriented toward opposite directions and lie within the same plane of the Fe-O(H)-Fe bridge. Similarly, to the cobalt case, the observed distortion appears largely determined by the structural constrain exerted by the chelating pentadentate ligand. The two iron complexes within the dimeric species are similar in terms of coordination motif and geometry, although they are not completely identical since slightly different bond distances and angles are measured (Table 5B.4), likely attributable to different intramolecular interactions in the solid state.[14] More importantly, the average Fe-N bond length (2.147 Å) and the mean Fe-O distance (1.944 Å) are comparable to those found for related iron(III) complexes featuring a similar ligand environment[14,15] and thus confirm the presence of a 3+ metal center. Also, the Fe(1)···Fe(2) distance (3.710 Å) and the Fe(1)-O(3)-Fe(2) bond angle (142.07°, see Table 5B.5) fall within the range typically observed for unsupported μ-OH-bridged Fe(III) dimers featuring similar coordination motifs.[14] While showing up as a dinuclear species in the solid state, complex **20c** appears as a monomeric compound in fluid solution, as demonstrated by ESI-MS analysis. In fact, this is not unexpected in view of the potential liability of the hydroxo bridge in a strongly coordinating environment.

5B.2.1. Electrochemical and Catalytical Studies

The catalytical investigations of the described transition metal complexes were done in collaboration with Dr. Mirco Natali (University of Ferrara). The preliminary redox studies involving complexes **20a-c** showed their potential ability to act as competent hydrogen evolving catalysts under light-activated conditions. All complexes presented changes on their electrochemical profiles with the crescent addition of acetic acid aliquots. The required potentials to power hydrogen evolution appeared substantially negative.

Two different photochemical systems were tested i) Ru(bpy)32+/ascorbic acid and ii) the Ir(ppy)2(bpy)+/TEA sensitizer/sacrificial donor couples. The electrochemical results show that all redox-active metal complexes **20a-c** may actually behave as competent HECs. Although only the cobalt compound presented substantial hydrogen evolving activity, under photochemical conditions, in both systems achieving TONs up to 10 and **19**, respectively, with maximum TOFs of 7.2 and 16.2 h^{-1}, respectively. The nickel and iron complexes, on the other hand, exhibit appreciable photocatalytic activity only in the iridium-based photochemical system, while showing negligible hydrogen evolution in the ruthenium one, similarly to what observed with the inactive zinc complex **20d**. Complexes **20a-c**, however, display considerably lower activity toward proton reduction with respect to state-of-the-art polypyridine metal complexes reported in the literature.

Table 5B.4. Relevant bond angles of the **(20c)$_2$OH** dimer.

Angle	(°)
N(1)-Fe(1)-N(2)	73.69
N(2)-Fe(1)-O(1)	79.46
O(1)-Fe(1)-O(3)	100.27
N(1)-Fe(1)-O(3)	106.59
N(3)-Fe(1)-O(3)	92.82
N(4)-Fe(1)-O(3)	89.69
N(4)-Fe(1)-N(2)	90.26
N(3)-Fe(1)-N(2)	87.36
N(3)-Fe(1)-O(1)	103.73
N(3)-Fe(1)-N(1)	76.64
N(4)-Fe(1)-N(1)	76.97
N(4)-Fe(1)-O(1)	102.16
Fe(1)-O(3)-Fe(2)	142.07
O(3)-Fe(2)-O(2)	92.02
N(6)-Fe(2)-O(2)	78.75
N(6)-Fe(2)-N(5)	74.26
O(3)-Fe(2)-N(5)	115.02
N(6)-Fe(2)-N(8)	88.79
N(8)-Fe(2)-O(3)	91.77
N(7)-Fe(2)-O(3)	92.63
N(6)-Fe(2)-N(7)	91.42
N(7)-Fe(2)-O(2)	102.90
N(5)-Fe(2)-N(7)	76.14
N(8)-Fe(2)-O(2)	105.51
N(5)-Fe(2)-N(8)	76.10

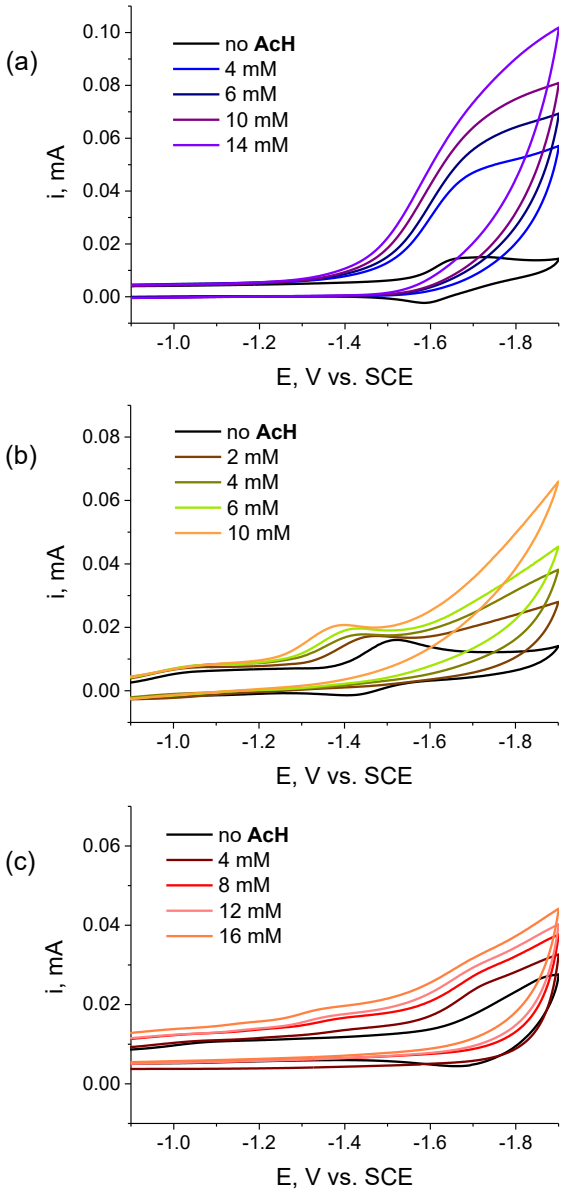

Figure 5B.2. Cyclic voltammetry of (a) 1 mM **20a**, (b) 1 mM **20b**, and (c) 1 mM **20c** in acetonitrile solution (0.1 M TBAPF6) upon addition of several aliquots of acetic acid (AcH). Experimental conditions: GC as WE, Pt as CE, SCE as reference, scan rate v = 100 mV/s

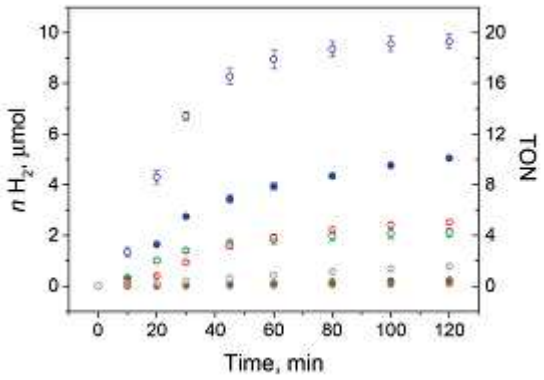

Figure 5B.3. Photocatalytic hydrogen evolution kinetics (average of two independent experiments) using complexes **20a** (blue dots), **20b** (green dots), **20c** (red dots) and **20d** (grey dots) in the ruthenium- (full dots) and iridium-based (empty dots) photochemical systems.

5B.3. Conclusions

New first-row transition metal complexes **20a-d** based on the 8-hydroxyquinoline-di(2-picolyl)amine ligand have been prepared and those based on redox active metal centers (**20a-c**) studied as potential hydrogen evolving catalysts under both electrochemical and light-driven conditions. The chelating properties of the new 8-hydroxyquinoline-di(2-picolyl)amine ligand are favorable toward the stabilization of the metal complexes in their coordination geometry also leaving a labile (and thus potentially available) coordination site to enable proton binding, the enhanced electron donating effect of the hydroxyquinoline moiety apparently increases the electronic density on the metal center thus shifting the metal-based reduction processes toward highly negative potentials. In this respect the formation of the nucleophilic M(I) species which is required to favor protonation as well as the subsequent reduction of the M(III)-H intermediate turn out to be thermodynamically more demanding than commonly observed with other polypyridine complexes. Therefore, catalyst activation by the photogenerated reducing agent, either in the ruthenium- and iridium-based photochemical systems, may actually compete unfavourably with side-reaction phenomena thereby leading to rapid abatement of the photocatalytic activity.

5B.4. Experimental Section

5B.4.1. General Remarks

Milli-Q Ultrapure water and spectroscopic grade acetonitrile (Sigma-Aldrich) were used for the photocatalysis experiments. Anhydrous acetonitrile (Alfa Aesar) was used for the electrochemical measurements. $Ru(bpy)_3Cl_2 \cdot 6H_2O$ was purchased from Sigma-Aldrich and used as received. All other reagents were purchased from commercially available suppliers and used as received.

The supplementary crystallographic data were deposited as CCDC 1556115-1556116. Copies of the data can be obtained, free of charge, at the Cambridge Crystallographic Data Centre.

^1H and $^{13}C\{^1H\}$ NMR spectra were recorded at 301 K on a Bruker AC-400, AC-300, and AC-200 MHz instruments. The ^1H NMR spectra were referenced to the solvent residual peak of MeOD-d_4 (3.31 ppm) or CD_3CN-d_3 (1.94 ppm); the ^{13}C NMR spectra (50 MHz) were referenced to MeOD (49.00 ± 0.02 ppm) or CD_3CN peaks (1.32 ± 0.02 and 118.26 ± 0.02 ppm). UV-Vis absorption spectra were recorded on a Jasco V-570 UV/Vis/NIR spectrophotometer. Cyclic Voltammetry (CV) measurements were carried out with a PC-interfaced Eco Chemie Autolab/Pgstat 30 Potentiostat. A conventional three-electrode cell assembly was adopted: a saturated calomel electrode (SCE, Amel) and a platinum electrode were used as reference and counter electrodes, respectively; a glassy carbon (GC) electrode (7 mm^2 surface area) was used as the working

electrode. All experiments were performed in nitrogen-purged acetonitrile solutions. The $TBAPF_6$ supporting electrolyte was dried overnight before use. The GC electrode was accurately polished with alumina slurry after every scan. The hydrogen evolution experiments were carried out upon continuous visible light irradiation with a 175 W Xe arc-lamp (CERMAX PE175BFA) of a reactor containing the solution (a 10 mm pathlength pyrex glass cuvette with head space obtained from a round-bottom flask). A cut-off filter at λ < 400 nm and a hot mirror (IR filtering) have been used in order to provide the useful wavelength range (400-800 nm). The gas phase of the reaction vessel was analyzed on an Agilent Technologies 490 microGC equipped with a 5 Å molecular sieve column (10 m), a thermal conductivity detector, and using Ar as carrier gas.

5B.4.2. Synthetic procedures

5B.4.2.1. General procedure for synthesis of 8-hydroxyquinoline-2-carbaldehyde (18):

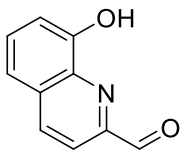

It was adopted a reported synthetic procedure with minor modifications.[16] Commercially available 8-hydroxy-2-methyl-quinoline (25.1 mmol) was added to a suspension of selenium oxide (8.364 g, 75.4 mmol) in dioxane (100 ml) under N_2 atmosphere. The mixture was heated at 95 °C during 21 h. After cooling at room temperature, the mixture was filtered on celite. The filtrate was concentrated under vacuum. Purification of the resulting crude product on silica column chromatography (dichloromethane) afforded the desired product as a yellow solid. Yield: 65%. ^{1}H NMR (200 MHz, $CDCl_3$): δ (ppm) = 10.26 (s, 1H, CHO), 8.36 (d, 1H, HAr), 8.21 (s, 1H, OH), 8.09 (d, 1H, HAr), 7.67 (t, 1H, HAr), 7.48 (dd, 1H, HAr), 7.34 (dd, 1H, HAr). ^{13}C NMR (62 MHz, $CDCl_3$): δ (ppm) = 192.94, 137.72, 131.17, 118.26, 111.43. ESI-MS m/z_{calc}: 173.1 Found $[MH]^+$ m/z: 174.1.

5B.4.2.2. General procedure for synthesis of 2-((bis(pyridin-2-ylmethyl)amino)methyl)quinolin-8-ol (19):

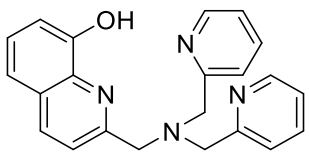

We adopted a reported synthetic procedure with minor modifications.[17] 2-dipicolylamine (0.945 mL, 5.3 mmol) and 8-hydroxyquinoline-2-carbaldehyde (1g, 5.8 mmol) were stirred in anhydrous dichloromethane (30 mL) under N_2 atmosphere. After 3 h, sodium triacetoxy borohydride (1.446 g, 6.8 mmol) was added and the mixture was stirred under N_2 atmosphere overnight at room temperature. The mixture was washed three times with saturated $NaHCO_3$ solution and the organic phase was dried over Na_2SO_4. The solvent was removed under reduced pressure and gave the pure product as a light yellow oil. Yield: 98%. ^{1}H NMR (200 MHz, CD_3CN): δ (ppm) = 8.54 (dq, 2H, HAr), 8.24 (d, 1H, HAr), 7.70 (m, 5H, HAr), 7.43 (m, 2H, HAr), 7.18 (m, 3H, HAr), 4.03 (s, 2H, CH_2), 3.93 (s, 4H, CH_2). ^{13}C NMR (62

MHz, $CDCl_3$): δ (ppm) = 160.71, 158.62, 153.88, 150.63, 137.92, 128.90, 124.74, 123.60, 118.92, 111.56, 61.72, 61.17. ESI-MS m/z_{calc}: 356.4 Found $[MH]^+$ m/z: 357.4.

5B.4.2.3. General procedure for the synthesis of metal complexes 20a-d

2-((bis(pyridin-2-ylmethyl)amino)methyl)quinolin-8-ol (50 mg, 0.14 mmol) was dissolved in the minimum amount of anhydrous acetonitrile and the desired metal salt (1 eq) was added. The solution was let stirring at room temperature for 15 min and then, diethyl ether was slowly added to the mixture to obtain the desired products by crystallization. *Caution!* Perchlorate salts of metal complexes with organic ligands are potentially explosive. They should be handled in small quantities and with caution.

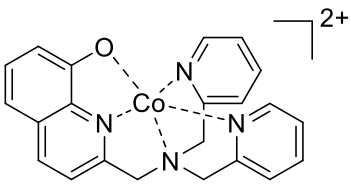

20a Dark brown crystal [74%]. ESI-MS m/z_{calc}: 513.0 Found $[MClO_4]^+$ m/z: 512.9. **Elemental Analysis (calc.)** $C_{22}H_{19}CoN_4O{*}2ClO_4{*}3H_2O{*}CH_3CN$ = C: 40.70%; H: 3.98%; N: 9.89% **Found** = C: 40.64%; H: 3.99%; N: 9.27%.

IR (KBr, cm^{-1})

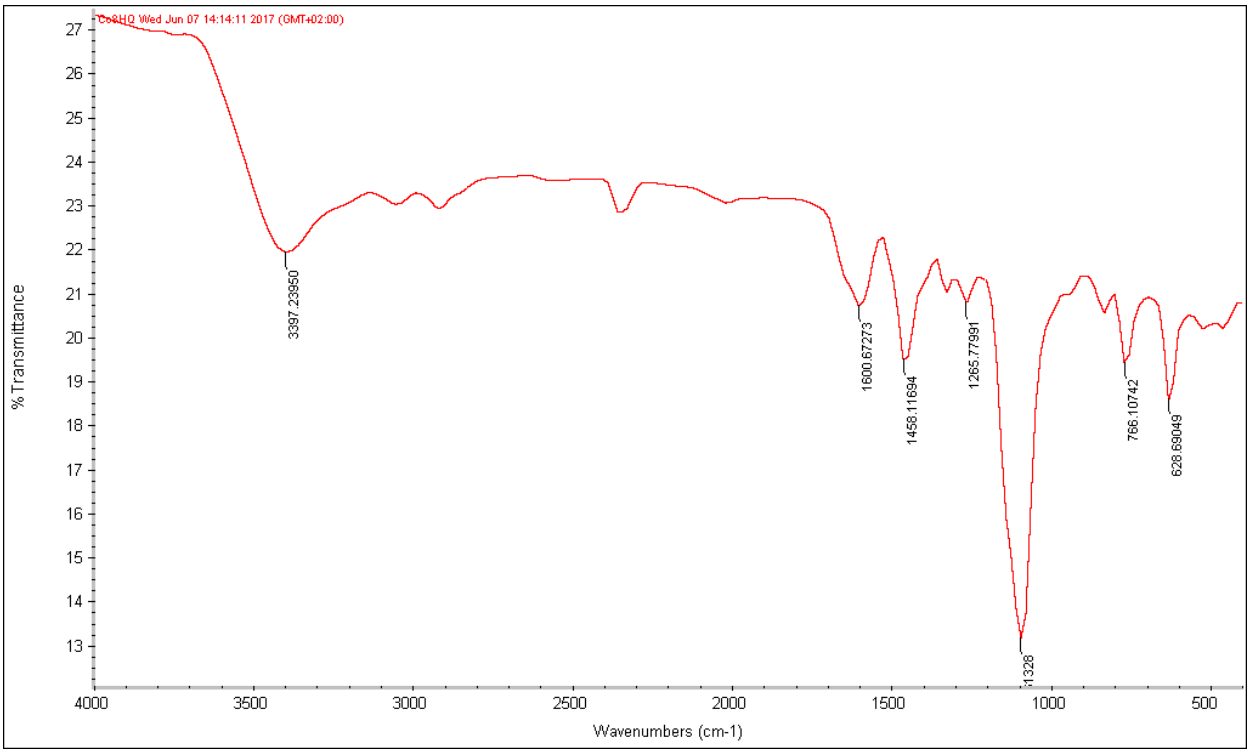

ESI+ MS (m/z)

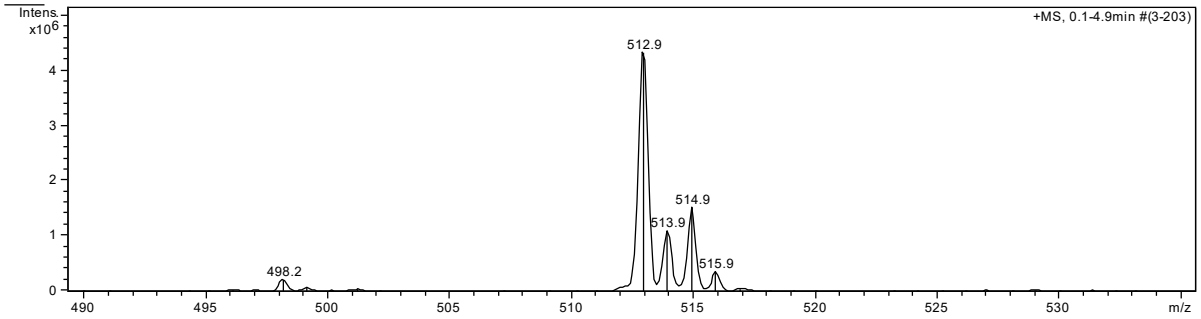

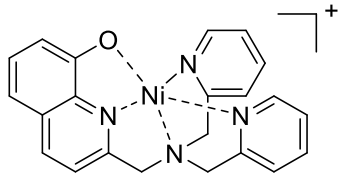

20b Ochre crystal [83%]. ESI-MS m/z_{calc}: 413.1 Found $[M]^+$ m/z: 413.1 **Elemental Analysis (calc.)** $C_{22}H_{19}NiN_4O*ClO_4*2H_2O$= C: 48.08%; H: 4.22%; N: 10.19% **Found** = C: 48.43%; H: 3.86%; N: 9.77%.

IR (KBr, cm^{-1})

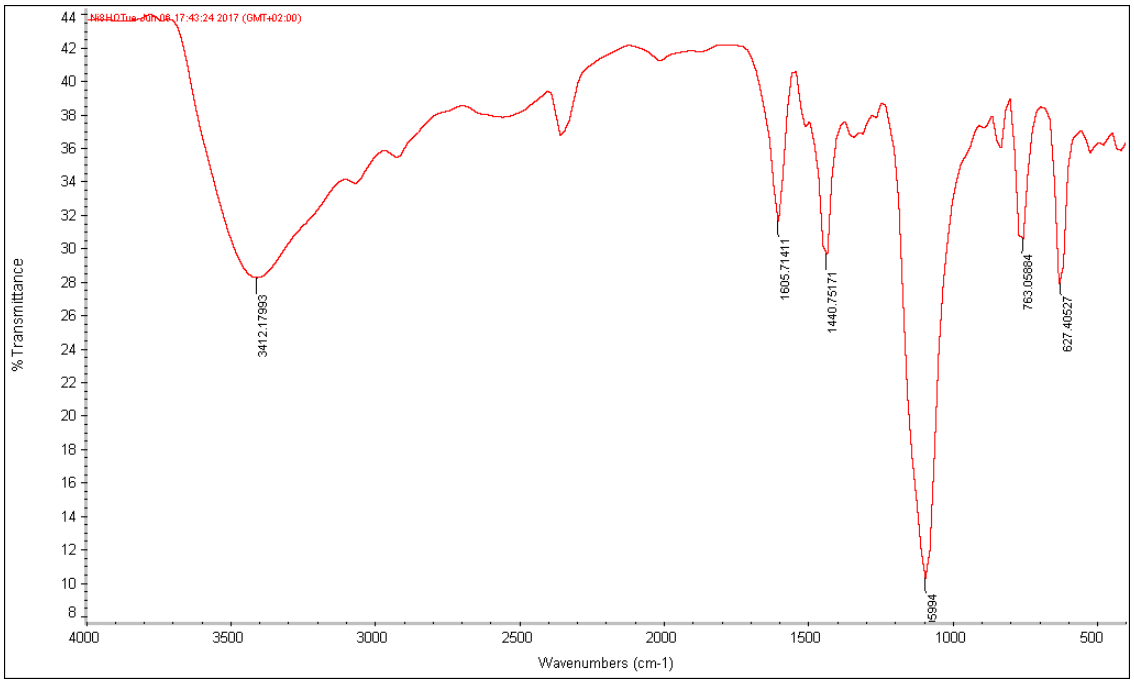

ESI+ MS (m/z)

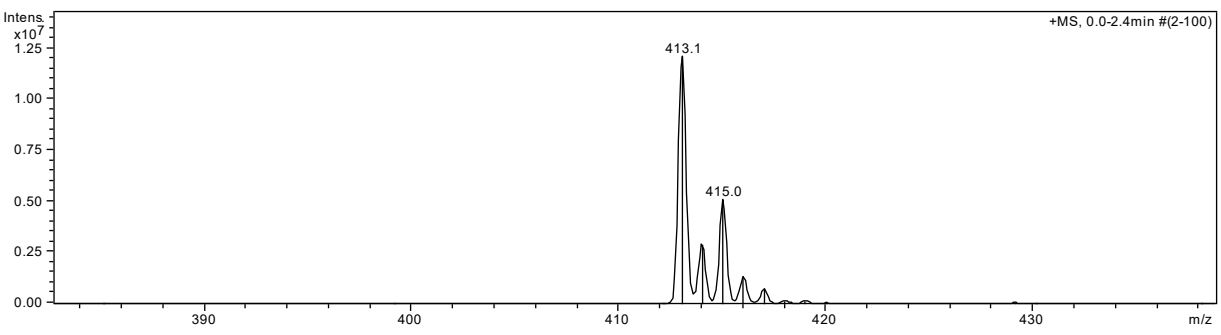

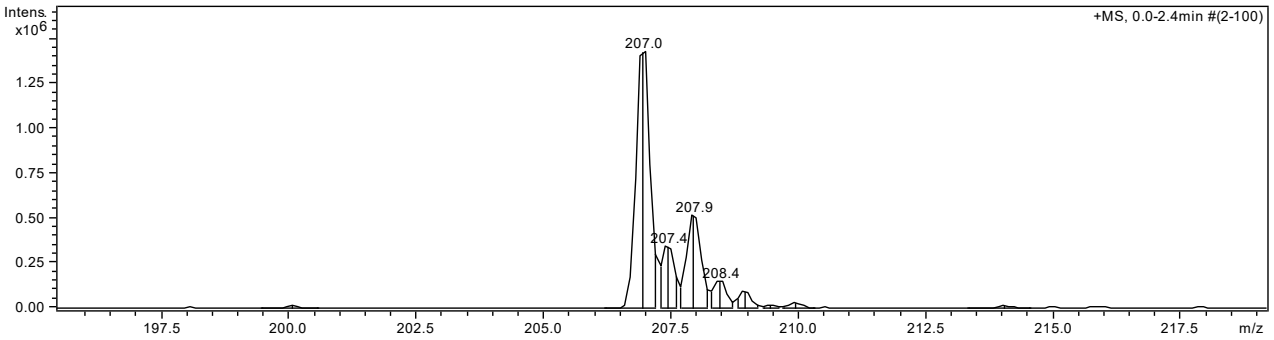

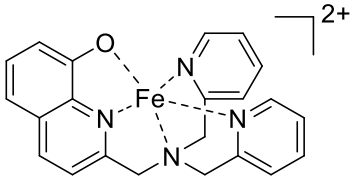

20c Dark green crystal [71%]. ESI-MS m/z $_{calc}$: 456.1 Found [MHCOO] $^{+}$ m/z: 456.1. **Elemental Analysis (calc.)** $C_{22}H_{19}FeN_4O*2ClO_4*H_2O$ = C: 42.07%; H: 3.37%; N: 8.92% **Found** = C: 42.47%; H: 3.36%; N: 9.12%.

IR (KBr, cm^{-1})

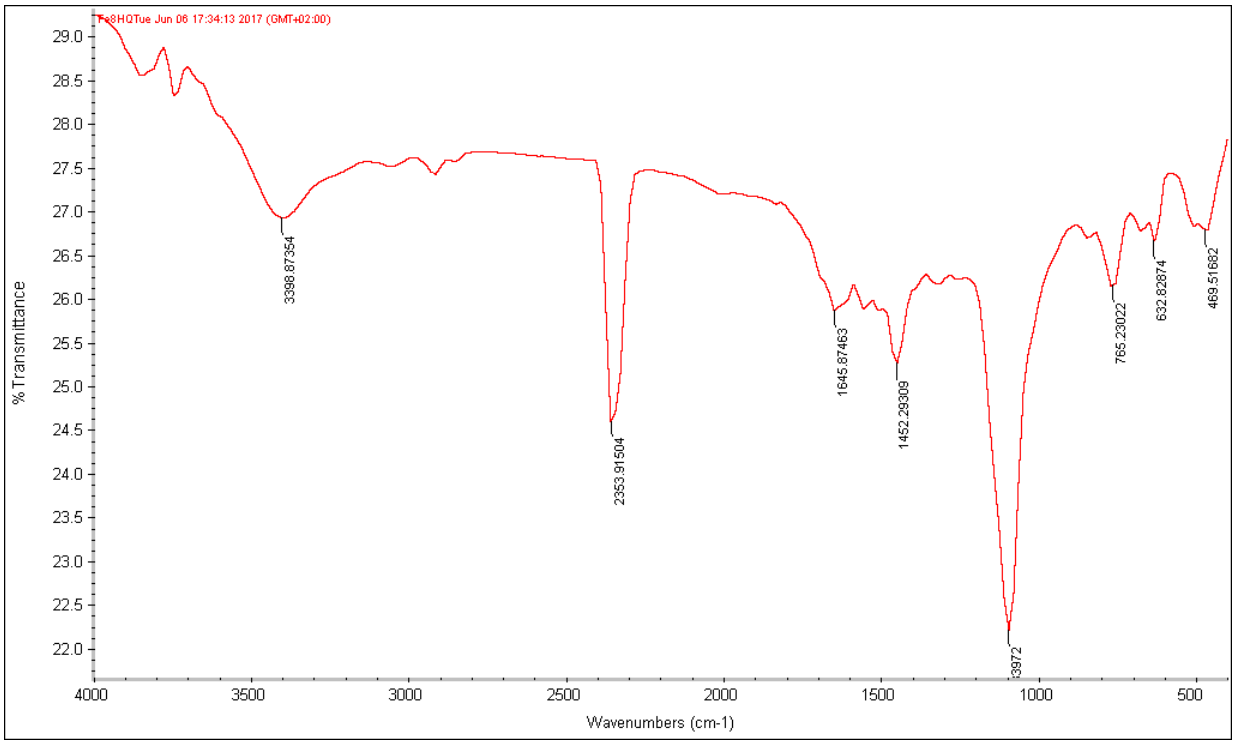

ESI+ MS (m/z)

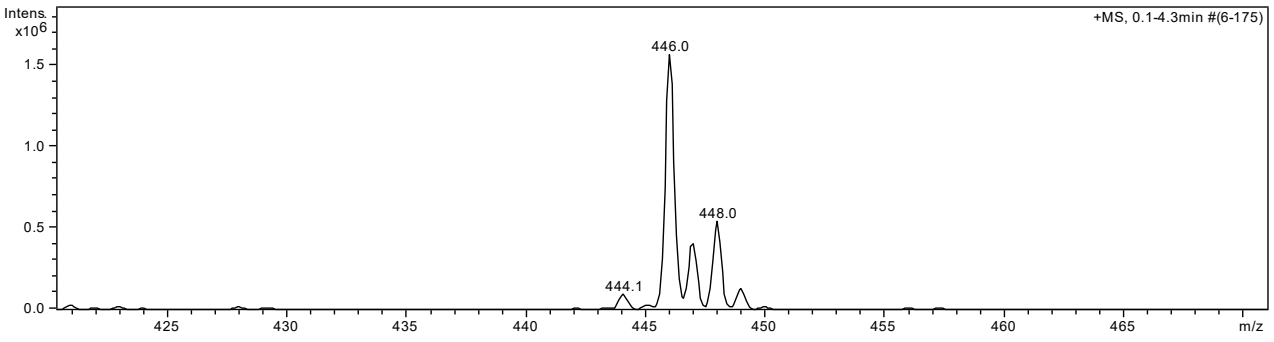

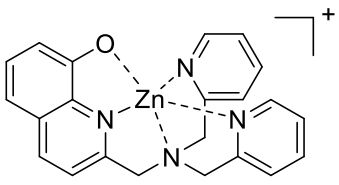

20d Dark yellow solid [87%]. ^{1}H NMR (200 MHz, CD_3CN): δ (ppm) = 8.81 (d, 2H, HAr), 8.52 (d, 1H, HAr), 8.12 (dt, 2H, HAr), 7.63 (m, 9H, HAr), 4.47 (d, 4H, CH_2), 4.39 (s, 2H, CH_2).Esi-MS m/z_{calc}: 419.1 Found $[M]^+$ m/z: 419.1. **Elemental Analysis (calc.)** $C_{22}H_{19}ZnN_4O{*}ClO_4{*}H_2O{*}CH_3CN$ = C: 49.76%; H: 4.18%; N: 12.09% **Found** = C: 49.90%; H: 3.93%; N: 12.41%.

IR (KBr, cm^{-1})

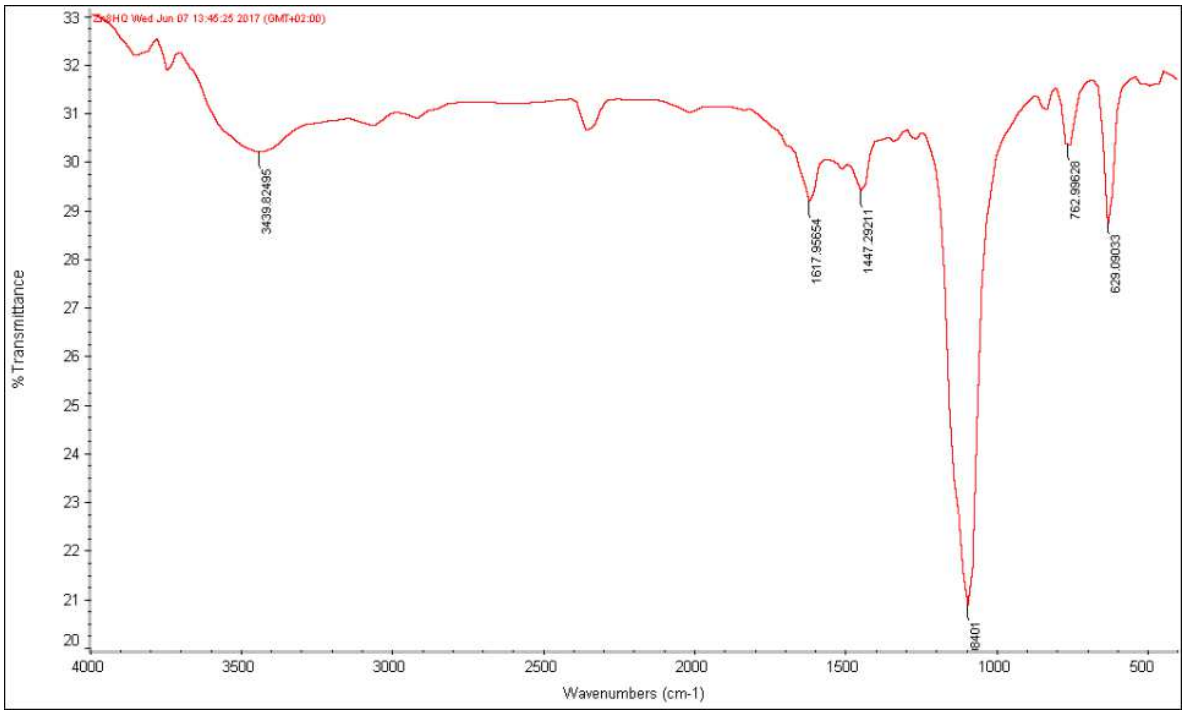

ESI+ MS (m/z)

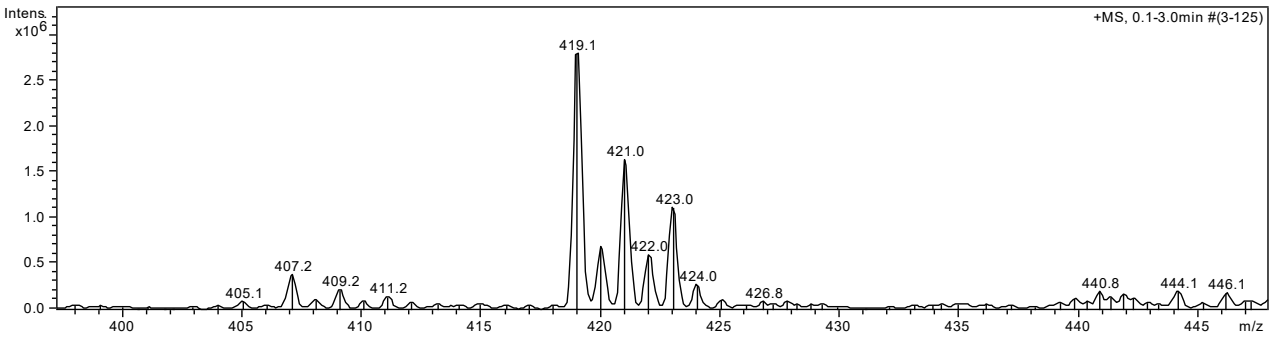

^{1}H NMR (200 MHz, CD_3CN):

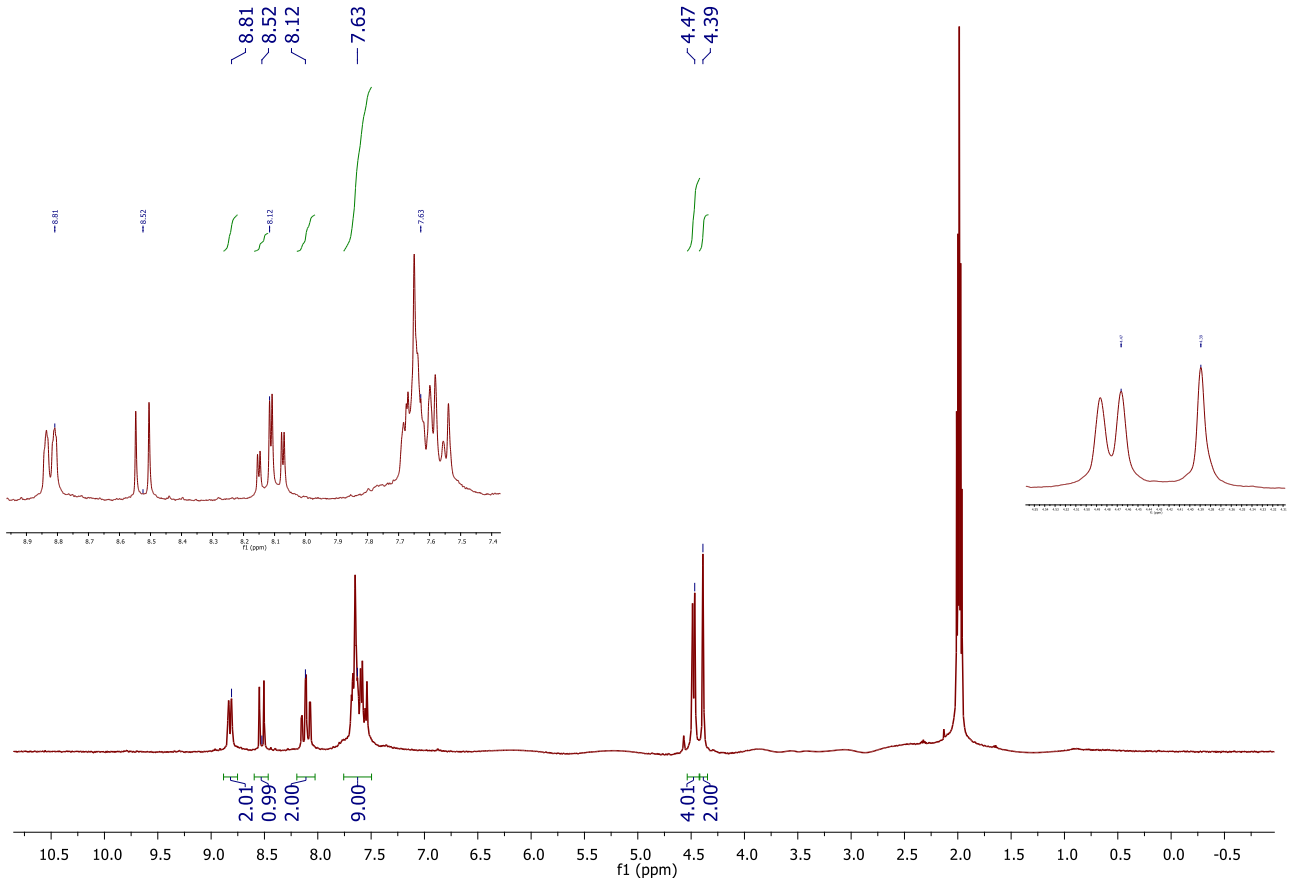

5B.5. References

[1] (a) N. S. Lewis and D. G. Nocera, *Proc. Natl. Acad. Sci. U.S.A.*, 2006, **103**, 15729. (b) N. Armaroli and V. Balzani, *Angew. Chem., Int. Ed.*, 2007, **46**, 52. (c) J. R. McKone, D. C. Crans, C. Martin, J. Turner, A. R. Duggal and H. B. Gray, *Inorg. Chem.*, 2016, **55**, 9131.

[2] (a) J. H. Alstrum-Acevedo, M. K. Brennaman and T. J. Meyer, *Inorg. Chem.*, 2005, **44**, 6802. (b) T. R. Cook, D. K. Dogutan, S. Y. Reece, Y. Surendranath, T. S. Teets and D. G. Nocera, *Chem. Rev.*, 2010, **110**, 6474. (c) D. Gust, T. A. Moore and A. L. Moore, *Faraday Disc.*, 2012, **155**, 9. (d) J. R. McKone, N. S. Lewis and H. B. Gray, *Chem. Mater.*, 2014, **26**, 407. (e) M. Natali and F. Scandola. *Supramolecular Artificial Photosynthesis*. G. Bergamini, S. Silvi (eds.), *Applied Photochemistry*, *Lecture Notes in Chemistry* **92**, DOI: 10.1007/978-3-319-31671-0_1, Springer 2016.

[3] (a) V. Artero, M. Chavarot-Kerlidou and M. Fontecave, *Angew. Chem., Int. Ed.*, 2011, **50**, 7238. (b) W. T. Eckenhoff, and R. Eisenberg, *Dalton Trans.*, 2012, **41**, 13004. (c) J. R. McKone, S. C. Marinescu, B. S. Brunschwig, J. R. Winkler and H. B. Gray, *Chem. Sci.*, 2014, **5**, 865.

[4] (a) Y. Halpin, M. T. Pryce, S. Rau, D. Dini and J. G. Vos, *Dalton Trans.* 2013, **42**, 16243. (b) Z. Han and R. Eisenberg, *Acc. Chem. Res.*, 2014, **47**, 2537. (c) K. Ladomenou, M. Natali, E. Iengo, G. Charalampidis, F. Scandola and A. G. Coutsolelos, *Coord. Chem. Rev.*, 2015, **304-305**, 38. (d) M. Wang, K. Han, S. Zhang and L. Sun, *Coord. Chem. Rev.*, 2015, **287**, 1.

[5] (a) P. Du, K. Knowles and R. Eisenberg, *J. Am. Chem. Soc.*, 2008, **130**, 12576. (b) A. Fihri, V. Artero, M. Razavet, C. Baffert, W. Leibl and M. Fontecave, *Angew. Chem., Int. Ed.*, 2008, **47**, 564. (c) W. T. Eckenhoff, W. R. McNamara, P. Du and R. Eisenberg, *Biochim. Biophys. Acta*, 2013, **1827**, 958. (d) F. Lakadamyali and E. Reisner, *Chem. Commun.*, 2011, **47**, 1695. (e) M. Natali, R. Argazzi, C. Chiorboli, E. Iengo and F. Scandola, *Chem. Eur. J.*, 2013, **19**, 9261. (f) E. Deponti and M. Natali, *Dalton Trans.*, 2016, **45**, 9136.

[6] (a) S. Losse, J. G. Vos and S. Rau, *Coord. Chem. Rev.*, 2010, **254**, 2492. (b) C. C. L. McCrory, C. Uyeda and J. C. Peters, *J. Am. Chem. Soc.*, 2012, **134**, 3164. (c) C. Gimbert-Suriñach, J. Albero, T. Stoll, J. Fortage, M.-N. Collomb, A. Deronzier, E. Palomares and A. Llobet, *J. Am. Chem. Soc.*, 2014, **136**, 7655. (d) M. Natali, A. Luisa, E. Iengo and F. Scandola, *Chem. Commun.*, 2014, **50**, 1842. (e) S. Roy, M. Bacchi, G. Berggren and V. Artero, *ChemSusChem*, 2015, **8**, 3632.

[7] (a) M. L. Helm, M. P. Stewart, R. M. Bullock, M. Rakowski DuBois and D. L. DuBois, *Science*, 2011, **333**, 863. (b) M. P. McLaughlin, T. M. McCormick, R. Eisenberg and P. L. Holland, *Chem. Commun.*, 2011, **47**, 7989. (c) Z. Han, L. Shen, W. W. Brennessel, P. L. Holland and R. Eisenberg, *J. Am. Chem. Soc.*, 2013, **135**, 14659. (d) M. A. Gross, A. Reynal, J. Durrant and E. Reisner, *J. Am. Chem. Soc.*, 2014, **136**, 356. (e) A. S. Weingarten, R. V. Kazantsev, L. C. Palmer, M. McClendon, A. R. Koltonow, A. P. S. Samuel, D. J. Kiebala, M. R. Wasielewski and S. I. Stupp, *Nat. Chem.*, 2014, **6**, 964. (f) P. H. A. Kankanamalage, S. Mazumder, V. Tiwari, K. K. Kpogo, H. B. Schelegel and C. N. Verani, *Chem. Commun.*, 2016, **52**, 13357.

[8] (a) C. Tard and C. J. Pickett, *Chem. Rev.*, 2009, **109**, 2245. (b) R. Lomoth and S. Ott, *Dalton Trans.*, 2009, 9952. (c) D. Streich, Y. Astuti, M. Orlandi, L. Schwartz, R. Lomoth, L. Hammarström and S. Ott, *Chem. Eur. J.*, 2010, **16**, 60; (d) S. Pullen, H. Fei, A. Orthaber, S. Cohen and S. Ott, *J. Am. Chem. Soc.*, 2013, **135**, 16997. (e) G. P. Connor, K. J. Meyer, C. S. Tribble and W. R. McNamara, *Inorg. Chem.*, 2014, **53**, 5408. (f) A. C. Cavell, C. L. Hartley, D. Liu, C. S. Tribble and W. R. McNamara, *Inorg. Chem.*, 2015, **54**, 3325. (g) C. L. Hartley, R. J. DiRisio, M. E. Screen, K. J. Mayer and W. R. McNamara, *Inorg. Chem.*, 2016, **55**, 8865.

[9] (a) C.-F. Leung, S.-M. Ng, C.-C. Ko, W.-L. Man, J. Wu, L. Chen and T.-C. Lau, *Energy Environ. Sci.*, 2012, **5**, 7903. (b) M. Nippe, R. S. Khnayzer, J. A. Panetier, D. Z. Zee, B. S. Olaiya, M. Head-Gordon, C. J. Chang, F. N. Castellano and J. R. Long, *Chem. Sci.*, 2013, **4**, 3934. (c) B. Shan, T. Baine, X. A. N. Ma, X. Zhao and R. H. Schmehl, *Inorg. Chem.*, 2013, **52**, 4853. (d) C. Bachmann, M. Guttentag, B. Spingler and R. Alberto, *Inorg. Chem.*, 2013, **52**, 6055. (e) R. S. Khnayzer, V. A. Thoi, M. Nippe, A. E. King, J. W. Jurss, K. A. El Roz, J. R. Long, C. J. Chang and F. N. Castellano, *Energy Environ. Sci.*, 2014, **7**, 1477. (f) L. Tong, R. Zong and R. P. Thummel, *J. Am. Chem. Soc.*, 2014, **136**, 4881. (g) E. Deponti, A. Luisa, M. Natali, E. Iengo and F. Scandola, *Dalton Trans.*, 2014, **43**, 16345. (h) A. Call, Z. Codolá, F. Acuña-Pares and J. Lloret-Fillol, *Chem. Eur. J.*, 2014, **20**, 6171. (i) D. Z. Zee, T. Chantarojsiri, J. R. Long and C. J. Chang, *Acc. Chem. Res.*, 2015, **48**, 2027. (j) N. Queyriaux, R. T. Jane, J. Massin, V. Artero and M. Chavarot-Kerlidou, *Coord. Chem. Rev.*, 2015, **304-305**, 3. (k) W. K. C. Lo, C. E. Castillo, R. Gueret, J. Fortage, M. Rebarz, M. Sliwa, F. Thomas, C. J. McAdam, G. B. Jameson, D. A. McMorran, J. D. Crowley, M.-N. Collomb and A. G. Blackman, *Inorg. Chem.*, 2016, **55**, 4564. (l) M. Natali, E. Badetti, E. Deponti, M. Gamberoni, F. A. Scaramuzzo, A. Sartorel and C. Zonta, *Dalton Trans.*, 2016, **45**, 14764.

[10] (a) F. A. Scaramuzzo, G. Licini and C. Zonta, *Chem. Eur. J.*, 2013, **19**, 16809. (b) E. Badetti, K. Wurst, G. Licini and C. Zonta, *Chem. Eur. J.*, 2016, **22**, 6515. (c) F. A. Scaramuzzo, E. Badetti, G. Licini and C. Zonta, *Eur. J. Org. Chem.*, 2017, **11**, 1438. (d) C. Bravin, E. Badetti, F. A. Scaramuzzo, G. Licini and C. Zonta, *J. Am. Chem. Soc.*, 2017, **139**, 6456–6460.

[11] G. Tallec, D. Imbert, P. H. Friesa and M. Mazzanti, *Dalton Trans.*, 2010, **39**, 9490.

[12] (a) E. C. Niederhoffer, A. E. Martell, P. Rudolf and A. Clearfield, *Inorg. Chem.*, 1982, **21**, 3734. (b) S. Ghosh, A. C. Barve, A. A. Kumbhar, A. S. Kumbhar, V. G. Puranik, P. A. Datar, U. B. Sonawane and R. R. Joshi, *J. Inorg. Biochem.*, 2006, **100**, 331.

[13] A. Albert and J. N. Phillips, *J. Chem. Soc.*, 1956, 1294.

[14] (a) J. Jullien, G. Juhasz, P. Mialane, E. Dumas, C. R. Mayer, J. Marrot, E. Rivière, E. L. Bominaar, E. Münck and F. Sécheresse, *Inorg. Chem.*, 2006, **45**, 6922. (b) R. Shakya, D. R. Powell and R. P. Houser, *Eur. J. Inorg. Chem*., 2009, 5319.

[15] J. P. López, F. W. Heinemann, R. Prakash, B. A. Hess, O. Horner, C. Jeandey, J.-L. Oddou, J.-M. Latour and A. Grohmann, *Chem. Eur. J.*, 2002, **8**, 5709.

[16] (a) G. Tallec, D. Imbert, P. H. Fries, M. Mazzanti, *Dalton Trans* 2010, **39**, 9490. (b) V. G. Ramsey, *J Am Pharm Assoc* 1951, **40,** 564. (c) L. Chen, C. Yan, B.-B. Du, K. Wu, L.-Y. Zhang, S.-Y. Yin, M. Pan, *Inorg Chem Commun* 2014, **47**, 13.

[17] K. J. Barnham, E. C. L. Gautier, G. B. Kok, G. Krippner, US20080161353 A1, 2008.

Abbreviations

ac	Absolute Configuration
BINOL	1,1'-Bi-2-naphthol
ARGET	Activators Regenerated by Electron Transfer
ESI-FAIMS-MS	Asymmetric Waveform Ion Mobility Spectrometry-Mass Spectrometry
ATRP	Atom Transfer Radical Polymerization
CSA	Chiral Solvating Agents
CPS	Chiral Stationary Phase
CIMS	Chiral Ion Mobility Spectrometry
COSY	COrrelation SpectroscopY
MOMCl	Chloromethyl Methyl Ether
CD	Circular Dicroism
CPL	Circulary Polarized Luminescence
CEI	Coulomb Explosion Imaging
DFT	Density Functional Theory
DOSY	Diffusion Ordered SpectroscopY
DMSO	Dimethyl sulfoxide
DMF	Dimethylformamide
$\mathbf{g_{lum}}$	dissymmetry factor / assymetry factor
DCC	Dynamic Covalent Chemistry
eATRP	Electrochemically Mediated ATRP
ESI-MS	Electrospray Ionisation Mass Spectrometry
e.e.	Enantiomeric Excess
EBPA	ethyl 1-phenyl-1-bromoacetate
FTIR	Fourier-Transform Infrared Spectroscopy
GC	Gas Chromatography
HS-SPME	Headspace Solid-Phase Microextraction
HMQC	Heteronuclear Multiple-Quantum Correlation
HPLC	High Performance Liquid Cromatography

HRMS	High Resolution Mass Spectra
HTS	High Throughput Screening
HEC	Hydrogen Evolving Catalysts
i2PEPICO	Imaging Photoelectron/Photoion Coincidence
IR	Infrared
ICAR	Initiators For Continuous Activator Regeneration
IM	Inverse Method
IM–HRMS	Ion Mobility High-Resolution Mass Spectroscopy
k_a	Activation rate constant
K_d	Deactivation rate constant
k_p	Propagation rate constant
k_t	Termination rate constant
LC/MSD	Liquid Chromatography/Mass Selective Detector
L	Ligand
MS-PECD	Mass Selective - Photo Electron Circular Dichroism
MS	Mass Spectroscopy
MALDI	Matrix-Assisted Laser Desorption/Ionization
MA	Methyl Acrylate
MMA	Methyl Methacrylate
M	Metal or Monomer (unless it is a measurement unit)
H2bpcd	*N,N'*-bis(2-pyridylmethyl)-trans-1,2-diaminocyclohexane-*N,N'*-diacetic acid
NBS	N-bromosuccinimide
NMR	Nuclear Magnetic Resonance Spectroscopy
OEOMA	Ooligo(ethylene glycol) methyl ether methacrylate
ORD	Optical Rotatory Dispersion
PBI	Perylenebisimide
PECD	Photoelectron Circular Dichroism
PEPICO	Photoelectron Photoion Coincidence
ROA	Raman Optical Activity
R-X	Alkyl halide (or dormant polymer chain)

R	Alkyl (or polymeric) radical
SARA	Supplemental Activator and Reducing Agent
TDDFT	Time-Dependent Density Functional Theory
TOF	Time-Of-Flight
TEA	Triethylamine
TPMA	Tris(2-Pyridylmethyl)Amine
2D-NMR	Two-Dimensional Nuclear Magnetic Resonance
UPLC	Ultra-Performance Liquid Chromatography
UV	Ultraviolet
UV-Vis	Ultraviolet-Visible
VT-NMR	Variable Temperature NMR
VCD	Vibrational Circular Dichroism
X	Halogen substituent